bioRxiv preprint doi: https://doi.org/10.1101/2020.02.19.956060; this version posted February 20, 2020. The copyright holder for this preprint (which was not certified by peer review) is the author/funder. All rights reserved. No reuse allowed without permission.

Chronic chemogenetic activation of forebrain excitatory neurons in postnatal life evokes long-lasting changes in mood-related behavior

Sthitapranjya Pati[1*], Kamal Saba[2#], Sonali S. Salvi[1#], Praachi Tiwari[1], Pratik R. Chaudhari[1], Vijaya Verma[3], Sourish Mukhopadhyay[1], Darshana Kapri[1], Shital Suryavanshi[1], James P. Clement[3], Anant B. Patel[2], Vidita A. Vaidya[1*]

[*]Equal corresponding authors

[#]Equal second authors

[1]Department of Biological Sciences, Tata Institute of Fundamental Research, Mumbai 400005, India. [2]Centre for Cellular and Molecular Biology, Hyderabad, Telangana 500007, India, [3]Neuroscience Unit, Jawaharlal Nehru Centre for Advanced Scientific Research, Bengaluru, Karnataka 560064, India

Address correspondence to:

*Dr. Vidita A. Vaidya
Department of Biological Sciences,
Tata Institute of Fundamental Research,
Homi Bhabha Road, Mumbai 400005, India
Telephone Number: +91 22 22782608
Fax Number: + 91-22 22804610
E-mail: vvaidya@tifr.res.in

*Dr. Sthitapranjya Pati
Department of Biological Sciences,
Tata Institute of Fundamental Research,
Homi Bhabha Road, Mumbai 400005, India
Telephone Number: +91 22 22782743
Fax Number: + 91-22 22804610
E-mail: sthitapati@tifr.res.in

bioRxiv preprint doi: https://doi.org/10.1101/2020.02.19.956060; this version posted February 20, 2020. The copyright holder for this preprint (which was not certified by peer review) is the author/funder. All rights reserved. No reuse allowed without permission.

Abstract

Early adversity is a key risk factor for the development of adult psychopathology, including anxiety, depression and schizophrenia. Rodent models of early adversity program persistent behavioral, molecular, metabolic, and neurophysiological changes. Perturbed signaling via forebrain Gq-coupled neurotransmitter receptors is a common feature across multiple models of early adversity. We addressed whether enhanced Gq-mediated signaling in forebrain excitatory neurons during postnatal life can evoke long-lasting mood-related behavioral changes. Excitatory hM3Dq DREADD-mediated chemogenetic activation of CamKIIα-positive forebrain excitatory neurons during postnatal life (P2-14) increased anxiety- and despair-like behavior, and evoked sensorimotor gating deficits in adulthood. In contrast, chronic chemogenetic hM3Dq DREADD activation of forebrain excitatory neurons in the juvenile or adult window did not evoke any mood-related behavioral alterations, highlighting the criticality of the postnatal temporal window. The enhanced anxiety-, despair- and schizophrenia-like behavioral changes evoked by chronic chemogenetic activation of forebrain excitatory neurons in postnatal life, was accompanied by an increased cortical and hippocampal metabolic rate of glutamatergic and GABAergic neurons in adulthood. Furthermore, animals with a history of postnatal hM3Dq activation exhibited a decline in the expression of activity-dependent and plasticity-associated markers within the hippocampus, along with perturbed hippocampal excitatory and inhibitory currents in adulthood. These results indicate that Gq signaling mediated activation of forebrain excitatory neurons during the critical postnatal window is sufficient to program altered mood-related behavior, as well as metabolic and neurophysiological changes in forebrain glutamate and GABA systems, recapitulating specific aspects of the consequences of early adversity.

bioRxiv preprint doi: https://doi.org/10.1101/2020.02.19.956060; this version posted February 20, 2020. The copyright holder for this preprint (which was not certified by peer review) is the author/funder. All rights reserved. No reuse allowed without permission.

Introduction

Early life experience plays a crucial role in the maturation and fine-tuning of neurocircuitry that drives emotional behavior in adulthood[1–6]. Both clinical and preclinical evidence indicates that early life adversity serves as a key risk factor for the development of adult psychopathology, increasing susceptibility to psychiatric disorders like anxiety, major depression and schizophrenia[5,7–10]. Stressful experiences in adulthood can produce behavioral alterations that are often transient in nature, however perturbations in the vulnerable perinatal 'critical window' can program lasting changes in emotional behavior[11–13]. Several animal models have been used to study the persistent behavioral changes caused by early life perturbations, and have been instrumental in understanding specific underlying neural mechanisms involved in the programming of adult emotional behavior[10,11,14–19].

The prenatal period and the first few weeks after birth are marked by the establishment and functional maturation of several neurocircuits in rodent models, representing a critical period in which these circuits are particularly amenable to modification by environmental stimuli[2,5]. Rodent models of early life perturbations encompass those based on gestational stress[10], maternal immune activation[8,9], disruption of dam-pup interaction[20,21] or pharmacological treatments[22–24], and exhibit both distinct and overlapping behavioral and physiological effects in adulthood[5,11]. Strikingly, a commonality noted across these animal models is the fact that multiple molecular, cellular, functional and behavioral changes often persist throughout the animal's lifespan[5,11,25]. Amongst the underlying mechanisms implicated in the establishment of such long-lasting changes in response to early life perturbations are a dysregulation of the hormonal stress response pathway[22,26–30], serotonergic system[31–33], and emergence of excitation-inhibition balance within key cortical neurocircuits[34,35].

Common across several rodent models of early life perturbations are alterations in G protein-coupled receptor (GPCR) signaling, including via the serotonin$_{1A}$ (5-HT$_{1A}$) receptor[36–38], serotonin$_{2A}$ (5-HT$_{2A}$) receptor[39–43], metabotropic glutamate receptors 1 and 5 (mGluR1/5)[44,45], muscarinic acetylcholine receptor 1 (M1)[46] and α_1 adrenergic receptors[47]. The emergence of aberrant emotional behavior in these animal models has been suggested to involve a key role for both excitatory Gq-coupled and inhibitory Gi-coupled GPCRs, in particular an appropriate balance of signaling between the Gq-coupled 5-HT$_{2A}$ receptor and the Gi-coupled 5-HT$_{1A}$ receptor in the forebrain has been hypothesized to be a critical determinant of the establishment of emotional behavior[48–51]. Enhanced signaling via the cortical 5-HT$_{2A}$ receptor is thought to be one of the common features noted across distinct models of early life

bioRxiv preprint doi: https://doi.org/10.1101/2020.02.19.956060; this version posted February 20, 2020. The copyright holder for this preprint (which was not certified by peer review) is the author/funder. All rights reserved. No reuse allowed without permission.

perturbations, including maternal separation[39,40], postnatal fluoxetine[48] and maternal immune activation[42,52]. Interestingly, a systemic blockade of the Gq-coupled 5-HT_{2A} receptor overlapping with early stress or postnatal fluoxetine treatment can prevent the emergence of adult anxiety and depressive behavior, and associated molecular and cellular correlates[40,48]. Furthermore, pharmacological stimulation of the 5-HT_{2A} receptor during the postnatal critical window is sufficient to evoke a persistent increase in anxiety in adulthood[48]. Collectively, these observations motivate the key question of whether perturbed Gq-coupled signaling within the forebrain in the critical postnatal window plays an important role in the establishment of persistent changes in mood-related behaviors.

Here, we have tested the hypothesis that enhanced Gq-mediated signaling in forebrain excitatory neurons during the postnatal critical window may be sufficient to program persistent alterations in mood-related behavior in adulthood. To address this central question we expressed the excitatory Designer Receptors Exclusively Activated by Designer Drugs (DREADD) in CamKIIα-positive forebrain excitatory neurons using a bigenic mouse line (CamKIIα-tTA::TetO hM3Dq)[53], and chemogenetically activated Gq signaling through oral administration of the DREADD agonist clozapine-N-oxide (CNO; 1 mg/kg) from postnatal day 2 to 14 prior to behavioral analysis in adulthood. Our findings demonstrate that chemogenetic activation of Gq signaling in CamKIIα-positive forebrain excitatory neurons by chronic postnatal CNO (PNCNO) treatment enhances anxiety- and despair-like behavior, accompanied by impaired sensorimotor gating in adulthood. These long-lasting behavioral changes evoked by PNCNO treatment are associated with a persistent dysregulation of cortical and hippocampal glutamate/GABA metabolism, and perturbed hippocampal excitatory and inhibitory neurotransmission. The criticality of the postnatal time window is highlighted by our observation that the same perturbation performed in the juvenile window or in adulthood has no effect on mood-related behavior. Our findings provide evidence in support of the hypothesis that enhanced Gq signaling within forebrain excitatory neurons during the critical postnatal window is sufficient to evoke perturbed mood-related behavior in adulthood, recapitulating the enhanced vulnerability to psychopathology associated with early adversity.

bioRxiv preprint doi: https://doi.org/10.1101/2020.02.19.956060; this version posted February 20, 2020. The copyright holder for this preprint (which was not certified by peer review) is the author/funder. All rights reserved. No reuse allowed without permission.

Results

Selective expression and activation of hM3Dq DREADD in CamKIIα-positive forebrain excitatory neurons in CamKIIα-tTA::TetO-hM3Dq bigenic mice during the postnatal window

To examine the persistent behavioral, metabolic, molecular and electrophysiological consequences of postnatal chemogenetic hM3Dq DREADD activation of forebrain excitatory neurons, CamKIIα-tTA::TetO-hM3Dq bigenic mice were generated (Figure 1A). This bigenic mouse line is reported to exhibit selective expression of the hM3Dq DREADD in Ca^{2+}/calmodulin-dependent protein kinase α (CamKIIα)-positive excitatory neurons in the forebrain[53] (Figure 1B). Western blotting and immunofluorescence analysis confirmed the presence of the HA-tagged hM3Dq DREADD in both the hippocampus and cortex of bigenic mouse pups (P7) (Figure 1C, D). Expression of the HA-tagged hM3Dq DREADD was not observed in either the hippocampal subfields or cortex of single-positive, genotype-control mouse pups (P7) (Figure 1D).

We next assessed whether, acute stimulation of the hM3Dq DREADD by the exogenous ligand, clozapine-N-oxide (CNO) at postnatal day 7 (P7), resulted in enhanced neuronal activation within the forebrain, using two distinct strategies. First, we performed western blotting analysis to determine the expression levels of the neuronal activity markers, c-Fos and phospho-ERK, following a single dose of CNO (1 mg/kg) administered via feeding to bigenic mouse pups at P7 (Figure 1E, F). Western blotting analysis revealed a significant increase in both p-ERK/ ERK (Figure 1G, $p = 0.02$) and c-Fos (Figure 1H, $p = 0.002$) levels in the hippocampus of CNO-treated bigenic mouse pups. We also observed a trend towards an increase in p-ERK/ ERK levels (Figure 1I, $p = 0.07$) and significant increase in c-Fos levels (Figure 1J, $p < 0.0001$) in the cortex of CNO-treated bigenic mouse pups. Second, we carried out whole-cell patch clamp recordings in current clamp mode from the somata of CA1 pyramidal neurons in acute hippocampal slices derived from bigenic mouse pups (P7) following CNO bath application (Figure 1K, L). Bath application of 1 μM CNO evoked robust spiking activity in CA1 pyramidal neurons (Figure 1M). These two approaches confirmed that as anticipated, acute postnatal hM3Dq DREADD activation of forebrain excitatory neurons resulted in enhanced neuronal activation.

Given our treatment paradigm involved chronic administration of CNO to mouse pups during the early postnatal window (P2-P14), we further sought to understand the effects of chronic CNO-mediated hM3Dq DREADD activation in CamKIIα-positive forebrain excitatory

bioRxiv preprint doi: https://doi.org/10.1101/2020.02.19.956060; this version posted February 20, 2020. The copyright holder for this preprint (which was not certified by peer review) is the author/funder. All rights reserved. No reuse allowed without permission.

neurons on neuronal activity, at an interim time point in the midst of chronic CNO administration (P7). Bigenic mouse pups were orally administered CNO (1 mg/kg; PNCNO) from P2-P7, and then assessed via western blotting analysis for cortical and hippocampal levels of the neuronal activity marker, p-ERK (Figure 1 – figure supplement 1A), or through electrophysiological measurements of spontaneous excitatory/ inhibitory currents in the hippocampus (Figure 1N; Figure 1 – figure supplements 2A, 3A). We detected a significant increase in p-ERK/ ERK levels in the hippocampus (Figure 1 – figure supplement 1B, C, p = 0.04) and the cortex (Figure 1 – figure supplement 1B, D, p = 0.0001) of PNCNO-treated mouse pups. Whole-cell patch clamp recording to measure sPSCs and intrinsic membrane properties in CA1 pyramidal neurons from acute hippocampal slices revealed a significant difference in sPSC amplitude in the PNCNO treatment group, with a small but significant decrease in low amplitude events (< 100 pA; Figure 1 – figure supplement 2B, C, $p < 0.0001$), accompanied by a significant increase in large amplitude events characterized by the presence of a long-tail in sPSC amplitude event distribution (Figure 1 – figure supplements 2C, 3B, 3C). We also observed a significant reduction in the cumulative probability of sPSC interevent intervals in CA1 pyramidal neurons from the PNCNO treatment group (Figure 1 – figure supplement 2D, $p < 0.0001$). CA1 pyramidal neurons in PNCNO-treated hippocampal slices displayed large network activity, characterized by compound negative peaks (Figure 1 – figure supplement 3B). Out of the total number of events analyzed, the frequency of events greater than 100 pA were almost double in PNCNO-treated CA1 neurons (4.85%) as compared to controls (2.57%). We also noted a small fraction of events (0.8%) with amplitudes greater than 250 pA in CA1 pyramidal neurons from PNCNO-treated mouse pups, which were not detected in vehicle-treated controls (Figure 1 – figure supplement 3D). In order to understand the influence of CNO-mediated hM3Dq DREADD activation of CamKIIα-positive excitatory neurons during the postnatal window on intrinsic excitability, we plotted an input-output curve by injecting increasing step currents and measured the number of action potentials (Figure 1 – figure supplement 2E). We observed no change in the number of action potentials generated in CA1 pyramidal neurons of PNCNO-treated mouse pups (Figure 1 – figure supplement 2F). Measurements of key intrinsic membrane properties revealed no change in input resistance (R_N), membrane time constant (τ), sag voltage, and accommodation index in CA1 pyramidal neurons of PNCNO-treated mouse pups (Table 1). We did note a trend towards a depolarizing shift in the resting membrane potential (RMP) in CA1 pyramidal neurons of the PNCNO treatment group as compared to their vehicle-treated controls (Table 1, p = 0.06).

bioRxiv preprint doi: https://doi.org/10.1101/2020.02.19.956060; this version posted February 20, 2020. The copyright holder for this preprint (which was not certified by peer review) is the author/funder. All rights reserved. No reuse allowed without permission.

We next sought to parcellate the influence of chronic CNO-mediated hM3Dq DREADD activation of CamKIIα-positive forebrain excitatory neurons in the postnatal window on excitatory and inhibitory neurotransmission. Whole-cell patch clamp analysis was carried out to measure sEPSCs and sIPSCs in CA1 pyramidal neurons in acute hippocampal slices derived from bigenic mouse pups treated with CNO (1 mg/kg) or vehicle (Figure 1N). We observed a significant difference in sEPSC amplitude in CA1 pyramidal neurons of PNCNO-treated mouse pups as compared to vehicle-treated controls, as revealed by a small but significant decrease in low amplitude events (< 100 pA), and a significant increase in large amplitude events characterized by the presence of a long-tail in sEPSC amplitude event cumulative distribution (Figure 1O, Q, $p < 0.0001$). CA1 pyramidal neurons in hippocampal slices from PNCNO-treated mouse pups displayed large sEPSC events characterized by compound negative peaks as compared to vehicle-treated controls (Fig 1O; bottom traces). We also noted a significant decline in the cumulative probability of sEPSC interevent intervals in CA1 pyramidal neurons from the PNCNO treatment group (Figure 1R, $p < 0.0001$). Further, we observed a significant reduction in the cumulative probability of sIPSC amplitude (Figure 1P, S, $p < 0.0001$) and an increase in the cumulative probability of sIPSC interevent intervals (Figure 1T, $p < 0.0001$) in CA1 pyramidal neurons from PNCNO-treated mouse pups.

Our findings demonstrate the selective expression of the hM3Dq DREADD in the forebrain of CamKIIα-tTA::TetO-hM3Dq bigenic mouse pups, and indicate that acute CNO treatment during postnatal life increases neuronal activity in the hippocampus and cortex. Further, as the main treatment paradigm used in our study is based on chronic CNO-mediated hM3Dq DREADD activation of CamKIIα-positive forebrain excitatory neurons during the postnatal window, our experiments at an interim juncture during postnatal treatment reveal significant changes in both neuronal activity marker expression and electrophysiological measures. Collectively, our results demonstrate that chronic CNO-mediated hM3Dq DREADD activation during the postnatal window results in enhanced expression levels of neuronal activity markers, elevated spontaneous network activity, an increase in spontaneous excitatory currents, and a concomitant decrease in spontaneous inhibitory currents in CA1 pyramidal neurons of the PNCNO treatment group.

bioRxiv preprint doi: https://doi.org/10.1101/2020.02.19.956060; this version posted February 20, 2020. The copyright holder for this preprint (which was not certified by peer review) is the author/funder. All rights reserved. No reuse allowed without permission.

Chronic chemogenetic activation of CamKIIα-positive forebrain excitatory neurons during the early postnatal window results in a long-lasting increase in anxiety- and despair-like behavior in adult mice

We next sought to assess the persistent behavioral consequences of perturbing neuronal activity of CamKIIα-positive forebrain excitatory neurons during the early postnatal window using chronic CNO-mediated hM3Dq DREADD activation. CamKIIα-tTA::TetO-hM3Dq bigenic mouse pups were orally administered the DREADD ligand, CNO (1 mg/kg), or vehicle, once daily from P2-P14 (Figure 2A). Postnatal treatment with CNO did not alter the body weight, measured across the period of postnatal treatment or in adulthood (Figure 2 – figure supplement 1A-C). Chronic CNO-mediated hM3Dq DREADD activation in the early postnatal window did not alter the normal trajectory of sensorimotor development, as indicated by no change in the ontogeny of reflex behaviors, namely surface righting and negative geotaxis, in PNCNO-treated mouse pups as compared to their vehicle-treated controls (Figure 2 – figure supplement 2A-C).

We examined the influence of chronic CNO-mediated hM3Dq DREADD activation of CamKIIα-positive forebrain excitatory neurons during the early postnatal window on long-lasting changes in anxiety- and despair-like behavior. We subjected bigenic adult mice with a history of PNCNO or vehicle treatment to a battery of behavioral tasks, commencing three-months post cessation of PNCNO treatment. We performed the open field test (OFT), elevated plus maze (EPM) test, and the light-dark (LD) avoidance test to assess anxiety-like behavior, followed by the forced swim test (FST) to assess despair-like behavior in PNCNO-treated adult bigenic male and female mice (Figure 2A, Figure 2 – figure supplement 3A). We noted a significant increase in anxiety-like behavior in adult male mice with a history of PNCNO treatment on the OFT (Figure 2B). The PNCNO treatment group showed a significant decrease in percent distance travelled in the center (Figure 2C, $p = 0.03$), number of entries to the center (Figure 2E, $p = 0.02$), and total distance travelled in the OFT arena (Figure 2F, $p = 0.003$). The percent time spent in the center of the OFT arena was unchanged across treatment groups (Figure 2D). We also noted an increase in anxiety-like behavior in the EPM (Figure 2G) in the PNCNO-treated adult male mice, with a significant decline in the number of entries to the open arms (Figure 2J, $p = 0.02$) and a trend towards a decrease in the percent time spent in the open arms (Figure 2I, $p = 0.08$). The percent distance travelled in the open arms (Figure 2H) and the total distance traversed in the EPM (Figure 2K) were unchanged. Behavioral analysis on the LD avoidance test (Figure 2L), revealed an anxiogenic effect of PNCNO treatment in bigenic

bioRxiv preprint doi: https://doi.org/10.1101/2020.02.19.956060; this version posted February 20, 2020. The copyright holder for this preprint (which was not certified by peer review) is the author/funder. All rights reserved. No reuse allowed without permission.

adult male mice, with a significant decrease in the number of entries to the light box (Figure 2M, $p = 0.04$) and a trend towards a decrease in the time spent in the light box (Figure 2N, $p = 0.07$). We then evaluated the influence of chronic CNO-mediated hM3Dq DREADD activation of forebrain excitatory neurons in the early postnatal window on despair-like behavior in adulthood using the FST (Figure 2O). We observed increased despair-like behavior in CamKIIα-tTA::TetO-hM3Dq bigenic adult male mice with a history of PNCNO treatment, as noted by a significant increase in the time spent immobile in the FST (Figure 2P, $p = 0.02$). Taken together, these results indicate that chronic CNO-mediated hM3Dq DREADD activation of CamKIIα-positive forebrain excitatory neurons during the early postnatal window results in long-lasting increases in anxiety- and despair-like behavior in adult male mice.

Following this, we sought to ascertain whether chronic CNO-mediated hM3Dq DREADD activation of CamKIIα-positive forebrain excitatory neurons during the early postnatal window, evokes a similar anxiogenic and despair-like behavioral phenotype in adult female mice (Figure 2 – figure supplement 3A). Bigenic adult female mice with a history of PNCNO treatment exhibited enhanced anxiety-like behavior on the OFT and EPM tests. In the OFT we noted a significant decrease in percent distance travelled in the center (Figure 2 – figure supplement 3B, C, $p = 0.01$), with no change observed in other measures (Figure 2 – figure supplement 3D-F). In the EPM, bigenic adult female mice with a history of PNCNO treatment, showed a significant decrease in the percent distance travelled (Figure 2 – figure supplement 3G, H, $p = 0.04$) and the percent time spent in the open arms (Figure 2 – figure supplement 3I, $p = 0.004$) as compared to their vehicle-treated controls, with no difference observed on other measures (Figure 2 – figure supplement 3J, K). PNCNO-treated bigenic adult female mice did not show any change in anxiety-like behavior on the LD avoidance test (Figure 2 – figure supplement 3L-N). PNCNO-treated bigenic adult female mice did not show any change in despair-like behavior assessed on the FST (Figure 2 – figure supplement 3O, P). Taken together, these results indicate that chronic CNO-mediated hM3Dq DREADD activation of forebrain excitatory neurons during the early postnatal window results in long-lasting increases in both anxiety- and despair-like behavior in adult male mice, whereas it evokes a persistent increase in anxiety-, but not despair-like behavior, in adult female mice. Henceforth, all our studies to assess the behavioral, metabolic, molecular and electrophysiological influence of chronic CNO-mediated hM3Dq DREADD activation of forebrain excitatory neurons during the early postnatal window have been restricted to male mice.

bioRxiv preprint doi: https://doi.org/10.1101/2020.02.19.956060; this version posted February 20, 2020. The copyright holder for this preprint (which was not certified by peer review) is the author/funder. All rights reserved. No reuse allowed without permission.

Chronic chemogenetic activation of CamKIIα-positive forebrain excitatory neurons during the early postnatal window does not influence novel object recognition memory and repetitive behavior in adult male mice

We next sought to determine the influence of chronic CNO-mediated hM3Dq DREADD activation of CamKIIα-positive forebrain excitatory neurons during the early postnatal window on cognitive performance and stereotypic behavior. We subjected CamKIIα-tTA::TetO-hM3Dq bigenic adult male mice, with a history of PNCNO treatment, to the novel object recognition test (Figure 2 – figure supplement 4A-C) and the marble burial test (Figure 2 – figure supplement 5A, B). With reference to object discrimination memory, we noted no change in the discrimination index, frequency of interaction and time spent with the novel object (Figure 2 – figure supplement 4D-F) across treatment groups. There was no object exploration bias in the PNCNO or vehicle-treated control groups (Figure 2 – figure supplement 4G). Interestingly, we did note a reduction in total object exploration time in the PNCNO-treated cohort (Figure 2 – figure supplement 4H, $p = 0.02$), which has been suggested to be a measure of enhanced anxiety-like behavior[54,55]. Further, we observed no change in stereotypic behavior on the marble burial test, with no difference in the number of marbles buried by the PNCNO or vehicle-treated bigenic adult male mice (Figure 2 – figure supplement 5A-C). Our observations indicate that chronic CNO-mediated hM3Dq DREADD activation of CamKIIα-positive forebrain excitatory neurons during the early postnatal window does not influence object discrimination memory or repetitive behavior in CamKIIα-tTA::TetO-hM3Dq bigenic adult male mice.

Chronic CNO administration during the early postnatal window does not influence anxiety- and despair-like behavior in genotype-control or background strain, adult male mice

Considering the evidence that CNO metabolites can produce off-target behavioral effects[56,57], we designed two sets of control experiments which assessed the influence of postnatal CNO administration in genotype-control or background strain mouse pups, and the resultant effects on the programming of adult anxiety- and despair-like behavior. First, we administered CNO (1 mg/kg) or vehicle to genotype-control mouse pups, single positive for either CamKIIα-tTA or TetO-hM3Dq once daily from P2 to P14 (Figure 2 – figure supplement 6A). Following a three month washout period post cessation of CNO treatment, we assayed these mice for anxiety and depressive-like behavior. We did not observe any difference in anxiety-like behavior in the OFT (Figure 2 – figure supplement 6B-E) in the PNCNO-treated

bioRxiv preprint doi: https://doi.org/10.1101/2020.02.19.956060; this version posted February 20, 2020. The copyright holder for this preprint (which was not certified by peer review) is the author/funder. All rights reserved. No reuse allowed without permission.

genotype-control cohort as compared to vehicle-treated controls. We did note a small, but significant decrease in total distance travelled in the OFT arena (Figure 2 – figure supplement 6F, $p = 0.03$) in the PNCNO-treated genotype-control group. Behavioral analysis on the EPM indicated no change in anxiety-like behavior in adult genotype-control mice with a history of PNCNO treatment (Figure 2 – figure supplement 6G-K). In addition, we did not observe any change in anxiety-like behavior in the LD avoidance test (Figure 2 – figure supplement 6L-N) as a consequence of PNCNO treatment in genotype-control mice. Despair-like behavior was also unchanged across treatment groups, indicating that CNO treatment in genotype-control mice during the postnatal window does not alter behavior on the FST (Figure 2 – figure supplement 6O, P).

The second control experiment to rule out potential off-target effects of chronic postnatal CNO treatment was performed in the background strain (C57BL/6J). C57BL/6J mouse pups received oral administration of CNO (1 mg/kg) or vehicle once daily from P2 to P14, followed by behavioral testing commencing three months post cessation of the CNO treatment regime (Figure 2 – figure supplement 7A). To assess anxiety-like behavior C57BL/6J adult male mice with a history of PNCNO treatment were tested on the OFT, EPM, and LD avoidance test. We did not observe any change in anxiety-like behavior in the OFT (Figure 2 – figure supplement 7B-F), EPM (Figure 2 – figure supplement 7G-K) and the LD avoidance test (Figure 2 – figure supplement 7L-N) in the PNCNO-treated C57BL/6J adult male mice as compared to their vehicle-treated controls. Despair-like behavior, as assessed by immobility time on the FST was also unchanged across treatment groups, indicating no effect of postnatal CNO treatment in the C57BL/6J background strain (Figure 2 – figure supplement 7O, P). Collectively, these control experiments indicate postnatal CNO administration does not evoke off-target effects that influence anxiety- and despair-like behavior.

Chronic chemogenetic activation of CamKIIα-positive forebrain excitatory neurons during the juvenile window or in adulthood does not evoke any long-lasting changes in anxiety- and despair-like behavior

Given we observed that chronic CNO-mediated hM3Dq DREADD activation of CamKIIα-positive forebrain excitatory neurons in the early postnatal window can program persistent changes in anxiety- and despair-like behavior, we next sought to ascertain whether the temporal window in which this perturbation is performed is critical to the establishment of these long-lasting behavioural changes. To address this question, we used chronic CNO-

bioRxiv preprint doi: https://doi.org/10.1101/2020.02.19.956060; this version posted February 20, 2020. The copyright holder for this preprint (which was not certified by peer review) is the author/funder. All rights reserved. No reuse allowed without permission.

mediated hM3Dq DREADD activation of CamKIIα-positive forebrain excitatory neurons in two distinct temporal windows, namely juvenile life (P28-40) and adulthood. The time duration and dose of CNO treatment was maintained constant across the postnatal, juvenile, and adult treatment paradigms.

CamKIIα-tTA::TetO-hM3Dq bigenic juvenile male mice received CNO (1 mg/kg; JCNO) via oral administration once daily from P28-P40 (Figure 3A; Figure 3 – figure supplement 1A). Following a washout period, we subjected bigenic adult male mice with a history of JCNO treatment to behavioral tests for anxiety- and despair-like behavior. We observed no change in anxiety-like behavior in JCNO-treated mice in the OFT (Figure 3B), with no difference noted for the percent distance travelled in the center (Figure 3C), percent time spent in the center (Figure 3D), number of entries to the center (Figure 3 – figure supplement 1B) and the total distance traversed in the OFT arena (Figure 3 – figure supplement 1C). Behavioral testing on the EPM (Figure 3E) revealed no influence of JCNO treatment on anxiety-like behavior, with no difference noted for the percent distance travelled in the open arms (Figure 3F), percent time spent in the open arms (Figure 3G), number of entries to the open arms (Figure 3 – figure supplement 1D), and total distance travelled in the EPM arena (Figure 3 – figure supplement 1E). Further, we did not observe any difference in the number entries to the light box (Figure 3H) and the time spent in the light box (Figure 3I) in JCNO-treated mice on the LD avoidance test. JCNO and vehicle-treated bigenic male mice did not differ on despair-like behavioral measures on the FST, with no significant change in immobility time (Figure 3J). These results indicate that chronic CNO-mediated hM3Dq DREADD activation of CamKIIα-positive forebrain excitatory neurons in the juvenile window does not program any persistent changes in anxiety- and despair-like behavior.

In order to test the effects of chronic CNO-mediated hM3Dq DREADD activation of CamKIIα-positive forebrain excitatory neurons in adulthood, we treated adult CamKIIα-tTA::TetO-hM3Dq bigenic male mice (3-4 months of age) with CNO (1 mg/kg; i.p.; ACNO) or vehicle once daily for thirteen days (Figure 3K; Figure 3 – figure supplement 1F), following which we performed behavioral assays. Behavioral testing was carried out at two time windows of the treatment regime. The first round of behavioral testing was conducted during and soon after the cessation of CNO treatment to assess any immediate consequences on anxiety-like behavior (Figure 3 – figure supplement 2A). The second phase of behavioral testing commenced after a three-month washout period to assess long-lasting consequences of chronic

bioRxiv preprint doi: https://doi.org/10.1101/2020.02.19.956060; this version posted February 20, 2020. The copyright holder for this preprint (which was not certified by peer review) is the author/funder. All rights reserved. No reuse allowed without permission.

CNO-mediated hM3Dq DREADD activation of forebrain excitatory neurons in adulthood on anxiety- and despair-like behavior (Figure 3K; Figure 3 – figure supplement 1F).

The first phase of behavioral testing involved assays for anxiety-like behavior on the OFT, EPM and LD avoidance test during and soon after the cessation of CNO treatment. OFT was performed on day 8 while the chronic CNO treatment was ongoing, and the EPM and LD avoidance test were carried out on day 15 and day 22 respectively soon after cessation of CNO treatment (Figure 3 – figure supplement 2A). No change in anxiety-like behavior was observed on the OFT (Figure 3 – figure supplement 2B-F), EPM (Figure 3 – figure supplement 2G-K), and LD avoidance test (Figure 3 – figure supplement 2L-N) in the ACNO treatment group, during and soon after the cessation of CNO treatment. In the adult CNO treatment regime we did not subject mice to behavioral testing for despair-like behavior on the FST immediately after treatment, as swimming can serve as a strong stressor[58,59] and we intended to assess for anxiety- and despair-like behavior following a three-month washout period in the same cohort. These findings indicate that chronic CNO-mediated hM3Dq DREADD activation of CamKIIα-positive forebrain excitatory neurons in adulthood does not evoke any change in anxiety-like behavior, during or in the short duration after the cessation of CNO treatment.

The second phase of behavioral testing involved assessing for the long-lasting consequences of chronic CNO-mediated hM3Dq DREADD activation of CamKIIα-positive forebrain excitatory neurons in adulthood, with behavioral tests for anxiety- and despair-like behavior commencing three months post cessation of CNO treatment (Figure 3K; Figure 3 – figure supplement 1F). We did not observe any change in anxiety-like behavior on the OFT in the ACNO-treated bigenic adult male mice (Figure 3L), with no change in the percent distance travelled in center (Figure 3M), percent time spent in the center (Figure 3N), number of entries to the center (Figure 3 – figure supplement 1G), and the total distance travelled in the OFT arena (Figure 3 – figure supplement 1H). Behavioral analysis of the EPM (Figure 3O), indicated that the ACNO-treated group did not differ in the percent distance travelled in the open arms (Figure 3P), percent time spent in the open arms (Figure 3Q), number of entries to the open arms (Figure 3 – figure supplement 1I), and the total distance travelled in the EPM (Figure 3 – figure supplement 1J). Similarly, we did not observe any change in anxiety-like behavior in the LD avoidance test with no difference noted in the number of entries to the light box (Figure 3R) and the time spent in the light box (Figure 3S) across treatment groups. Further, we subjected ACNO and vehicle-treated bigenic adult male mice to the FST to assess for despair-like behavior, and noted no difference in the immobility time (Figure 3T). These

bioRxiv preprint doi: https://doi.org/10.1101/2020.02.19.956060; this version posted February 20, 2020. The copyright holder for this preprint (which was not certified by peer review) is the author/funder. All rights reserved. No reuse allowed without permission.

observations reveal that chronic CNO-mediated hM3Dq DREADD activation of CamKIIα-positive forebrain excitatory neurons in adulthood does not result in any long-lasting consequences in anxiety- and despair-like behavior.

These observations collectively underscore the critical importance of the postnatal window in the long-term programming of anxiety- and despair-like behavior, as chronic CNO-mediated hM3Dq DREADD activation of CamKIIα-positive forebrain excitatory neurons is sufficient to establish persistent changes in these behaviors only when administered during the postnatal window, with no such effect noted when the same chemogenetic activation is performed either in juvenile life or in adulthood.

Chronic chemogenetic activation of CamKIIα-positive forebrain excitatory neurons during the early postnatal window programs impaired sensorimotor gating in adulthood

Given prior evidence that a dysregulation of cortical excitation/inhibition balance during postnatal life contributes to the establishment of endophenotypes linked to schizophrenia[60], we next sought to examine whether chronic CNO-mediated hM3Dq DREADD activation of CamKIIα-positive forebrain excitatory neurons in the early postnatal window influenced sensorimotor gating behavior in adulthood (Figure 4A). In order to assess for sensorimotor gating, we subjected CamKIIα-tTA::TetO-hM3Dq bigenic adult male mice with a history of PNCNO treatment to the pre-pulse inhibition (PPI) test (Figure 4B). We did not observe any significant alterations in the basal startle response across treatment groups (Figure 4C). Strikingly, we noticed a significant PPI deficit at all prepulse tones, with a decline in percent prepulse inhibition to tone (120 dB) following a pre-pulse of + 4 dB (69 dB; Figure 4D, $p = 0.024$), + 8 dB (73 dB; Figure 4D, $p = 0.017$), and + 16 dB (81 dB; Figure 4D, $p = 0.041$, n = 12/ group) above the background noise in PNCNO-treated bigenic adult male mice. These findings indicate that chronic CNO-mediated hM3Dq DREADD activation of CamKIIα-positive forebrain excitatory neurons during the early postnatal window results in long-lasting deficits in sensorimotor gating.

Next, we attempted to understand whether chronic CNO-mediated hM3Dq DREADD activation of CamKIIα-positive forebrain excitatory neurons in the juvenile time window or in adulthood can exert similar long-term effects on sensorimotor gating behavior. CamKIIα-tTA::TetO-hM3Dq bigenic male mice (Juvenile group: P28-40; Adult group: 3-4 months of age) were administered CNO (1 mg/kg) or vehicle treatment once daily for thirteen days (Figure 4 – figure supplement 1A, 2A). Behavioral testing for sensorimotor gating on the PPI

bioRxiv preprint doi: https://doi.org/10.1101/2020.02.19.956060; this version posted February 20, 2020. The copyright holder for this preprint (which was not certified by peer review) is the author/funder. All rights reserved. No reuse allowed without permission.

test (Figure 4 – figure supplement 1B, 2B) commenced post a three-month washout period for both the JCNO and ACNO experiments. We did not observe any significant change in the basal startle response (Figure 4 – figure supplement 1C, 2C) in either the JCNO or ACNO treatment groups as compared to their respective vehicle-treated controls. Further, we noted no significant difference in percent PPI in the JCNO or ACNO bigenic adult male mice to a 120 dB tone at all prepulse tones above the background noise (Figure 4 – figure supplement 1D, 2D).

These behavioral experiments reveal that chronic CNO-mediated hM3Dq DREADD activation of CamKIIα-positive forebrain excitatory neurons programs long-lasting changes in sensorimotor gating when the hM3Dq DREADD activation is performed in the postnatal window, but not in either the juvenile time window or in adulthood.

Chronic chemogenetic activation of CamKIIα-positive forebrain excitatory neurons during the early postnatal window results in long-lasting alterations in neuronal metabolic rate in the hippocampus and cortex.

Dysregulation of glutamatergic and GABAergic neurotransmission within forebrain neurocircuitry, including the hippocampus and several cortical regions, is thought to causally contribute to the pathogenesis of several mood-related disorders including anxiety, major depression, and schizophrenia[61–64]. In particular, metabolic dysfunction of glutamate and GABA systems are considered to be important endophenotypes of mood-related disorders[65–68]. Hence, we next sought to investigate the effects of chronic CNO-mediated hM3Dq DREADD activation of CamKIIα-positive forebrain excitatory neurons during the early postnatal window on the metabolic activity in glutamatergic and GABAergic neurons in the hippocampus and cortex in adulthood. We orally administered CNO (PNCNO; 1 mg/kg) or vehicle to CamKIIα-tTA::TetO-hM3Dq bigenic mouse pups once daily from P2-P14, and performed metabolic analysis in adulthood using a trace approach by infusing [1,6-$^{13}C_2$]glucose (Figure 5A; Figure 5 – figure supplements 1, 2A, 3A). [1,6-$^{13}C_2$]Glucose is transported and metabolized in the brain to $Pyruvate_{C3}$ via glycolysis. The $pyruvate_{C3}$ is subsequently oxidized through the TCA cycles of glutamatergic and GABAergic neurons, and astrocytes to produce ^{13}C labelled metabolites (Figure 5 – figure supplement 1). The ^{13}C labeling of brain metabolites was measured in ^{1}H-[^{13}C]-NMR spectra of brain tissue extracts. The metabolic rate of glucose oxidation in excitatory and inhibitory neurons was determined by using the three-compartment metabolic rate model [69–71].

bioRxiv preprint doi: https://doi.org/10.1101/2020.02.19.956060; this version posted February 20, 2020. The copyright holder for this preprint (which was not certified by peer review) is the author/funder. All rights reserved. No reuse allowed without permission.

First, we measured the concentration of different metabolites in the hippocampus and cortex from the non-edited ^{1}H-[^{13}C]-NMR spectrum using [2-^{13}C]glycine as the reference (Figure 5 – figure supplement 2B). We did not observe any significant difference in the levels of glutamate, GABA, glutamine, aspartate, N-acetylaspartate, lactate, inositol, taurine, choline and creatine in the hippocampus and cerebral cortex of PNCNO-treated bigenic adult male mice as compared to their vehicle-treated controls (Table 2). We observed a significant decline in the levels of alanine in the hippocampus (p = 0.047), but not in the cortex, of bigenic adult male mice with a history of PNCNO treatment (Table 2).

Further, we measured the ^{13}C labeling of amino acids from [1,6-$^{13}C_2$]glucose TCA from the ^{13}C edited spectrum (^{13}C only) (Figure 5 – figure supplement 2C). The metabolic rate glucose oxidation in excitatory and inhibitory neurons from the hippocampus and cortex was determined from the ^{13}C label trapped into different amino acids[69,72]. Bigenic adult male mice with a history of PNCNO treatment exhibited an elevated rate of hippocampal glutamate and GABA synthesis from [1,6-$^{13}C_2$]glucose as revealed by a significant increase in the concentration of ^{13}C labelled Glu_{C4} (Figure 5B, p = 0.05), $GABA_{C2}$ (Figure 5E, p = 0.045) and the metabolic rate of glucose oxidation in GABAergic neurons (Figure 5G, p = 0.001) in the hippocampus of PNCNO-treated adult mice. We did not note any difference in the concentration of ^{13}C labelled Glu_{C3} (Figure 5C), $GABA_{C4}$ (Figure 5F), and the metabolic rate of glucose oxidation in glutamatergic neurons (Figure 5D) in the hippocampus. We also observed an overall increase in total neuronal metabolic rate of glucose oxidation in the hippocampus of PNCNO-treated mice as compared to vehicle-treated controls (Figure 5H, p = 0.05). PNCNO-treated mice also showed a trend towards an increase in the concentration of ^{13}C labelled Asp_{C3} (Figure 5 – figure supplement 3C, p = 0.074) with no change noted in the concentration of ^{13}C labelled Gln_{C4} (Figure 5 – figure supplement 3B).

In the cortex, PNCNO-treated adult mice significantly higher levels of ^{13}C-labelled metabolites Glu_{C4} (Figure 5I, p = 0.009), Glu_{C3} (Figure 5J, p = 0.026) from [1,6-$^{13}C_2$]glucose, and the metabolic rate of glucose oxidation in glutamatergic neurons of the cortex (Figure 5K, p = 0.007). We observed a trend towards an increase in levels of ^{13}C-labelled metabolite $GABA_{C2}$ (Figure 5L, p = 0.09) and the metabolic rate of glucose oxidation in GABAergic neurons of the cortex (Figure 5N, p = 0.067), with no change noted in ^{13}C-labelled $GABA_{C4}$ (Figure 5M) in the PNCNO treatment group. There was a significant increase in the overall neuronal metabolic rate of glucose oxidation in the cortex (Figure 5O, p = 0.012) of the PNCNO treatment group.

bioRxiv preprint doi: https://doi.org/10.1101/2020.02.19.956060; this version posted February 20, 2020. The copyright holder for this preprint (which was not certified by peer review) is the author/funder. All rights reserved. No reuse allowed without permission.

Taken together, our data suggests a long-lasting increase in metabolic rate of neuronal glucose oxidation within the hippocampus and cortex following chronic CNO-mediated hM3Dq DREADD activation of CamKIIα-positive forebrain excitatory neurons during the early postnatal window. This suggests a persistent alteration in glutamatergic and GABAergic neurotransmission in the forebrain in adulthood as a consequence of postnatal chronic CNO-mediated hM3Dq DREADD activation of CamKIIα-positive forebrain excitatory neurons. To examine the influence of hM3Dq DREADD activation of forebrain excitatory neurons on neuronal activity, we focused on the hippocampus for the subsequent experiments.

Chronic chemogenetic activation of CamKIIα-positive forebrain excitatory neurons during the early postnatal window results in a long-lasting reduction in neuronal activity-related gene expression, and in c-Fos immunopositive cell numbers, in the adult hippocampus.

In order to investigate the influence of chronic CNO-mediated hM3Dq DREADD activation of CamKIIα-positive forebrain excitatory neurons during the early postnatal window on hippocampal neuronal activity, we adopted two complementary approaches. First, we performed qPCR analysis for neuronal activity and plasticity related gene expression in hippocampi derived from PNCNO and vehicle-treated CamKIIα-tTA::TetO-hM3Dq bigenic adult male mice (Figure 6A; Table 3)[35,73]. We observed a significant decline in the expression of several neuronal activity regulated genes namely *c-Fos*, *Erk1*, *Npas4*, *Staufen1*, *Staufen2*, *Nrxn1*, *Gphn*, *Shank*, *Psd95*, *Fmrp*, and *Synapsin1b* in the hippocampi derived from bigenic adult male mice with a history of PNCNO treatment (Figure 6B). We did not observe any alteration in expression levels of *Nr4a1*, *JunB*, *Nlgn1*, *Nlgn2*, *Mecp2*, and *Mef2C* across treatment groups (Figure 6B). The second approach we took was to perform cell counting analysis of c-Fos immunoreactive cell numbers within the hippocampal subfields namely, CA1, CA3, dentate gyrus (DG), and the hilus of PNCNO and vehicle administered bigenic adult male mice (Figure 6A). We observed a significant decline in c-Fos immunopositive cell number within the CA1 (Figure 6C, $p = 0.004$) and CA3 (Figure 6D, $p = 0.012$) subfields of the hippocampus in the PNCNO treatment group. We noted a trend towards a decline in c-Fos immunopositive cell numbers in the DG subfield (Figure 6E, $p = 0.08$), with no change observed in the hilus (Figure 6F) in the PNCNO group. Collectively, our findings provide evidence that chronic CNO-mediated hM3Dq DREADD activation of CamKIIα-positive forebrain excitatory neurons during the early postnatal window can program a persistent decline in the expression of several neuronal activity and plasticity-associated genes within the

bioRxiv preprint doi: https://doi.org/10.1101/2020.02.19.956060; this version posted February 20, 2020. The copyright holder for this preprint (which was not certified by peer review) is the author/funder. All rights reserved. No reuse allowed without permission.

hippocampus, also accompanied by a reduction in the number of c-Fos immunopositive cells suggestive of an alteration in hippocampal neuronal activity.

Chronic chemogenetic activation of CamKIIα-positive forebrain excitatory neurons during the early postnatal window alters excitatory and inhibitory spontaneous currents in the hippocampi of adult male mice.

Given that our gene expression profiling and c-Fos counting analyses pointed towards a possible change in hippocampal neuronal activity in adulthood as a consequence of postnatal hM3Dq DREADD activation of CamKIIα-positive forebrain excitatory neurons, we next performed electrophysiological studies to assess effects on hippocampal neurotransmission. Whole-cell patch clamp analysis was carried out in the somata of CA1 pyramidal neurons in acute hippocampal slices derived from PNCNO or vehicle-treated CamKIIα-tTA::TetO-hM3Dq bigenic adult male mice (Figure 7A; Figure 7 – figure supplements 1A, 2A). In order to determine the long-lasting influence of chronic hM3Dq DREADD activation of forebrain excitatory neurons during the postnatal window on intrinsic excitability in adulthood, we plotted an input-output curve by injecting increasing step currents and measured the number of action potentials (Figure 7 – figure supplement 1B). No change was noted in the input-output curves obtained from CA1 pyramidal neurons in acute hippocampal slices derived from bigenic adult male mice with as history of PNCNO treatment (Figure 7 – figure supplement 1C). We then measured key intrinsic membrane properties using a hyperpolarizing current step of -100 pA for 500 ms. We did not observe any change in the resting membrane potential (RMP), input resistance (RN), membrane time constant (τ), sag voltage, and accommodation index in CA1 pyramidal neurons of the PNCNO treatment group (Table 4).

Measurement of sPSCs in CA1 pyramidal neurons in acute hippocampal slices derived from PNCNO-treated bigenic adult male mice revealed a significant increase in the cumulative probability of sPSC amplitude characterized by a long-tail in sPSC amplitude event distribution (Figure 7 – figure supplement 1D, E; Figure 7 – figure supplement 2B, C; $p < 0.0001$), accompanied by a significant reduction in the cumulative probability of sPSC interevent intervals (Figure 7 – figure supplement 1F; $p = 0.0009$). Out of the total number of sPSCs analyzed, we noted events with an amplitude greater than 100 pA occurred with a significantly greater frequency in CA1 neurons from the PNCNO treatment group (2.2%), as compared to controls (0.32%). Further, we also observed a small fraction of events (0.66%) with amplitudes

bioRxiv preprint doi: https://doi.org/10.1101/2020.02.19.956060; this version posted February 20, 2020. The copyright holder for this preprint (which was not certified by peer review) is the author/funder. All rights reserved. No reuse allowed without permission.

greater than 250 pA in CA1 pyramidal neurons from the PNCNO-treated cohort, that were not detected in vehicle-treated controls (Figure 7 – figure supplement 2D).

We next sought to distinguish the influence of chronic CNO-mediated hM3Dq DREADD activation of CamKIIα-positive forebrain excitatory neurons during the early postnatal window on hippocampal excitatory and inhibitory neurotransmission in adulthood. We performed whole-cell patch clamp analysis to measure sEPSCs and mEPSCs in CA1 pyramidal neurons in acute hippocampal slices derived from bigenic adult male mice with a history of PNCNO treatment (Figure 7A). We noted a significantly altered sEPSC amplitude distribution in CA1 pyramidal neurons of PNCNO-treated adult male mice (Figure 7B, C; $p < 0.0001$), with a small but significant increase in low amplitude events (< 30 pA), and a significant decline in large amplitude events. Further, we observed a significant decrease in cumulative probability of sEPSC interevent intervals in CA1 pyramidal neurons from the PNCNO treatment group (Figure 7D; $p < 0.0001$). We observed a small, but significantly enhanced cumulative probability of mEPSC amplitude (Figure 7E, F; $p < 0.0001$), with no change observed in the cumulative probability of mEPSC interevent intervals (Figure 7G) in bigenic adult male mice with a history of PNCNO treatment.

To assess effects on hippocampal inhibitory neurotransmission, we measured sIPSCs and mIPSCs in CA1 pyramidal neurons in acute hippocampal slices. We noted a significant increase in the cumulative probability of sIPSC amplitude (Figure 7H, I; $p < 0.0001$), concommitant with a significant reduction in the cumulative probability of sIPSC interevent intervals (Figure 7J; $p < 0.0001$) in bigenic adult male mice with a history of PNCNO treatment. Further, we noted a significant reduction in the cumulative probability of mIPSC amplitude (Figure 7K, L; $p < 0.0001$), with no change noted in the cumulative probability of mIPSC interevent intervals (Figure 7M) in CA1 neurons of PNCNO-treated adult male mice.

Our electrophysiological studies performed on CA1 neurons in acute hippocampal slices of adult male mice with a history of chemogenetic activation of CamKIIα-positive forebrain excitatory neurons during the early postnatal window demonstrates the programming of persistent increases in spontaneous network activity, accompanied by significantly altered hippocampal excitatory and inhibitory neurotransmission.

bioRxiv preprint doi: https://doi.org/10.1101/2020.02.19.956060; this version posted February 20, 2020. The copyright holder for this preprint (which was not certified by peer review) is the author/funder. All rights reserved. No reuse allowed without permission.

Discussion

The major finding of our study is that chronic chemogenetic hM3Dq DREADD activation of CamKIIα-positive forebrain excitatory neurons in the first two weeks of postnatal life is sufficient to program the emergence of enhanced anxiety-, despair- and schizophrenia-like behavior in adult male mice. In contrast, chronic chemogenetic activation of CamKIIα-positive forebrain excitatory neurons in either the juvenile or adult temporal window did not result in any persistent changes in mood-related behavior. Chronic chemogenetic activation of forebrain excitatory neurons in postnatal life also resulted in persistent changes in glutamate/GABA metabolism in the hippocampus and cortex, accompanied by a long-lasting decline in hippocampal activity and plasticity-associated gene expression, and altered hippocampal spontaneous excitatory and inhibitory currents. Given prior reports that several models of early adversity exhibit enhanced signaling via Gq-coupled neurotransmitter receptors in the forebrain[39,40,42,46,48,52], our findings posit that enhanced Gq-signaling mediated activation of forebrain excitatory neurons in the critical temporal window of postnatal life may serve as a putative mechanism to program enhanced risk for adult psychopathology, a hallmark feature of models of early adversity.

Results from multiple rodent models including maternal separation (MS), maternal neglect, and postnatal fluoxetine (PNFlx) indicate that the first two weeks of postnatal life are critical to the long-lasting programming of anxiety- and despair-like behavior[74–77]. Evidence from several of these rodent models suggests enhanced functionality of Gq-coupled neurotransmitter receptors in the forebrain[39,40,42,46,48,52]. Furthermore, pharmacological studies indicate that stimulation of the Gq-coupled 5-HT_{2A} receptor during the early postnatal window can program persistent mood-related behavioral changes[48], and that 5-HT_{2A} receptor blockade overlapping with MS or PNFLx can prevent the emergence of adult anxiety- and despair-like behavior[40,48]. Our study directly tests the role of enhanced Gq signaling mediated activation of forebrain excitatory neurons in the early postnatal window in programming mood-related behavioral changes, and demonstrates that this perturbation when performed in the critical postnatal window, but not in juvenile or adult life, is sufficient to program the emergence of anxiety-, despair- and schizophrenia-like behaviors in adulthood.

Adult male mice with a history PNCNO treatment showed both enhanced anxiety- and despair-like behavior, whereas adult female mice exhibited enhanced anxiety-, but not despair-like behavioral changes. Sexually dimorphic effects of early adversity have been previously

bioRxiv preprint doi: https://doi.org/10.1101/2020.02.19.956060; this version posted February 20, 2020. The copyright holder for this preprint (which was not certified by peer review) is the author/funder. All rights reserved. No reuse allowed without permission.

reported, with females suggested to be resistant to some of the behavioral consequences of early adversity, in particular the programming of despair-like behavioral changes[27,78–82]. Our results suggest the possibility of sexually dimorphic behavioral consequences of early postnatal chemogenetic activation of forebrain excitatory neurons. Our work motivates further investigation to systematically assess whether enhanced Gq signaling driven within forebrain excitatory neurons in postnatal life evokes sex-specific behavioral, metabolic and electrophysiological consequences.

Given that thus far very few studies have used chemogenetic strategies during developmental time windows[83,84], we characterized the consequences of hM3Dq DREADD activation of forebrain excitatory neurons in the postnatal window using both electrophysiological and biochemical approaches. Our observation of hM3Dq DREADD-mediated induction of robust spiking activity in postnatal slices parallels observations made in adulthood[53,85]. Chronic chemogenetic hM3Dq DREADD activation during postnatal life enhanced neuronal activity marker expression in the hippocampus and cortex, as well as increased network activity, enhanced spontaneous excitatory events, and reduced spontaneous inhibitory events in CA1 pyramidal neurons in PNCNO-treated mouse pups. Our studies also indicated that chronic chemogenetic hM3Dq DREADD activation of forebrain excitatory neurons during postnatal life does not impact normal physical growth, developmental milestones such as eye opening or ontogeny of reflex development. We also addressed the possibility that off-target effects of CNO[56,57] may impact our interpretations by extensively addressing effects of postnatal CNO treatment to genotype-control or background strain mouse pups, and noted no change in the emergence of anxiety- or despair-like behaviors in adulthood. These controls are particularly relevant given that very few reports have used chemogenetic perturbations during these early postnatal windows[83,84]. Our results exclude the possibility that the behavioral consequences of chemogenetic hM3Dq DREADD activation of forebrain excitatory neurons arise due to off-target effects of CNO.

We next addressed whether chronic chemogenetic activation of CamKIIα-positive forebrain excitatory neurons in postnatal life recapitulates the effects of early adversity in programming changes in schizophrenia-like behavior[86,87], cognition[88,89] and repetitive behavior[90]. We noted a significant impairment in sensorimotor gating indicated by prepulse inhibition (PPI) deficits, but no change in object memory or stereotypic behavior, in adult mice with a history of PNCNO treatment. Deficient PPI is considered to be a behavioral deficit associated with schizophrenia-like behavior in both genetic or environmental perturbation

bioRxiv preprint doi: https://doi.org/10.1101/2020.02.19.956060; this version posted February 20, 2020. The copyright holder for this preprint (which was not certified by peer review) is the author/funder. All rights reserved. No reuse allowed without permission.

based animal models[87,91–94]. Preclinical genetic models targeting signaling pathways downstream to Gq (PLC-β1$^{-/-}$ mice) exhibit enhanced schizophrenia-like behavior[95]. Further, loss of function of the Gq-coupled mGluR5 receptor in parvalbumin-positive interneurons increased both compulsive behavior and aberrant sensorimotor gating[96]. It is important to note that PPI deficits are also common across various other neuropsychiatric conditions, in addition to schizophrenia[97,98]. Several reports indicate that early adversity during the perinatal window results in PPI impairments in adulthood[87,99–101]. However, both the intensity and timing of the early stressor could program differing outcomes on PPI[87,101,102]. For example, severe maternal deprivation evokes robust PPI deficits, whereas short duration maternal separation has no effect on PPI[87,102]. In this regard, our findings that chemogenetic activation of forebrain excitatory neurons produces an entire spectrum of mood-related behavioral changes, namely enhanced anxiety-, despair- and schizophrenia-like behaviors is suggestive of behavioral endophenotypes noted with the more severe of early stress models[98,103,104].

Our results that the timing of the chronic chemogenetic activation of forebrain excitatory neurons is central to determining consequent changes in mood-related behavior underscores the key importance of 'critical' periods for programming emotionality[105,106]. We observed no change in anxiety-, despair- and schizophrenia-like behaviors in either the juvenile or adult chronic CNO paradigms, indicating that the chemogenetic activation of Gq signaling in forebrain excitatory neurons needs to be performed in the postnatal window (P2-14) to program persistent mood-related behavioral changes. While our studies do not allow us to parcellate out the exact duration of this critical window, it likely encompasses the first two weeks of life. In this regard, both the MS and PNFLx models have critical periods spanning from P2-14 and P2-11 respectively[74,76,77]. These temporal windows overlap with distinct critical periods including the stress hyporesponsive period[107–109], a neurodevelopmental window for the refinement of multiple cortical circuits[1,2], including the maturation of serotonergic afferents to the cortex[110,111], and the tuning of excitation-inhibition balance across cortical microcircuits[34,112,113]. A recent report indicates that hM3Dq DREADD activation of the medial prefrontal cortex during postnatal life can abrogate the influence of maternal separation on oligodendrogenesis and despair-like behavior[83]. However, the use of a pan-neuronal human synapsin promoter to drive the hM3Dq DREADD[83], and the absence of a non-maternal separation cohort makes it difficult to directly compare with our results. Our observations support the view that chemogenetic activation of forebrain excitatory neurons

bioRxiv preprint doi: https://doi.org/10.1101/2020.02.19.956060; this version posted February 20, 2020. The copyright holder for this preprint (which was not certified by peer review) is the author/funder. All rights reserved. No reuse allowed without permission.

from P2-14 could impinge on several key neurodevelopmental processes, thus establishing a substrate for the emergence of perturbed mood-related behaviors in adulthood.

Associated with the long-lasting behavioral changes programmed by chronic DREADD activation of CamKIIα-positive forebrain excitatory neurons, we noted persistent dysregulation of glutamate and GABA neurotransmitter metabolism, a decline in the expression of neuronal activity- and plasticity-related markers, as well as alterations in hippocampal spontaneous excitatory and inhibitory currents. The dysregulation of both glutamate and GABA systems is amongst the key factors in the pathophysiology of several psychiatric disorders including anxiety, depression, and schizophrenia[61,62,64,114,115]. Neuroimaging studies on human subjects with mood-disorders and schizophrenia demonstrate altered volume and resting state functional activity in several forebrain regions, including hippocampus, sensory and frontal cortices[116–118]. A major endophenotype that reflects persistent alterations in neuronal activity in mood-related disorders is the levels and neurometabolic activity of glutamate and GABA, the major excitatory and inhibitory neurotransmitters respectively[61,62,64–68]. Although ^{1}H-MRS has been widely used to examine the levels of these neurotransmitters in both human patients and rodents[119,120], there has been a scarcity of studies to investigate neurometabolic activity, which represent a functional readout of metabolic dynamics in these neurocircuits[121,122]. We employed ^{1}H-[^{13}C]-NMR spectroscopy to measure the metabolic rate of excitatory and inhibitory neurons in conjunction with infusion of [1,6-$^{13}C_2$]glucose[69,70,121,122]. The glutamate hypothesis of mood disorders is based on observations of elevated glutamate levels, associated with changes in glutamate receptors, biosynthetic and regulatory pathways both in human patients and rodent models of anxiety/despair-like behavior and schizophrenia[61,64]. Consistent with this hypothesis, we observed an increase in glucose oxidation in the TCA cycle of glutamatergic neurons in the hippocampus and cortex of adult mice with a history of PNCNO treatment. The rate of neuronal glucose oxidation and neurotransmitter cycle are stoichiometrically coupled during the entire range of brain activity[69,123,124]. Hence, increased neuronal glucose oxidation in PNCNO-treated mice suggests enhanced excitatory and inhibitory neurotransmission. Furthermore, we observed an increase in metabolic rate of hippocampal GABAergic neurons, and a trend towards an increase in this measure in the cortex. It is important to note that though we see an increase in metabolic rate of both glutamatergic and GABAergic neurons, a history of PNCNO treatment does not influence the neurotransmitter pool of glutamate or GABA either in the hippocampus or cortex. While our observations for enhanced glutamatergic metabolic rate in PNCNO-treated animals are

bioRxiv preprint doi: https://doi.org/10.1101/2020.02.19.956060; this version posted February 20, 2020. The copyright holder for this preprint (which was not certified by peer review) is the author/funder. All rights reserved. No reuse allowed without permission.

consistent with clinical and preclinical reports of enhanced glutamate function in mood disorders[61,64], our observations with GABA differ from the reports of reduced GABA levels observed in human subjects and several adult-onset stress based rodent models of mood-related behavioral changes[64,125,126]. Thus far, neurometabolic studies on preclinical models of early life stress, or in patients with a life history of early adversity have not been carried out, making it difficult to directly compare our observations. Collectively, our results suggest that driving enhanced Gq signaling based activation of forebrain excitatory neurons in the postnatal window can evoke persistent dysregulation of amino acid neurotransmitter system metabolism, which may contribute to the long-lasting behavioral changes.

We focused our gene expression and electrophysiological studies on the hippocampus, which has been strongly implicated in mood-related disorders[127–129]. Early stress influences both hippocampal neuronal morphology and plasticity, features that contribute to the behavioral sequelae of early trauma[130–133]. We noted a decreased expression of several activity- and plasticity-related markers within the hippocampus, observed months post the cessation of PNCNO treatment, indicative of persistent molecular changes that ensue from the transient postnatal perturbation. These markers included transcription/translation factors, scaffolding proteins, cell adhesion molecules, and ion channels previously implicated in the regulation of excitation-inhibition balance[35,73]. These results are suggestive of the programming of an altered excitation/inhibition within the hippocampus, which is supported by our electrophysiological observations. Several studies in the past have investigated neurophysiological consequences of early adversity[134]. Previous results indicate persistent dysregulation of signaling via Gq-coupled neurotransmitter receptors (M1 and 5-HT_{2A}) in the neocortex of maternally separated animals[39,46]. Rodent models of rearing in an impoverished environment[135,136], poor maternal care[137–139], neonatal novelty exposure[140], and maternal separation[141–143] are all associated with impairment of hippocampal long term potentiation (LTP). Further, *in vivo* electrophysiological recordings in a model of neonatal isolation indicate a decline in hippocampal outputs[144,145]. Our observations of reduced expression of the activity marker c-Fos in all hippocampal subfields, concomitant with an increase in cumulative probabilities of sIPSC amplitude and a reduction of sIPSC interevent intervals, is indicative of decreased activity in hippocampal networks in keeping with observations in early stress models[134]. Our results support an overall increase in inhibitory neurotransmission within the hippocampi of adult mice with a history of PNCNO treatment. The increase in GABA flux, enhanced metabolic rate of GABAergic neurons, and the shift towards increased inhibition noted in hippocampi of PNCNO-treated mice could arise

bioRxiv preprint doi: https://doi.org/10.1101/2020.02.19.956060; this version posted February 20, 2020. The copyright holder for this preprint (which was not certified by peer review) is the author/funder. All rights reserved. No reuse allowed without permission.

as an adaptive compensation to increased DREADD-mediated excitation during the postnatal window. The effect on hippocampal excitatory neurotransmission on the other hand appears more complex, with an increase in low amplitude and a decline in larger amplitude spontaneous events, along with an increase in the frequency of sEPSC events. This was concomitant with an increase in the cumulative probability of mEPSC amplitude, and a decline in high amplitude mIPSC events. This suggests that the overall decline in inhibition is unlikely to be cell-autonomous, and probably emerges as a consequence of an alteration in the excitatory-inhibitory recurrent network of the hippocampus. Our results do not allow us to distinguish whether the dysfunctional glutamate/GABA metabolism and neurotransmission observed in PNCNO-treated mice serve as instructive/permissive to the development of psychopathology, or simply arise as compensatory adaptations due to increased neuronal activation of forebrain excitatory neurons in the postnatal window. This motivates future experiments to address the influence of driving Gq signaling mediated activation of forebrain excitatory neurons in the postnatal window on excitatory and inhibitory neurotransmission in both cortical and hippocampal networks, as well as the emergence of excitation-inhibition balance within these neurocircuits.

In conclusion, we show that chemogenetic activation of forebrain excitatory neurons during postnatal life evokes a long-lasting increase in anxiety-, despair-, and schizophrenia-like behavior. These behavioral changes are accompanied by a dysregulation of glutamate/GABA metabolism in the cortex and hippocampus, as well as perturbed inhibitory and excitatory neurotransmission within the hippocampus in adulthood. Our perturbation evokes several of pathophysiological features associated with preclinical and clinical studies of early adversity. These findings suggest the intriguing possibility that early adversity could program specific aspects of long-lasting behavioral, molecular, metabolic and functional changes via a modulation of Gq signaling mediated neuronal activation of forebrain excitatory neurons within the critical temporal window of postnatal life.

bioRxiv preprint doi: https://doi.org/10.1101/2020.02.19.956060; this version posted February 20, 2020. The copyright holder for this preprint (which was not certified by peer review) is the author/funder. All rights reserved. No reuse allowed without permission.

Materials and Methods

Animals

The CamKIIα-tTA transgenic mice[146] were gifted by Dr. Christopher Pittenger, Department of Psychiatry, Yale School of Medicine. The TetO-hM3Dq mice (Cat. No. 014093; Tg (TetO-CHRM3*)1Blr/J) and C57BL6/J mice were purchased from Jackson Laboratories, USA. The genotypes of CamKIIα-tTA::TetO-hM3Dq animals were confirmed by PCR-based genotyping analysis. Single-positive animals, positive for either CamKIIα-tTA or TetO-hM3Dq, as well as the background strain C57BL6/J were used for control experiments. The animals were bred in the Tata Institute of Fundamental Research (TIFR) animal house facility. All animals were maintained on a 12-hour light-dark cycle (7 am to 7 pm), with *ad libitum* access to food and water. Slice electrophysiology experiments were carried out at the Jawaharlal Nehru Centre for Advanced Scientific Research (JNCASR), Bengaluru and ^{1}H-[^{13}C]-NMR experiments were carried out at the Centre for Cellular and Molecular Biology (CCMB), Hyderabad. Experimental procedures were carried out as per the guidelines of the Committee for the Purpose of Control and Supervision of Experiments on Animals (CPCSEA), Government of India and were approved by the TIFR, JNCASR, and CCMB animal ethics committees. Care was taken across all experiments to minimize animal suffering and restrict the number of animals used.

Drugs

DREADD agonist, Clozapine-N-oxide (CNO; Cat. No. 4936, Tocris, UK) was used to selectively activate the excitatory DREADD, hM3Dq. CNO was dissolved in 5% aqueous sucrose solution for oral delivery in postnatal and juvenile treatment experiments, and in physiological saline for intraperitoneal delivery in adult-onset treatments. For vehicle treatment, the base solution without the drugs was used. For slice electrophysiology experiments, stock solutions of CNO, 6-Cyano-7-nitroquinoxaline-2,3-dione disodium (CNQX disodium salt; Cat. No. 1045, Tocris, UK), DL-2-Amino-5-phosphonopentanoic acid sodium salt (AP5, Cat. No. 3693, Tocris, UK), (-)-Bicuculline methochloride (Cat. No. 0131, Tocris, UK), and Tetrodotoxin citrate (TTX; Cat. No. ab120055, Abcam, UK) were prepared and aliquots were stored at -20°C. For all slice electrophysiology experiments, acute slice preparations had bath application of drugs in artificial CSF (aCSF) using a perfusion system.

bioRxiv preprint doi: https://doi.org/10.1101/2020.02.19.956060; this version posted February 20, 2020. The copyright holder for this preprint (which was not certified by peer review) is the author/funder. All rights reserved. No reuse allowed without permission.

Western Blotting

To assess HA-tagged hM3Dq DREADD expression in the hippocampus and cortex of CamKIIα-tTA::TetO-hM3Dq bigenic mice on postnatal day 7 (P7), we performed western blotting analysis for the HA antigen. To examine the influence of CNO-mediated hM3Dq DREADD activation on expression levels of neuronal activity markers (c-Fos, phospho-ERK/ERK), we fed a single dose of 1 mg/kg CNO or vehicle to CamKIIα-tTA::TetO-hM3Dq bigenic mouse pups (P7) and sacrificed them 15 minutes post-feeding. In order to examine the effect of chronic CNO-mediated hM3Dq DREADD activation on expression levels of the neuronal activity marker pERK/ERK, we fed 1 mg/kg CNO or vehicle to CamKIIα-tTA::TetO-hM3Dq bigenic mouse pups once daily from P2-P7 and sacrificed them 15 minutes post-feeding on P7. Tissue samples were dissected and stored at -80 °C, and then homogenized in Radioimmunoprecipitation assay (RIPA) buffer (10 mM Tris-Cl (pH 8.0), 1 mM EDTA, 0.5 mM EGTA, 1% Triton X-100, 0.1% sodium deoxycholate, 0.1% SDS, 140 mM NaCl) using a Dounce homogenizer. The lysis buffer contained protease and phosphatase inhibitors (Sigma Aldrich, United States). Following the estimation of protein concentration using the Quantipro BCA assay kit (Sigma-Alrich, United States), equal amounts of lysate were resolved on a 10% sodium dodecyl sulfate polyacrylamide gel and then transferred onto polyvinylidene fluoride membranes. Blots were blocked in 5% milk dissolved in TBST for one hour, and subsequently incubated overnight with respective primary antibodies i.e. rabbit anti-HA (1:1500 in 5% milk, Cat. No. H6908, Sigma-Aldrich, United States), rabbit anti-c-Fos (1:1000 in 5% milk, Cat. No. 2250, Cell Signalling Technology, United States), rabbit anti-actin (1: 10,000 in 5% BSA, Cat. No. AC026, Abclonal Technology, United States), rabbit anti p-ERK1/2 (Thr202/Tyr204) (1:1000 in 5% BSA, Cat. No. 9101, Cell Signalling Technology, United States), or rabbit anti ERK1/2 (1:1000 in 5% BSA, Cat. No. 9102, Cell Signalling Technology, United States). Following subsequent washes, blots were exposed to HRP conjugated goat anti-rabbit secondary antibody (1:6000, Cat. No. AS014, Abclonal Technology, United States) for one hour. Signal was visualized using a GE Amersham Imager 600 (GE life sciences, United States) with a western blotting detection kit (WesternBright ECL, Advansta, United States). Densitometric quantitative analysis was performed using ImageJ software.

Immunofluorescence

HA-tagged hM3Dq DREADD expression in the hippocampus and cortex of CamKIIα-tTA::TetO-hM3Dq bigenic mice (P7) was visualized using immunofluorescent staining for the

bioRxiv preprint doi: https://doi.org/10.1101/2020.02.19.956060; this version posted February 20, 2020. The copyright holder for this preprint (which was not certified by peer review) is the author/funder. All rights reserved. No reuse allowed without permission.

HA epitope. Pups single-positive for either CamKIIα-tTA or TetO-hM3Dq were used as the genotype-controls. Mice were sacrificed by transcardial perfusion with 4 % paraformaldehyde, and 40 μm thick serial coronal sections were obtained using a vibratome (Leica, Germany). Following a permeabilization step at room temperature in phosphate-buffered saline with 0.4% Triton X-100 (PBSTx) for one hour, the sections were then incubated in the blocking solution [1% Bovine Serum Albumin (Roche, Cat. No. 9048-49-1), 5% Normal Goat Serum (Thermoscientific, Cat. No. PI-31873) in 0.4% PBSTx] at room temperature for one hour. The sections were incubated with primary antibody, rabbit anti HA (1:250; Rockland, Cat. No. 600-401-384, USA) for 4 days at 4°C. Following sequential washes with 0.4% PBSTx, the sections were incubated with the secondary antibody, goat anti rabbit IgG conjugated to Alexa Fluor 568 (1:500; Invitrogen, Cat. No. A-11079, USA) for two and a half hours at room temperature, followed by washes with 0.4% PBSTx. Sections were mounted on to slides using Vectashield Antifade Mounting Medium with DAPI (Vector, H-1200, USA) and images were visualized on a LSM5 exciter confocal microscope (Zeiss, Germany).

Experimental Paradigms

Postnatal Treatment

CamKIIα-tTA::TetO-hM3Dq bigenic males were mated with CamKIIα-tTA::TetO-hM3Dq bigenic females. CamKIIα-tTA::TetO-hM3Dq bigenic females were housed as dyads, prior to single-housing commencing one to two days before parturition. Dams were provided with equal amount of paper shredding as nesting material. The litters were randomly assigned to postnatal CNO (PNCNO) treatment and vehicle-treated control groups. To determine the influence of chronic CNO-mediated hM3Dq DREADD activation of CamKIIα-positive forebrain excitatory neurons during the early postnatal window, CamKIIα-tTA::TetO-hM3Dq bigenic mouse pups were fed either CNO (1 mg/kg) or vehicle for thirteen days from postnatal day 2 (P2) to postnatal day 14 (P14) using a micropipette (0.5-10 μL; Cat. No. 3123000020; Eppendorf, Germany). Mouse pups for each postnatal treatment experiment were selected from at least six different dams to minimize any litter-related bias. The weight of the pups was measured daily during the course of treatment. Reflex behavior was assayed at postnatal days 9 and 12, and eye-opening time was observed. The pups were weaned between postnatal days 25-30, and then housed in identical group-housing conditions till adulthood (three months onwards) following which a battery of behavioral assays was performed in order to test for persistent alterations in behavior. Adult male and female mice were assayed for anxiety- and

bioRxiv preprint doi: https://doi.org/10.1101/2020.02.19.956060; this version posted February 20, 2020. The copyright holder for this preprint (which was not certified by peer review) is the author/funder. All rights reserved. No reuse allowed without permission.

depressive-like behavior, and male mice were assessed for effects on object recognition memory, stereotypy, and sensorimotor gating.

In order to control for possible off-target effects of postnatal administration of the hM3Dq DREADD agonist CNO, two different experimental paradigms were performed using mice that did not express the hM3Dq DREADD. The first experiment involved single-positive mouse pups that were positive for either CamKIIα-tTA or TetO-hM3Dq (genotype-control). The second control experiment involved the use of mouse pups from the background strain C57BL6/J. In both the experiments, the litters were randomly assigned to vehicle (Veh) or postnatal CNO (PNCNO) treatment groups. The pups were weaned between postnatal days 25-30, and then housed in identical group-housing conditions till adulthood (three months onwards) following which behavioral analysis was performed. Adult male mice from both control experiments were assayed for anxiety- and depressive-like behavior.

Juvenile Treatment

CamKIIα-tTA::TetO-hM3Dq bigenic male mice were weaned between postnatal days 26-28, and then randomly assigned to vehicle (Veh) or juvenile CNO (JCNO) treatment groups. To determine the influence of chronic CNO-mediated hM3Dq DREADD activation of CamKIIα-positive forebrain excitatory neurons in the juvenile window, CamKIIα-tTA::TetO-hM3Dq bigenic male mice were fed either CNO (1 mg/kg) or vehicle for thirteen days from postnatal day 28 (P28) to postnatal day 40 (P40) using a micropipette (0.5-10 µL; Cat. No. 3123000020; Eppendorf, Germany). Following JCNO treatment, mice were housed in identical group-housing conditions, and tested for anxiety and depressive-like behavior from the age of three months onwards, followed by assessment of sensorimotor gating.

Adult Treatment

Adult CamKIIα-tTA::TetO-hM3Dq bigenic male mice (3-4 months of age) were randomly assigned to either vehicle or adult CNO (ACNO) treatment groups. Mice were taken from at least four different litters to minimize any litter-related bias. CamKIIα-tTA::TetO-hM3Dq bigenic male mice received either vehicle (0.9 % saline) or CNO (1 mg/kg CNO in 0.9 % saline) for thirteen days once daily via intraperitoneal injections. The influence of CNO-mediated hM3Dq DREADD activation on anxiety-like behavior was assessed both during and soon after cessation of the treatment paradigm. Anxiety-like behavior was assessed using the open field test (OFT) performed on day 8 of treatment paradigm, the elevated plus maze (EPM) test performed on day 15, and the light-dark avoidance test carried out on day 22, with the

bioRxiv preprint doi: https://doi.org/10.1101/2020.02.19.956060; this version posted February 20, 2020. The copyright holder for this preprint (which was not certified by peer review) is the author/funder. All rights reserved. No reuse allowed without permission.

treatment paradigm being carried out from day 1 to day 13. To assay for persistent alterations in emotional behavior following chronic CNO-mediated hM3Dq DREADD activation, CamKIIα-tTA::TetO-hM3Dq bigenic male mice treated chronically with either vehicle/CNO as described above, were given a wash-out period of three months and then were assayed for anxiety- and depressive-like behavior, followed by the prepulse inhibition test for sensorimotor gating.

Behavioral Tests

Reflex behaviors

To assess the influence of chronic CNO-mediated hM3Dq DREADD activation of CamKIIα-positive forebrain excitatory neurons in the early postnatal window on the emergence of reflex behaviors, vehicle and PNCNO-treated CamKIIα-tTA::TetO-hM3Dq bigenic mouse pups were assayed for surface righting and negative geotaxis on postnatal day 9 and 12. For surface righting behavior, pups were placed in the home cage upside down, and the time taken to stand on all four paws was noted. For negative geotaxis, the pups were placed on a slanted platform 30° to horizontal, facing the ground and the time taken to face upwards (180° from the initial position) was noted. In addition, the eye-opening time for all mouse pups across postnatal treatment groups was noted.

Anxiety-like behavior

In order to determine the influence of postnatal, juvenile, and adult treatments on anxiety-like behaviors, CamKIIα-tTA::TetO-hM3Dq bigenic mice from the PNCNO (males and females), JCNO (males), and ACNO (males) treatment groups with their respective vehicle-treated controls were subjected to the open field test (OFT), elevated plus maze test (EPM), and light-dark (LD) avoidance test. Further, PNCNO-treated genotype-control and C57BL6/J male mice, with their individual vehicle-treated control groups were also assessed on the OFT, EPM and LD avoidance test.

Open field test

Mice were released into one corner of the open field box (40 cm x 40 cm x 40 cm), the center area (20 cm x 20 cm) of which is considered to be anxiogenic. They were released in different corners of the arena in each trial to remove any side bias. Behavior was recorded for 10 minutes using an overhead analog camera. The captured video was digitized at 25 fps using an analog to digital converter (Startech, UK) and then tracked using an automated on-line

bioRxiv preprint doi: https://doi.org/10.1101/2020.02.19.956060; this version posted February 20, 2020. The copyright holder for this preprint (which was not certified by peer review) is the author/funder. All rights reserved. No reuse allowed without permission.

behavioral analysis software (Ethovision XT 11; Noldus, Netherlands). The total distance travelled, percent distance travelled in the center, percent time spent in the center, and number of entries to the center of the arena were calculated.

Elevated plus maze

The elevated plus maze consisted of a plus-shaped platform with two closed and two open arms (30 cm x 5 cm each) that was elevated 50 cm above the ground. The height of the closed arm walls was 15 cm. The mice were introduced to the arena facing the open arm and behavior was recorded for 10 minutes using an overhead camera. Following digitization at 25 fps, the behavior was tracked online using the automated behavior analysis platform Ethovision XT 11. The total distance travelled, percent distance travelled in the open arms, percent time spent in the open arms, and number of entries to the open arms were calculated to assess anxiety-like behavior.

Light-dark avoidance test

The light-dark box consisted of a rectangular box with a light chamber (25 cm x 25 cm) and a dark chamber (15 cm x 25 cm) which were connected via a passage (10 cm x 10 cm). The mice were released into the behavioral arena facing the light box following which behavior was recorded for 10 minutes using an overhead camera, digitized at 25 fps. The time spent and number entries in the light box were then manually assessed by an experimenter blind to the experimental treatment groups.

Despair-like behavior

In order to test the effect of postnatal, juvenile, and adult treatments on despair-like behavior, forced swim test (FST) was performed with the PNCNO (males and females), JCNO (males), and ACNO (males) treatment groups. Further, FST was also performed on vehicle/PNCNO-treated genotype-control and C57BL6/J male mice.

Forced swim test

The forced swim test was performed in a transparent cylindrical chamber (30 cm height, outer diameter: 15 cm, inner diameter: 14 cm) filled with 25°C water to a height of 30 cm from the base. The mice were released into the water and behavior was recorded for 6 minutes using a side-mounted webcam (Logitech, Switzerland). The time spent immobile was calculated for

bioRxiv preprint doi: https://doi.org/10.1101/2020.02.19.956060; this version posted February 20, 2020. The copyright holder for this preprint (which was not certified by peer review) is the author/funder. All rights reserved. No reuse allowed without permission.

a duration of five minutes, with the first minute discarded from the analysis by an experimenter blind to the experimental treatment groups.

Sensorimotor gating

To determine the influence of chronic CNO-mediated hM3Dq DREADD activation of CamKIIα-positive forebrain excitatory neurons during the early postnatal window on sensorimotor gating behavior, vehicle and PNCNO-treated CamKIIα-tTA::TetO-hM3Dq bigenic male mice were assayed on the prepulse inhibition test performed using a startle and fear conditioning apparatus (Panlab, Spain). In addition, CamKIIα-tTA::TetO-hM3Dq bigenic mice treated with vehicle or CNO during the juvenile (JCNO) or adult (ACNO) window were also assayed for PPI to observe the long-term influence of chronic CNO-mediated hM3Dq DREADD activation of CamKIIα-positive forebrain excitatory neurons during different time epochs on sensorimotor gating behavior. The apparatus comprised of a soundproof chamber with metal grid flooring, a strain gauge coupled to load cells to transduce rapid load change during startle behavior, a load cell amplifier, and a control/interface unit connected to the computer. The load cell was calibrated prior to behavioral testing using a 20 g standard weight by setting the load cell amplifier in DC mode at a gain of 1000. The mouse was placed inside a restrainer to limit spatial location with respect to sound and habituated to the apparatus for four days, followed by habituation for three days with 65 dB background white noise. On the test day, the load cell amplifier was set in AC mode at a gain of 5000. Packwin software (Panlab, Spain) was used to program the protocol and acquire the data. A digital gain of 8 was applied while acquiring the data. The mouse was first habituated to the box for 5 min with 65 dB background white noise which was followed by the first block in which ten tone pulses (120 dB, 1s) were presented to measure basal startle response. In the second block, the mouse was presented with either only tone (120 dB, 1s; x10) or a 100 ms pre-pulse which was either + 4 dB, + 8 dB or + 16 dB higher than the background noise (69/73/81 dB, 1s; x5) which co-terminated with a 1s, 120 dB tone. The percent prepulse inhibition was calculated using the following formula: Percent prepulse inhibition = 100 × (average startle response with only tone − average startle response with the prepulse)/average startle response with only tone.

Novel object recognition

To determine the influence of chronic CNO-mediated hM3Dq DREADD activation of CamKIIα-positive forebrain excitatory neurons during the early postnatal window on object recognition memory, vehicle and PNCNO-treated CamKIIα-tTA::TetO-hM3Dq bigenic male

bioRxiv preprint doi: https://doi.org/10.1101/2020.02.19.956060; this version posted February 20, 2020. The copyright holder for this preprint (which was not certified by peer review) is the author/funder. All rights reserved. No reuse allowed without permission.

mice were subjected to the novel object recognition test. Mice were first habituated in the open field box (40 cm x 40 cm x 40 cm) for five minutes, twice a day for three days. On the fourth day, they were exposed to two identical objects (either sand-filled jugs or marble-filled transparent bottles) for ten minutes. Objects were interchangeably used as familiar or novel to avoid any object bias. On the fifth day, the object recognition memory test was performed. The mice were exposed to the familiar objects for five minutes which was replaced by a novel object for the next five minutes. Behavior was recorded using an overhead analog camera, digitized at 25 fps using an analog to digital converter (Startech, UK), and then tracked online using the automated behavior analysis software Ethovision XT 11. The discrimination index was calculated as the ratio of time spent exploring the novel object to the total time spent exploring both the novel and familiar object.

Marble burial

To determine the influence of chronic CNO-mediated hM3Dq DREADD activation of CamKIIα-positive forebrain excitatory neurons during the early postnatal window on repetitive behavior (stereotypy), vehicle and PNCNO-treated CamKIIα-tTA::TetO-hM3Dq bigenic male mice were tested on the marble burial test. The test mice were placed in a cage (30 cm x 15 cm) where twelve marbles were distributed at an equal interval of ~6 cm on a 4 cm deep bedding material (corn cob). The mice were then allowed to explore the arena for thirty minutes and the number of marbles buried were assessed by three different experimenters, blind to the experimental treatment groups. Marbles with more than two-thirds of the marble not visible above the surface were considered to be buried. The number of marbles buried per mouse was expressed as the average of the values observed by the three experimenters.

Neurometabolic analysis in hippocampus and cerebral cortex

To determine the influence of chronic CNO-mediated hM3Dq DREADD activation of CamKIIα-positive forebrain excitatory neurons during the early postnatal window on neurometabolism in the hippocampus and cerebral cortex of vehicle and PNCNO-treated CamKIIα-tTA::TetO-hM3Dq bigenic male mice, the ^{13}C labeling of brain metabolites were measured in tissue extracts using ^{1}H-[^{13}C]-NMR spectroscopy following infusion of [1,6-$^{13}C_2$]glucose.

bioRxiv preprint doi: https://doi.org/10.1101/2020.02.19.956060; this version posted February 20, 2020. The copyright holder for this preprint (which was not certified by peer review) is the author/funder. All rights reserved. No reuse allowed without permission.

Infusion of [1,6-$^{13}C_2$]Glucose

Vehicle and PNCNO-treated adult CamKIIα-tTA::TetO-hM3Dq bigenic male mice were subjected to 6 hours of fasting, and briefly restrained for the cannulation of the tail-vein to infuse ^{13}C labeled [1,6-$^{13}C_2$]glucose. [1,6-$^{13}C_2$]Glucose (ISOTEC, Miamisburg, United States) dissolved in deionized water (0.225 mol/L) was first administered as a bolus followed by an exponentially decreasing infusion rate for 2 min. Blood was withdrawn via retro-orbital bleeding under mild chloroform anesthesia just before the end of the experiment, centrifuged, and the plasma was collected and frozen in liquid N_2, and subsequently stored at -80°C. Exactly 6 min following the start of infusion, mice were sacrificed by Focused Micorwave Beam Irradiation (4KW for 0.94 s) in order to instantly arrest neurometabolic activity using the Muromachi Microwave Fixation System (MMW-05, Muromachi, Japan). The hippocampus and cortex tissues were dissected on ice, snap-frozen in liquid N_2, and stored at -80°C until further processing.

Preparation of brain extract

Metabolites were extracted from brain tissue using a modified protocol described previously[147]. In brief, the frozen hippocampal and cortical tissue samples were homogenized in 3X volume/weight of 0.1 mol/L HCl dissolved in methanol using a motorized homogenizer. [2-^{13}C]Glycine (0.2 µmol, 99 atom %, Cambridge Isotopes, Andover, MA, United States) was added to the homogenate as a concentration reference. Following further homogenization, 6X volume/weight of 90% ice-cold ethanol was added and the tissue was homogenized, which was then centrifuged at 16,000g for 45 min at 4°C. The supernatant was collected and passed through a custom made Chelex column (Biorad, USA). The pH of the extract was adjusted to 7.0, which was followed by lyophilization. The lyophilized powder was dissolved in phosphate-buffered deuterium oxide containing sodium trimethylsilylpropionate (0.25 mmol/L).

NMR analysis of plasma and brain extract

Blood plasma (100 µL) was mixed with deuterium oxide (450 µl) containing sodium formate (1 µmol/L) and then passed through a 10 KDa cutoff centrifugal filter (VWR, Radnor, PA, United States). ^{1}H-NMR spectra were acquired using a 600 MHz spectrometer (Bruker AVANCE II, Karlsruhe, Germany). Percent ^{13}C enrichment of glucose-C1 was calculated by dividing the area of the ^{13}C-coupled satellites by the total area ^{1}H area (^{12}C + ^{13}C) observed at 5.2 ppm. ^{1}H-[^{13}C]-NMR spectra of hippocampal and cortical tissue extracts were recorded as

bioRxiv preprint doi: https://doi.org/10.1101/2020.02.19.956060; this version posted February 20, 2020. The copyright holder for this preprint (which was not certified by peer review) is the author/funder. All rights reserved. No reuse allowed without permission.

described previously[122,148,149]. Briefly, two spin-echo ^{1}H NMR spectra were recorded with an OFF/ON ^{13}C inversion pulse. Free induction decays (FIDs) were zero-filled, apodized to Lorentzian line broadening, Fourier transformed, and phase-corrected. C-13 edited NMR was obtained by subtracting the sub-spectrum obtained with ^{13}C inversion pulse from that acquired without inversion. The concentration of metabolites was calculated by using [2-^{13}C]glycine as the relative standard. Percentage ^{13}C enrichment of the desired metabolites was determined as the ratio of the peak areas of the ^{1}H-[^{13}C]-NMR difference spectrum (^{13}C only) to the non-edited spectrum (^{12}C + ^{13}C). This was further corrected for the natural abundance (1.1%) of ^{13}C.

Estimation of metabolic rate of glucose oxidation

The metabolic rates of excitatory and inhibitory neurons were calculated using ^{13}C label trapped into brain metabolites as described previously[69,72]. The metabolic rate of glucose oxidation by glutamatergic neurons (MR_{Glu}) was calculated using the following formula:

$$MR_{Glu} = 0.5 \times (1/10) \times (1/Glc_{C1}) \times \{0.82[Glu](Glu_{C4} + 2Glu_{C3}) + 0.42[Asp](2Asp_{C3})\}$$

where Glu_{Ci} and Asp_{Ci} are percentage ^{13}C enrichment of glutamate and aspartate, respectively, at the 'i'th carbon during 6-min infusion, Glc_{C1} is the percent labeling of [1,6-$^{13}C_2$]glucose in blood plasma, and [Glu] and [Asp] are the concentrations of glutamate and aspartate, respectively. The metabolic rate of glucose oxidation by GABAergic neurons, MR_{GABA} was calculated by the following formula:

$$MR_{GABA} = 0.5 \times (1/10) \times (1/Glc_{C1}) \times \{0.02[Glu](Glu_{C4} + 2Glu_{C3}) + [GABA](GABA_{C2} + 2GABA_{C4}) + 0.42[Asp](2Asp_{C3})\}$$

$GABA_{Ci}$ is the percentage labeling of GABA at carbon 'i' and [GABA] is the concentration of GABA. The total metabolic rate of glucose oxidation was calculated using the following formula:

$$MR_{Total} = 0.5 \times (1/10) \times (1/Glc_{C1}) \times \{[Glu](Glu_{C4} + 2Glu_{C3}) + [GABA](GABA_{C2} + 2GABA_{C4}) + [Asp](2Asp_{C3}) + [Gln(Gln_{C4})\}$$

Gln_{C4} refers to the percentage ^{13}C labelling of glutamine.

bioRxiv preprint doi: https://doi.org/10.1101/2020.02.19.956060; this version posted February 20, 2020. The copyright holder for this preprint (which was not certified by peer review) is the author/funder. All rights reserved. No reuse allowed without permission.

Quantitative PCR

To determine the influence of chronic CNO-mediated hM3Dq DREADD activation of CamKIIα-positive forebrain excitatory neurons during the early postnatal window on persistent changes in gene expression within the hippocampus, hippocampi derived from vehicle and PNCNO-treated CamKIIα-tTA::TetO-hM3Dq bigenic adult male mice were subjected to qPCR analysis. Vehicle and PNCNO-treated adult CamKIIα-tTA::TetO-hM3Dq bigenic mice were anesthetized by CO_2 inhalation and sacrificed by rapid decapitation. The hippocampi were then dissected in ice-cold PBS, snap-frozen in liquid N_2, and stored at −80°C. RNA extraction was performed using Trizol (TRI reagent, Sigma-Aldrich, USA). The RNA was quantified using a Nanodrop (Thermo Scientific, USA) spectrophotometer followed by reverse transcription reaction to produce cDNA using PrimeScript RT Reagent Kit (Takara, Clonetech, Japan). Specific primers against the genes of interest (Table 3) were designed and qPCR was performed to amplify the genes of interest using the CF96X Real Time System (BioRad, USA). The qPCR data were analyzed using the ΔΔCt method as described previously[150]. Ct value for a particular gene was normalized to the endogenous housekeeping gene GAPDH (Glyceraldehyde 3-phosphate dehydrogenase), which was unchanged across treatment groups.

c-Fos immunohistochemistry and cell counting analysis

To determine the influence of chronic CNO-mediated hM3Dq DREADD activation of CamKIIα-positive forebrain excitatory neurons during the early postnatal window on persistent changes in neuronal activity within the hippocampus, brain sections were subjected to c-Fos immunohistochemistry and cell counting analysis. Vehicle and PNCNO-treated CamKIIα-tTA::TetO-hM3Dq bigenic adult male mice that were naïve for behavioral testing, were sacrificed by transcardial perfusion with 4% paraformaldehyde. Coronal sections of 40 µm thickness were obtained using the vibratome (Leica, Germany). Sections were then blocked at room temperature for 2 hours in 10% horse serum with 0.3% TritonX-100 (made in 0.1M Phosphate buffer) following which they were incubated with rabbit anti-c-Fos antibody (1:1000, Cat no. 2250, Cell Signalling Technology, United States) for 2 days at 4°C. Subsequently, they were subjected to incubation with the secondary antibody (biotinylated goat anti-rabbit, 1:500, Cat no. BA9400, Vector Labs, United States) for 2 hours at room temperature. Signal was amplified using an Avidin-biotin complex based system (Vector lab, Vectastain ABC kit Elite PK1600, United States) and then visualized using Diaminobenzidine tetrahydrochloride substrate (Cat no. D5905, SigmaAldrich, United States).

bioRxiv preprint doi: https://doi.org/10.1101/2020.02.19.956060; this version posted February 20, 2020. The copyright holder for this preprint (which was not certified by peer review) is the author/funder. All rights reserved. No reuse allowed without permission.

An experimenter blind to the treatment groups carried out cell counting of c-Fos immunopositive cells in the hippocampal subfields namely the CA1, CA3, and dentate gyrus (DG) using a brightfield microscope (Zeiss Axioskop 2 plus, Germany) at a magnification of 200X. Eight sections, separated by a periodicity of 200 µm, spanning the rostrocaudal extent of the hippocampus (four dorsal and four ventral) were selected from each mouse. Results are expressed as the number of c-Fos-positive cells per section for each hippocampal subfield.

Electrophysiological studies

In order to determine the influence of CNO-mediated hM3Dq DREADD activation on spiking activity, drug-naive CamKIIα-tTA::TetO-hM3Dq bigenic mouse pups were sacrificed on postnatal day 7 following which current clamp recordings were performed with CNO bath application. To observe the effects of CNO-mediated chronic postnatal hM3Dq DREADD activation of CamKIIα-positive excitatory neurons on hippocampal neurotransmission, CamKIIα-tTA::TetO-hM3Dq bigenic mice pups were treated once daily with CNO or vehicle from postnatal day 2-7 (P2-7) and sacrificed on P7 for whole-cell patch clamp recording. To determine the influence of chronic CNO-mediated hM3Dq DREADD activation of CamKIIα-positive forebrain excitatory neurons during the early postnatal window (P2-14) on hippocampal neurotransmission that persists into adulthood (3-4 months), whole-cell patch clamp recording was performed on acute hippocampal slices derived from PNCNO and vehicle-treated adult CamKIIα-tTA::TetO-hM3Dq bigenic male mice.

Preparation of hippocampal slices

Mice were sacrificed by cervical dislocation in accordance with the guidelines of the Jawaharlal Nehru Centre for Advanced Scientific Research (JNCASR, Bengaluru) Institutional Animal Ethics Committee. The mice were quickly decapitated following which the brain was transferred to ice-cold sucrose cutting solution (189 mM Sucrose, 10 mM D-glucose, 26 mM $NaHCO_3$, 3 mM KCl, 10 mM $MgSO_4.7H_2O$, 1.25 mM NaH_2PO_4, and 0.1 mM $CaCl_2$), bubbled continuously with 95% O_2 and 5% CO_2. The brain was then dissected in a petri dish containing an ice-cold cutting solution, the cerebellum was removed, and glued onto a brain holder before placing in a container filled with ice-cold cutting solution. Horizontal sections (300 µm) were obtained using a vibrating microtome (Leica, VT-1200, Germany) and transferred to a petri dish containing aCSF (124 mM NaCl, 3 mM KCl, 1 mM $MgSO_4.7H_2O$, 1.25 mM NaH_2PO_4, 10 mM D-glucose, 24 mM $NaHCO_3$, and 2 mM $CaCl_2$) at room temperature. The part of the sections containing the hippocampus was gently dissected out and transferred to a nylon mesh

bioRxiv preprint doi: https://doi.org/10.1101/2020.02.19.956060; this version posted February 20, 2020. The copyright holder for this preprint (which was not certified by peer review) is the author/funder. All rights reserved. No reuse allowed without permission.

chamber containing aCSF that was continuously bubbled with 95% O_2 and 5% CO_2 at 37°C. Following a recovery period of 45-60 min at 37°C to ensure a stable electrophysiological baseline response, slices were kept at room temperature and subsequently transferred to the recording chamber as required.

Recording Rig and data acquisition

The slice recording chamber was continuously circulated with aCSF at 1-2 mL min^{-1} using a combination of a peristaltic pump (BT-3001F, longer precision pump Co. Ltd., China) and gravity feed. The aCSF was pre-heated to 34°C using a single channel temperature controller (Cat. No. TC-324C, Warner Instruments, USA) with a feedback temperature control provided through a thermistor submerged in the recording chamber. In addition, an Ag/AgCl wire was submerged in the recording chamber and was used for referencing. The recording electrodes were held at approximately 45° to the vertical and were controlled using a micromanipulator (Cat. No. 1U RACK; Scientifica, UK). The neurons in the slice were visualized using an upright microscope (Slicescope pro 6000 Scientifica, UK) with specialized optics to visualize deep tissue. The recording set up was enclosed in a Faraday cage and placed on an anti-vibration table (Cat. No. 63P-541; TMC, USA). The electrical noise was eliminated by grounding all electrical connections to a single ground point in the amplifier.

Recording electrodes

Borosilicate glass capillaries (Cat. No. 30-0044/ GC120F-10; Harvard apparatus, UK) were used to pull recording electrodes using a horizontal micropipette puller (Cat. No. P97, Sutter Instruments Co., USA). Intracellular patch electrodes (6-8 MΩ) used to record spiking activity, intrinsic properties, spontaneous postsynaptic currents (sPSC), spontaneous excitatory postsynaptic currents (sEPSC), and miniature excitatory postsynaptic currents (mEPSC) were filled with potassium gluconate (KGlu) internal solution (130 mM KGlu, 20 mM KCl, 10 mM HEPES free acid, 0.2 mM EGTA, 0.3 mM GTP-Na salt, 4 mM ATP-Mg salt; osmolarity adjusted to 280-310 mOsm). Intracellular patch electrodes (6-8 MΩ) used to record spontaneous inhibitory postsynaptic currents (sIPSC) and miniature inhibitory postsynaptic currents (mIPSC) were filled with cesium chloride (CsCl) internal solution (120 mM CsCl, 10 mM HEPES free acid, 10 mM EGTA, 5 mM QX314-Br, 4 mM ATP disodium salt, 0.3 mM GTP disodium salt, 4 mM $MgCl_2$, osmolality adjusted to 280-310 mOsm). The microelectrodes were mounted to an electrode holder (Scientifica, UK), which was further mounted to a

bioRxiv preprint doi: https://doi.org/10.1101/2020.02.19.956060; this version posted February 20, 2020. The copyright holder for this preprint (which was not certified by peer review) is the author/funder. All rights reserved. No reuse allowed without permission.

headstage connected to the amplifier. All signals were amplified using a Multiclamp-700B (Molecular Devices, USA).

Whole-cell patch clamp recording

Somata of CA1 pyramidal neurons were patched in order to perform whole-cell patch clamp recording. A small positive pressure was applied to the patch pipette filled with appropriate intracellular recording solution using a mouth-operated syringe which was attached to the pipette holder using air-tight tubing. After setting current and voltage offset to zero, the resistance of the electrode was noted by applying a test voltage step and measuring the resulting current according to Ohm's law. When the pipette tip touched the cell surface which could be confirmed both by the appearance of "dimple shape" under the microscope and a change in resistance, the positive pressure was released. A subsequent negative pressure was applied by a gentle suction leading the pipette to form a tight seal with the somata, indicated by a gigaohm-seal (> 1 GΩ). The slow and fast capacitance were offset followed by the rupturing of the cell membrane by applying gentle suction. The cells with membrane potential more depolarized than -55 mV in adulthood and -45 mV at P7 were not considered. In addition, only cells having a series resistance in the range of 5-25 MΩ during the course of recording were considered.

Recording of spiking activity of CA1 pyramidal neurons following CNO administration at P7 was performed by holding cells in a current clamp mode. The identity of CA1 pyramidal neurons was confirmed qualitatively using the shape of action potential (characterized by the presence of an after-depolarization potential) by injecting a current of up to 2 nA for 2 ms through the patch electrode. A five-minute baseline was recorded followed by bath application of 1 µM for two minutes. The slices were then washed in aCSF and spiking activity was recorded. In order to measure intrinsic membrane properties and input-output characteristics, both at P7 and adulthood, a 500 ms, 7-step hyperpolarizing or depolarizing current (ranging from -100 pA to 180 pA) was injected through the patch electrode at an inter-sweep interval of 10s.

Spontaneous postsynaptic currents (sPSCs) were measured by holding the cell in voltage-clamp mode at -70 mV. sEPSCs were recorded in the presence of 10 µM bicuculline and mEPSCs were recorded in the presence of 1 µM TTX + 10 µM bicuculline, while cells were held in a voltage-clamp mode at -70 mV. Further, sIPSCs were recorded in the presence of 10 µM CNQX + 100 µM AP5 and mIPSCs were recorded in the presence of 1 µM TTX + 10 µM CNQX + 100 µM AP5 in a voltage-clamp mode at -70 mV.

bioRxiv preprint doi: https://doi.org/10.1101/2020.02.19.956060; this version posted February 20, 2020. The copyright holder for this preprint (which was not certified by peer review) is the author/funder. All rights reserved. No reuse allowed without permission.

Analysis of electrophysiology data

Whole-cell patch clamp data were analyzed offline using the Clampfit 10.5 (Molecular Devices, USA) and Mini Analysis program (Synaptosoft Inc., USA). Voltage deflection traces obtained from a 100 pA hyperpolarizing current pulse were used to calculate different intrinsic membrane properties as follows. The input resistance was calculated by applying Ohm's law, R = V/I. Where V = stable state voltage and I = injected current (100 pA). The voltage trace was fitted to a single exponential $Ae^{-t/\tau}$ and the decay constant was measured in order to calculate the membrane time constant (τ_m). Sag voltage was calculated by subtracting the steady-state voltage from the peak negative-going voltage. The accommodation index was calculated as the ratio of the maximum inter-spike interval (including the interval from the last spike to the end of the current injection) to the first inter-spike interval. The number of spikes fired in response to an increasing amplitude of current injection (0-180 pA) was calculated to generate the input-output curve. Amplitude and interevent intervals for all spontaneous currents were calculated by a semi-automated event-detection algorithm using the Mini Analysis program. At least 200 events from identical temporal bins were counted.

Statistics

All experiments had two treatment groups and were subjected to a two-tailed, unpaired Student's t-test using GraphPad Prism (Graphpad Software Inc., USA). One-sample Kolmogorov-Smirnov test was performed to confirm normality. All graphs were plotted using GraphPad Prism (Graphpad Software Inc., USA). Data are expressed as mean ± standard error of the mean (S.E.M) and statistical significance was set at $p < 0.05$. To account for type I errors, the qPCR data were further subjected to the two-stage linear step-up procedure of Benjamini, Krieger and Yekutieli method to calculate false discovery rate (FDR) at 5%. Vehicle and PNCNO treatment groups were subjected to linear regression followed by ANCOVA in order to compare input-output curves and statistical significance was set at $p < 0.05$. For the analysis of spontaneous current data, amplitudes and inter-event intervals of events recorded from vehicle or PNCNO treatment groups were converted to corresponding cumulative probability distributions and then subjected to Kolmogorov-Smirnov two-sample comparison. Statistical significance was set at $p < 0.001$.

bioRxiv preprint doi: https://doi.org/10.1101/2020.02.19.956060; this version posted February 20, 2020. The copyright holder for this preprint (which was not certified by peer review) is the author/funder. All rights reserved. No reuse allowed without permission.

Acknowledgements

We are grateful to Prof. Rishikesh Narayan (Molecular Biophysics Unit, Indian Institute of Science, Bangalore) for his valuable inputs on the manuscript. We thank all members of the Vaidya and Clement Lab for their technical help. We thank Monalisa Ghosh and Manish Biyani from the Patel Lab for their technical support during NMR experiments. We thank TIFR animal Facility personnel and Dr Sachin Atole for technical support.

Author Contributions

Sthitapranjya Pati- Conception and design, acquisition, analysis and interpretation of all data, writing the article

Kamal Saba- acquisition of NMR spectra and analysis

Sonali S. Salvi- animal treatments, acquisition and analysis of behavior data, qPCR and immunohistochemical analysis

Praachi Tiwari – animal treatments, acquisition and analysis of behavior data

Pratik R. Chaudhari – western blotting analysis

Vijaya Verma – acquisition of P7 electrophysiological data

Sourish Mukhopadhyay- animal treatment and acquisition of behavior data

Darshana Kapri - animal treatment and acquisition of behavior data

Shital Suryavanshi – animal breeding and treatments

James P. Clement – design, analysis and interpretation of electrophysiological experiments

Anant B. Patel - design, analysis and interpretation of NMR experiments

Vidita A. Vaidya- Conception and design, analysis and interpretation of all data, writing the article

Competing interests The authors have no competing interests to declare.

Funding Funding support was received via intramural funds from TIFR to V.V.

bioRxiv preprint doi: https://doi.org/10.1101/2020.02.19.956060; this version posted February 20, 2020. The copyright holder for this preprint (which was not certified by peer review) is the author/funder. All rights reserved. No reuse allowed without permission.

References

1. Hensch, T. K. Critical Period Regulation. *Annu. Rev. Neurosci.* **27**, 549–579 (2004).
2. Hensch, T. K. Critical period plasticity in local cortical circuits. *Nat. Rev. Neurosci.* **6**, 877–888 (2005).
3. Bale, T. L. *et al.* Early life programming and neurodevelopmental disorders. *Biological Psychiatry* **68**, 314–319 (2010).
4. Berardi, N., Pizzorusso, T. & Maffei, L. Critical periods during sensory development. *Current Opinion in Neurobiology* **10**, 138–145 (2000).
5. Carr, C. P., Martins, C. M. S., Stingel, A. M., Lemgruber, V. B. & Juruena, M. F. The Role of Early Life Stress in Adult Psychiatric Disorders. *J. Nerv. Ment. Dis.* **201**, 1007–1020 (2013).
6. Kessler, R. C. *et al.* Childhood adversities and adult psychopathology in the WHO world mental health surveys. *Br. J. Psychiatry* **197**, 378–385 (2010).
7. Anda, R. F. *et al.* The enduring effects of abuse and related adverse experiences in childhood. A convergence of evidence from neurobiology and epidemiology. *Eur. Arch. Psychiatry Clin. Neurosci.* **256**, 174–86 (2006).
8. Knuesel, I. *et al.* Maternal immune activation and abnormal brain development across CNS disorders. *Nat. Rev. Neurol.* **10**, 643–660 (2014).
9. Wright, P., Takei, N., Rifkin, L. & Murray, R. M. Maternal influenza, obstetric complications, and schizophrenia. *Am. J. Psychiatry* **152**, 1714–1720 (1995).
10. Glover, V. Annual Research Review: Prenatal stress and the origins of psychopathology: an evolutionary perspective. *J. Child Psychol. Psychiatry* **52**, 356–367 (2011).
11. Heim, C. & Nemeroff, C. B. The role of childhood trauma in the neurobiology of mood and anxiety disorders: Preclinical and clinical studies. *Biological Psychiatry* **49**, 1023–1039 (2001).
12. McEwen, B. S. Mood disorders and allostatic load. *Biological Psychiatry* **54**, 200–207 (2003).
13. Ogle, C. M., Rubin, D. C. & Siegler, I. C. The relation between insecure attachment and posttraumatic stress: Early life versus adulthood traumas. *Psychol. Trauma Theory, Res. Pract. Policy* **7**, 324–332 (2015).
14. Francis, D., Diorio, J., Liu, D. & Meaney, M. J. Nongenomic transmission across generations of maternal behavior and stress responses in the rat. *Science* **286**, 1155–8 (1999).
15. Walker, C.-D. & McCormick, C. M. Development of the Stress Axis: Maternal and Environmental Influences. in *Hormones, Brain and Behavior* 1931–1974 (Elsevier, 2009). doi:10.1016/B978-008088783-8.00061-9
16. Weinstock, M. The long-term behavioural consequences of prenatal stress. *Neurosci. Biobehav. Rev.* **32**, 1073–1086 (2008).
17. Welberg, L. A. M. & Seckl, J. R. Prenatal Stress, Glucocorticoids and the

bioRxiv preprint doi: https://doi.org/10.1101/2020.02.19.956060; this version posted February 20, 2020. The copyright holder for this preprint (which was not certified by peer review) is the author/funder. All rights reserved. No reuse allowed without permission.

Programming of the Brain. *J. Neuroendocrinol.* **13**, 113–128 (2008).

18. Ansorge, M. S., Hen, R. & Gingrich, J. A. Neurodevelopmental origins of depressive disorders. *Current Opinion in Pharmacology* **7**, 8–17 (2007).

19. Ansorge, M. S., Zhou, M., Lira, A., Hen, R. & Gingrich, J. A. Early-life blockade of the 5-HT transporter alters emotional behavior in adult mice. *Science (80-.).* **306**, 879–881 (2004).

20. Liu, D. *et al.* Maternal care, hippocampal glucocorticoid receptors, and hypothalamic-pituitary-adrenal responses to stress. *Science* **277**, 1659–62 (1997).

21. Levine, S. *et al.* Critical Period for Effects of Infantile Experience on Maturation of Stress Response. *Science (80-.).* **129**, 42–43 (1959).

22. Oberlander, T. F., Gingrich, J. A. & Ansorge, M. S. Sustained neurobehavioral effects of exposure to SSRI antidepressants during development: molecular to clinical evidence. *Clin. Pharmacol. Ther.* **86**, 672–7 (2009).

23. Cutler, A. R., Wilkerson, A. E., Gingras, J. L. & Levin, E. D. Prenatal cocaine and/or nicotine exposure in rats: Preliminary findings on long-term cognitive outcome and genital development at birth. *Neurotoxicol. Teratol.* **18**, 635–643 (1996).

24. Sarkar, A. *et al.* Hippocampal HDAC4 contributes to postnatal fluoxetine-evoked depression-like behavior. *Neuropsychopharmacology* **39**, 2221–32 (2014).

25. Suri, D. & Vaidya, V. A. The adaptive and maladaptive continuum of stress responses - a hippocampal perspective. *Rev. Neurosci.* **26**, 415–42 (2015).

26. Kalinichev, M., Easterling, K. W., Plotsky, P. M. & Holtzman, S. G. Long-lasting changes in stress-induced corticosterone response and anxiety-like behaviors as a consequence of neonatal maternal separation in Long–Evans rats. *Pharmacol. Biochem. Behav.* **73**, 131–140 (2002).

27. Leussis, M. P., Freund, N., Brenhouse, H. C., Thompson, B. S. & Andersen, S. L. Depressive-Like Behavior in Adolescents after Maternal Separation: Sex Differences, Controllability, and GABA. *Dev. Neurosci.* **34**, 210–217 (2012).

28. Wilber, A. A., Southwood, C. J. & Wellman, C. L. Brief neonatal maternal separation alters extinction of conditioned fear and corticolimbic glucocorticoid and NMDA receptor expression in adult rats. *Dev. Neurobiol.* **69**, 73–87 (2009).

29. Fish, E. W. *et al.* Epigenetic Programming of Stress Responses through Variations in Maternal Care. *Ann. N. Y. Acad. Sci.* **1036**, 167–180 (2006).

30. Gillespie, C. F., Phifer, J., Bradley, B. & Ressler, K. J. Risk and resilience: Genetic and environmental influences on development of the stress response. in *Depression and Anxiety* **26**, 984–992 (NIH Public Access, 2009).

31. Altieri, S. C. *et al.* Perinatal vs Genetic Programming of Serotonin States Associated with Anxiety. *Neuropsychopharmacology* **40**, 1456–1470 (2015).

32. Gross, C. & Hen, R. The developmental origins of anxiety. *Nature Reviews Neuroscience* **5**, 545–552 (2004).

33. Shah, R., Courtiol, E., Castellanos, F. X. & Teixeira, C. M. Abnormal serotonin levels during perinatal development lead to behavioral deficits in adulthood. *Frontiers in*

bioRxiv preprint doi: https://doi.org/10.1101/2020.02.19.956060; this version posted February 20, 2020. The copyright holder for this preprint (which was not certified by peer review) is the author/funder. All rights reserved. No reuse allowed without permission.

Behavioral Neuroscience **12**, 114 (2018).

34. Sohal, V. S. & Rubenstein, J. L. R. Excitation-inhibition balance as a framework for investigating mechanisms in neuropsychiatric disorders. *Mol. Psychiatry* **24**, 1248–1257 (2019).

35. Gatto, C. L. & Broadie, K. Genetic controls balancing excitatory and inhibitory synaptogenesis in neurodevelopmental disorder models. *Front. Synaptic Neurosci.* **2**, 4 (2010).

36. Gross, C. *et al.* Serotonin1A receptor acts during development to establish normal anxiety-like behaviour in the adult. *Nature* **416**, 396–400 (2002).

37. Richardson-Jones, J. W. *et al.* 5-HT1A Autoreceptor Levels Determine Vulnerability to Stress and Response to Antidepressants. *Neuron* **65**, 40–52 (2010).

38. Goodfellow, N. M., Benekareddy, M., Vaidya, V. A. & Lambe, E. K. Layer II/III of the prefrontal cortex: Inhibition by the serotonin 5-HT1A receptor in development and stress. *J. Neurosci.* **29**, 10094–103 (2009).

39. Benekareddy, M., Goodfellow, N. M., Lambe, E. K. & Vaidya, V. A. Enhanced Function of Prefrontal Serotonin 5-HT2 Receptors in a Rat Model of Psychiatric Vulnerability. *J. Neurosci.* **30**, 12138–12150 (2010).

40. Benekareddy, M., Vadodaria, K. C., Nair, A. R. & Vaidya, V. a. Postnatal serotonin type 2 receptor blockade prevents the emergence of anxiety behavior, dysregulated stress-induced immediate early gene responses, and specific transcriptional changes that arise following early life stress. *Biol. Psychiatry* **70**, 1024–32 (2011).

41. Weisstaub, N. V. *et al.* Cortical 5-HT2A receptor signaling modulates anxiety-like behaviors in mice. *Science (80-.).* **313**, 536–540 (2006).

42. Malkova, N. V., Gallagher, J. J., Yu, C. Z., Jacobs, R. E. & Patterson, P. H. Manganese-enhanced magnetic resonance imaging reveals increased DOI-induced brain activity in a mouse model of schizophrenia. *Proc. Natl. Acad. Sci. U. S. A.* **111**, E2492-500 (2014).

43. Wischhof, L., Irrsack, E., Dietz, F. & Koch, M. Maternal lipopolysaccharide treatment differentially affects 5-HT2A and mGlu2/3 receptor function in the adult male and female rat offspring. *Neuropharmacology* **97**, 275–288 (2015).

44. Genty, J., Nomigni, M. T., Anton, F. & Hanesch, U. The combination of postnatal maternal separation and social stress in young adulthood does not lead to enhanced inflammatory pain sensitivity and depression-related behavior in rats. *PLoS One* **13**, (2018).

45. Lin, T. *et al.* The Impact and Mechanism of Methylated Metabotropic Glutamate Receptors 1 and 5 in the Hippocampus on Depression-Like Behavior in Prenatal Stress Offspring Rats. *J. Clin. Med.* **7**, 117 (2018).

46. Proulx, É., Suri, D., Heximer, S. P., Vaidya, V. A. & Lambe, E. K. Early stress prevents the potentiation of muscarinic excitation by calcium release in adult prefrontal cortex. *Biol. Psychiatry* **76**, 315–23 (2014).

47. Loria, A. S. & Osborn, J. L. Maternal separation diminishes α-adrenergic receptor density and function in renal vasculature from male Wistar-Kyoto rats. *Am. J. Physiol.*

bioRxiv preprint doi: https://doi.org/10.1101/2020.02.19.956060; this version posted February 20, 2020. The copyright holder for this preprint (which was not certified by peer review) is the author/funder. All rights reserved. No reuse allowed without permission.

Physiol. **313**, F47–F54 (2017).

48. Sarkar, A., Chachra, P. & Vaidya, V. A. Postnatal fluoxetine-evoked anxiety is prevented by concomitant 5-HT2A/C receptor blockade and mimicked by postnatal 5-HT2A/C receptor stimulation. *Biol. Psychiatry* **76**, 858–68 (2014).

49. Sargin, D., Jeoung, H. S., Goodfellow, N. M. & Lambe, E. K. Serotonin Regulation of the Prefrontal Cortex: Cognitive Relevance and the Impact of Developmental Perturbation. *ACS Chem. Neurosci.* **10**, 3078–3093 (2019).

50. Lambe, E. K., Fillman, S. G., Webster, M. J. & Weickert, C. S. Serotonin receptor expression in human prefrontal cortex: Balancing excitation and inhibition across postnatal development. *PLoS One* **6**, (2011).

51. Vinkers, C. H., Oosting, R. S., van Bogaert, M. J. V., Olivier, B. & Groenink, L. Early-Life Blockade of 5-HT1A Receptors Alters Adult Anxiety Behavior and Benzodiazepine Sensitivity. *Biol. Psychiatry* **67**, 309–316 (2010).

52. Moreno, J. L. *et al.* Maternal influenza viral infection causes schizophrenia-like alterations of 5-HT2Aand mGlu2 receptors in the adult offspring. *J. Neurosci.* **31**, 1863–1872 (2011).

53. Alexander, G. M. *et al.* Remote control of neuronal activity in transgenic mice expressing evolved G protein-coupled receptors. *Neuron* **63**, 27–39 (2009).

54. Strekalova, T., Spanagel, R., Bartsch, D., Henn, F. A. & Gass, P. Stress-induced anhedonia in mice is associated with deficits in forced swimming and exploration. *Neuropsychopharmacology* **29**, 2007–2017 (2004).

55. Lueptow, L. M. Novel Object Recognition Test for the Investigation of Learning and Memory in Mice. *J. Vis. Exp.* (2017). doi:10.3791/55718

56. Gomez, J. L. *et al.* Chemogenetics revealed: DREADD occupancy and activation via converted clozapine. *Science* **357**, 503–507 (2017).

57. MacLaren, D. A. A. *et al.* Clozapine N-Oxide Administration Produces Behavioral Effects in Long-Evans Rats: Implications for Designing DREADD Experiments. *eNeuro* **3**, ENEURO.0219-16.2016 (2016).

58. Can, A. *et al.* The mouse forced swim test. *J. Vis. Exp.* (2011). doi:10.3791/3638

59. Yankelevitch-Yahav, R., Franko, M., Huly, A. & Doron, R. The forced swim test as a model of depressive-like behavior. *J. Vis. Exp.* **2015**, (2015).

60. Rosen, A. M., Spellman, T. & Gordon, J. A. Electrophysiological endophenotypes in rodent models of schizophrenia and psychosis. *Biological Psychiatry* **77**, 1041–1049 (2015).

61. Sanacora, G., Treccani, G. & Popoli, M. Towards a glutamate hypothesis of depression: An emerging frontier of neuropsychopharmacology for mood disorders. in *Neuropharmacology* **62**, 63–77 (2012).

62. Kendell, S. F., Krystal, J. H. & Sanacora, G. GABA and glutamate systems as therapeutic targets in depression and mood disorders. *Expert Opinion on Therapeutic Targets* **9**, 153–168 (2005).

63. Choudary, P. V. *et al.* Altered cortical glutamatergic and GABAergic signal

bioRxiv preprint doi: https://doi.org/10.1101/2020.02.19.956060; this version posted February 20, 2020. The copyright holder for this preprint (which was not certified by peer review) is the author/funder. All rights reserved. No reuse allowed without permission.

transmission with glial involvement in depression. *Proc. Natl. Acad. Sci. U. S. A.* **102**, 15653–15658 (2005).

64. Duman, R. S., Sanacora, G. & Krystal, J. H. Altered Connectivity in Depression: GABA and Glutamate Neurotransmitter Deficits and Reversal by Novel Treatments. *Neuron* **102**, 75–90 (2019).

65. Veeraiah, P. *et al.* Dysfunctional Glutamatergic and γ-Aminobutyric Acidergic Activities in Prefrontal Cortex of Mice in Social Defeat Model of Depression. *Biol. Psychiatry* **76**, 231–238 (2014).

66. Sekar, S. *et al.* Neuro-metabolite profiles of rodent models of psychiatric dysfunctions characterised by MR spectroscopy. *Neuropharmacology* **146**, 109–116 (2019).

67. Godfrey, K. E. M., Gardner, A. C., Kwon, S., Chea, W. & Muthukumaraswamy, S. D. Differences in excitatory and inhibitory neurotransmitter levels between depressed patients and healthy controls: A systematic review and meta-analysis. *Journal of Psychiatric Research* **105**, 33–44 (2018).

68. Hasler, G. & Northoff, G. Discovering imaging endophenotypes for major depression. *Molecular Psychiatry* **16**, 604–619 (2011).

69. Patel, A. B. *et al.* The contribution of GABA to glutamate/glutamine cycling and energy metabolism in the rat cortex in vivo. *Proc. Natl. Acad. Sci. U. S. A.* **102**, 5588–5593 (2005).

70. Tiwari, V., Ambadipudi, S. & Patel, A. B. Glutamatergic and GABAergic TCA cycle and neurotransmitter cycling fluxes in different regions of mouse brain. *J. Cereb. Blood Flow Metab.* **33**, 1523–1531 (2013).

71. Saba, K. *et al.* Energetics of Excitatory and Inhibitory Neurotransmission in Aluminum Chloride Model of Alzheimer's Disease: Reversal of Behavioral and Metabolic Deficits by Rasa Sindoor. *Front. Mol. Neurosci.* **10**, 323 (2017).

72. Mishra, P. K., Kumar, A., Behar, K. L. & Patel, A. B. Subanesthetic ketamine reverses neuronal and astroglial metabolic activity deficits in a social defeat model of depression. *J. Neurochem.* **146**, 722–734 (2018).

73. Loebrich, S. & Nedivi, E. The function of activity-regulated genes in the nervous system. *Physiological Reviews* **89**, 1079–1103 (2009).

74. Rebello, T. J. *et al.* Postnatal day 2 to 11 constitutes a 5-HT-sensitive period impacting adult mPFC function. *J. Neurosci.* **34**, 12379–12393 (2014).

75. Suri, D. & Vaidya, V. A. The adaptive and maladaptive continuum of stress responses – a hippocampal perspective. *Rev. Neurosci.* **26**, 415–442 (2015).

76. Roque, S., Mesquita, A. R., Palha, J. A., Sousa, N. & Correia-Neves, M. The behavioral and immunological impact of maternal separation: A matter of timing. *Front. Behav. Neurosci.* **8**, 192 (2014).

77. Freund, N., Thompson, B. S., DeNormandie, J., Vaccarro, K. & Andersen, S. L. Windows of vulnerability: Maternal separation, age, and fluoxetine on adolescent depressive-like behavior in rats. *Neuroscience* **249**, 88–97 (2013).

78. Roman, E., Ploj, K. & Nylander, I. Maternal separation has no effect on voluntary

bioRxiv preprint doi: https://doi.org/10.1101/2020.02.19.956060; this version posted February 20, 2020. The copyright holder for this preprint (which was not certified by peer review) is the author/funder. All rights reserved. No reuse allowed without permission.

ethanol intake in female Wistar rats. *Alcohol* **33**, 31–39 (2004).

79. Dimatelis, J. J., Vermeulen, I. M., Bugarith, K., Stein, D. J. & Russell, V. A. Female rats are resistant to developing the depressive phenotype induced by maternal separation stress. *Metab. Brain Dis.* **31**, 109–119 (2016).

80. Lundberg, S., Martinsson, M., Nylander, I. & Roman, E. Altered corticosterone levels and social play behavior after prolonged maternal separation in adolescent male but not female Wistar rats. *Horm. Behav.* **87**, 137–144 (2017).

81. Desgent, S. *et al.* Early-life stress is associated with gender-based vulnerability to epileptogenesis in rat pups. *PLoS One* **7**, (2012).

82. de Melo, S. R., de David Antoniazzi, C. T., Hossain, S. & Kolb, B. Neonatal Stress Has a Long-Lasting Sex-Dependent Effect on Anxiety-Like Behavior and Neuronal Morphology in the Prefrontal Cortex and Hippocampus. *Dev. Neurosci.* **40**, 93–103 (2018).

83. Teissier, A. *et al.* Early-life stress impairs postnatal oligodendrogenesis and adult emotional behaviour through activity-dependent mechanisms. *Mol. Psychiatry* 1–16 (2019). doi:10.1038/s41380-019-0493-2

84. Wong, F. K. *et al.* Pyramidal cell regulation of interneuron survival sculpts cortical networks . *Nature* **557**, 668–673 (2018).

85. Pati, S. *et al.* Chemogenetic activation of excitatory neurons alters hippocampal neurotransmission in a dose-dependent manner. *eNeuro* **6**, (2019).

86. Girardi, C. E. N., Zanta, N. C. & Suchecki, D. Neonatal stress-induced affective changes in adolescent wistar rats: Early signs of schizophrenia-like behavior. *Front. Behav. Neurosci.* **8**, (2014).

87. Ellenbroek, B. A., Van Den Kroonenberg, P. T. J. M. & Cools, A. R. The effects of an early stressful life event on sensorimotor gating in adult rats. *Schizophr. Res.* **30**, 251–260 (1998).

88. Suri, D. *et al.* Early stress evokes age-dependent biphasic changes in hippocampal neurogenesis, Bdnf expression, and cognition. *Biol. Psychiatry* **73**, 658–666 (2013).

89. Naninck, E. F. G. *et al.* Chronic early life stress alters developmental and adult neurogenesis and impairs cognitive function in mice. *Hippocampus* **25**, 309–328 (2015).

90. Malkova, N. V., Yu, C. Z., Hsiao, E. Y., Moore, M. J. & Patterson, P. H. Maternal immune activation yields offspring displaying mouse versions of the three core symptoms of autism. *Brain. Behav. Immun.* **26**, 607–616 (2012).

91. Khan, A. & Powell, S. B. Sensorimotor gating deficits in “two-hit” models of schizophrenia risk factors. *Schizophr. Res.* **198**, 68–83 (2018).

92. Mena, A. *et al.* Reduced prepulse inhibition as a biomarker of schizophrenia. *Front. Behav. Neurosci.* **10**, (2016).

93. Geyer, M. A., Krebs-Thomson, K., Braff, D. L. & Swerdlow, N. R. Pharmacological studies of prepulse inhibition models of sensorimotor gating deficits in schizophrenia: A decade in review. *Psychopharmacology* **156**, 117–154 (2001).

bioRxiv preprint doi: https://doi.org/10.1101/2020.02.19.956060; this version posted February 20, 2020. The copyright holder for this preprint (which was not certified by peer review) is the author/funder. All rights reserved. No reuse allowed without permission.

94. Belforte, J. E. *et al.* Postnatal NMDA receptor ablation in corticolimbic interneurons confers schizophrenia-like phenotypes. *Nat. Neurosci.* **13**, 76–83 (2010).

95. Mcomish, C. *et al.* Phospholipase C-b1 knockout mice exhibit endophenotypes modeling schizophrenia which are rescued by environmental enrichment and clozapine administration. (2007). doi:10.1038/sj.mp.4002046

96. Barnes, S. A. *et al.* Disruption of mGluR5 in parvalbumin-positive interneurons induces core features of neurodevelopmental disorders. *Mol. Psychiatry* **20**, 1161–72 (2015).

97. Powell, S. B., Weber, M. & Geyer, M. A. Genetic models of sensorimotor gating: Relevance to neuropsychiatric disorders. *Curr. Top. Behav. Neurosci.* **12**, 251–318 (2012).

98. Nestler, E. J. & Hyman, S. E. Animal models of neuropsychiatric disorders. *Nat. Neurosci.* **13**, 1161–1169 (2010).

99. Ko, M.-C., Lee, L. J.-H., Li, Y. & Lee, L.-J. Long-term consequences of neonatal fluoxetine exposure in adult rats. *Dev. Neurobiol.* **74**, 1038–1051 (2014).

100. Smith, S. E. P., Li, J., Garbett, K., Mirnics, K. & Patterson, P. H. Maternal immune activation alters fetal brain development through interleukin-6. *J. Neurosci.* **27**, 10695–10702 (2007).

101. Fabricius, K., Wörtwein, G. & Pakkenberg, B. The impact of maternal separation on adult mouse behaviour and on the total neuron number in the mouse hippocampus. *Brain Struct. Funct.* **212**, 403–416 (2008).

102. Ellenbroek, B. A. & Cools, A. R. Early maternal deprivation and prepulse inhibition: The role of the postdeprivation environment. *Pharmacol. Biochem. Behav.* **73**, 177–184 (2002).

103. Bolton, J. L., Molet, J., Ivy, A. & Baram, T. Z. New insights into early-life stress and behavioral outcomes. *Current Opinion in Behavioral Sciences* **14**, 133–139 (2017).

104. Walker, C. D. *et al.* Chronic early life stress induced by limited bedding and nesting (LBN) material in rodents: critical considerations of methodology, outcomes and translational potential. *Stress* **20**, 421–448 (2017).

105. Bock, J., Rether, K., Gröger, N., Xie, L. & Braun, K. Perinatal programming of emotional brain circuits: An integrative view from systems to molecules. *Frontiers in Neuroscience* **8**, (2014).

106. Leonardo, E. D. & Hen, R. Anxiety as a developmental disorder. *Neuropsychopharmacology* **33**, 134–140 (2008).

107. Schmidt, M. *et al.* The postnatal development of the hypothalamic–pituitary–adrenal axis in the mouse. *Int. J. Dev. Neurosci.* **21**, 125–132 (2003).

108. Levine, S. Primary social relationships influence the development of the hypothalamic–pituitary–adrenal axis in the rat. *Physiol. Behav.* **73**, 255–260 (2001).

109. Suchecki, D. Maternal regulation of the infant's hypothalamic-pituitary-adrenal axis stress response: Seymour 'Gig' Levine's legacy to neuroendocrinology. *J. Neuroendocrinol.* **30**, e12610 (2018).

bioRxiv preprint doi: https://doi.org/10.1101/2020.02.19.956060; this version posted February 20, 2020. The copyright holder for this preprint (which was not certified by peer review) is the author/funder. All rights reserved. No reuse allowed without permission.

110. Teissier, A., Soiza-Reilly, M. & Gaspar, P. Refining the role of 5-HT in postnatal development of brain circuits. *Front. Cell. Neurosci.* **11**, (2017).

111. Vitalis, T. & Verney, C. Sculpting Cerebral Cortex with Serotonin in Rodent and Primate. in *Serotonin - A Chemical Messenger Between All Types of Living Cells* (InTech, 2017). doi:10.5772/intechopen.69000

112. Tatti, R., Haley, M. S., Swanson, O. K., Tselha, T. & Maffei, A. Neurophysiology and Regulation of the Balance Between Excitation and Inhibition in Neocortical Circuits. *Biological Psychiatry* **81**, 821–831 (2017).

113. Xue, M., Atallah, B. V. & Scanziani, M. Equalizing excitation-inhibition ratios across visual cortical neurons. *Nature* **511**, 596–600 (2014).

114. Brambilla, P., Perez, J., Barale, F., Schettini, G. & Soares, J. C. GABAergic dysfunction in mood disorders. *Molecular Psychiatry* **8**, 721–737 (2003).

115. Bergink, V., Van Megen, H. J. G. M. & Westenberg, H. G. M. Glutamate and anxiety. *European Neuropsychopharmacology* **14**, 175–183 (2004).

116. Koike, S. *et al.* Reduced but broader prefrontal activity in patients with schizophrenia during n-back working memory tasks: A multi-channel near-infrared spectroscopy study. *J. Psychiatr. Res.* **47**, 1240–1246 (2013).

117. Wolf, N. D. *et al.* Dysconnectivity of multiple resting-state networks in patients with schizophrenia who have persistent auditory verbal hallucinations. *J. Psychiatry Neurosci.* **36**, 366–374 (2011).

118. Kühn, S. & Gallinat, J. Resting-state brain activity in schizophrenia and major depression: A quantitative meta-analysis. *Schizophr. Bull.* **39**, 358–365 (2013).

119. Zieminska, E. *et al.* Glutamate, glutamine and GABA levels in rat brain measured using MRS, HPLC and NMR methods in study of two models of autism. *Front. Mol. Neurosci.* **11**, (2018).

120. Dyke, K. *et al.* Comparing GABA-dependent physiological measures of inhibition with proton magnetic resonance spectroscopy measurement of GABA using ultra-high-field MRI. *Neuroimage* **152**, 360–370 (2017).

121. Patel, A. B. *et al.* Glutamatergic neurotransmission and neuronal glucose oxidation are coupled during intense neuronal activation. *J. Cereb. Blood Flow Metab.* **24**, 972–85 (2004).

122. de Graaf, R. A., Mason, G. F., Patel, A. B., Behar, K. L. & Rothman, D. L. In vivo1H-[13C]-NMR spectroscopy of cerebral metabolism. *NMR Biomed.* **16**, 339–357 (2003).

123. Hyder, F. *et al.* Neuronal-glial glucose oxidation and glutamatergic-GABAergic function. *Journal of Cerebral Blood Flow and Metabolism* **26**, 865–877 (2006).

124. Sibson, N. R. *et al.* Functional energy metabolism: In vivo 13C-NMR spectroscopy evidence for coupling of cerebral glucose consumption and glutamatergic neuronal activity. in *Developmental Neuroscience* **20**, 321–330 (1998).

125. Pilc, A. & Nowak, G. GABAergic hypotheses of anxiety and depression: Focus on GABAB receptors. *Drugs of Today* **41**, 755–766 (2005).

126. Kalueff, A. V. & Nutt, D. J. Role of GABA in anxiety and depression. *Depress.*

bioRxiv preprint doi: https://doi.org/10.1101/2020.02.19.956060; this version posted February 20, 2020. The copyright holder for this preprint (which was not certified by peer review) is the author/funder. All rights reserved. No reuse allowed without permission.

Anxiety **24**, 495–517 (2007).

127. Santos, M. A. O., Bezerra, L. S., Carvalho, A. R. M. R. & Brainer-Lima, A. M. Global hippocampal atrophy in major depressive disorder: A meta-analysis of magnetic resonance imaging studies. *Trends in Psychiatry and Psychotherapy* **40**, 369–378 (2018).

128. Campbell, S. & MacQueen, G. The role of the hippocampus in the pathophysiology of major depression. *Journal of Psychiatry and Neuroscience* **29**, 417–426 (2004).

129. Femenía, T., Gómez-Galán, M., Lindskog, M. & Magara, S. Dysfunctional hippocampal activity affects emotion and cognition in mood disorders. *Brain Research* **1476**, 58–70 (2012).

130. Kim, J. J., Song, E. Y. & Kosten, T. A. Stress effects in the hippocampus: Synaptic plasticity and memory. *Stress* **9**, 1–11 (2006).

131. Fenoglio, K. A., Brunson, K. L. & Baram, T. Z. Hippocampal neuroplasticity induced by early-life stress: Functional and molecular aspects. *Frontiers in Neuroendocrinology* **27**, 180–192 (2006).

132. Maccari, S., Krugers, H. J., Morley-Fletcher, S., Szyf, M. & Brunton, P. J. The consequences of early-life adversity: Neurobiological, behavioural and epigenetic adaptations. *Journal of Neuroendocrinology* **26**, 707–723 (2014).

133. McEwen, B. S., Nasca, C. & Gray, J. D. Stress Effects on Neuronal Structure: Hippocampus, Amygdala, and Prefrontal Cortex. *Neuropsychopharmacology* **41**, 3–23 (2016).

134. Ali, I., Salzberg, M. R., French, C. & Jones, N. C. Electrophysiological insights into the enduring effects of early life stress on the brain. *Psychopharmacology* **214**, 155–173 (2011).

135. Cui, M. *et al.* Enriched environment experience overcomes the memory deficits and depressive-like behavior induced by early life stress. *Neurosci. Lett.* **404**, 208–212 (2006).

136. Brunson, K. L. *et al.* Mechanisms of late-onset cognitive decline after early-life stress. *J. Neurosci.* **25**, 9328–9338 (2005).

137. Bagot, R. C. *et al.* Maternal care determines rapid effects of stress mediators on synaptic plasticity in adult rat hippocampal dentate gyrus. *Neurobiol. Learn. Mem.* **92**, 292–300 (2009).

138. Weaver, I. C. G. *et al.* Epigenetic programming by maternal behavior. *Nat. Neurosci.* **7**, 847–854 (2004).

139. Meaney, M. J. & Szyf, M. Maternal care as a model for experience-dependent chromatin plasticity? *Trends Neurosci.* **28**, 456–463 (2005).

140. Zou, B., Golarai, G., Connor, J. A. & Tang, A. C. Neonatal exposure to a novel environment enhances the effects of corticosterone on neuronal excitability and plasticity in adult hippocampus. *Brain Res. Dev. Brain Res.* **130**, 1–7 (2001).

141. Kehoe, P., Hoffman, J. H., Austin-LaFrance, R. J. & Bronzino, J. D. Neonatal isolation enhances hippocampal dentate response to tetanization in freely moving juvenile male

bioRxiv preprint doi: https://doi.org/10.1101/2020.02.19.956060; this version posted February 20, 2020. The copyright holder for this preprint (which was not certified by peer review) is the author/funder. All rights reserved. No reuse allowed without permission.

rats. *Exp. Neurol.* **136**, 89–97 (1995).

142. Gruss, M., Braun, K., Frey, J. U. & Korz, V. Maternal separation during a specific postnatal time window prevents reinforcement of hippocampal long-term potentiation in adolescent rats. *Neuroscience* **152**, 1–7 (2008).

143. Salzberg, M. *et al.* Early postnatal stress confers enduring vulnerability to limbic epileptogenesisy. *Epilepsia* **48**, 2079–2085 (2007).

144. Bartesaghi, R. Effect of early isolation on the synaptic function in the dentate gyrus and field CA1 of the guinea pig. *Hippocampus* **14**, 482–498 (2004).

145. Bartesaghi, R., Raffi, M. & Ciani, E. Effect of early isolation on signal transfer in the entorhinal cortex-dentate-hippocampal system. *Neuroscience* **137**, 875–890 (2006).

146. Mayford, M. *et al.* Control of memory formation through regulated expression of a CaMKII transgene. *Science* **274**, 1678–83 (1996).

147. Patel, A. B., Rothman, D. L., Cline, G. W. & Behar, K. L. Glutamine is the major precursor for GABA synthesis in rat neocortex in vivo following acute GABA-transaminase inhibition. *Brain Res.* **919**, 207–220 (2001).

148. Saba, K. *et al.* Energetics of excitatory and inhibitory neurotransmission in aluminum chloride model of alzheimer's disease: Reversal of behavioral and metabolic deficits by rasa sindoor. *Front. Mol. Neurosci.* **10**, 323–323 (2017).

149. Bagga, P., Chugani, A. N., Varadarajan, K. S. & Patel, A. B. In vivo NMR studies of regional cerebral energetics in MPTP model of Parkinson's disease: Recovery of cerebral metabolism with acute levodopa treatment. *J. Neurochem.* **127**, 365–377 (2013).

150. Bookout, A. L. & Mangelsdorf, D. J. Quantitative real-time PCR protocol for analysis of nuclear receptor signaling pathways. *Nucl. Recept. Signal.* **1**, nrs.01012 (2003).

bioRxiv preprint doi: https://doi.org/10.1101/2020.02.19.956060; this version posted February 20, 2020. The copyright holder for this preprint (which was not certified by peer review) is the author/funder. All rights reserved. No reuse allowed without permission.

Figures and Figure legends

Figure 1 with 4 supplements

Selective expression and activation of hM3Dq DREADD in CamKIIα-positive forebrain excitatory neurons in CamKIIα-tTA::TetO-hM3Dq bigenic mice during the postnatal window

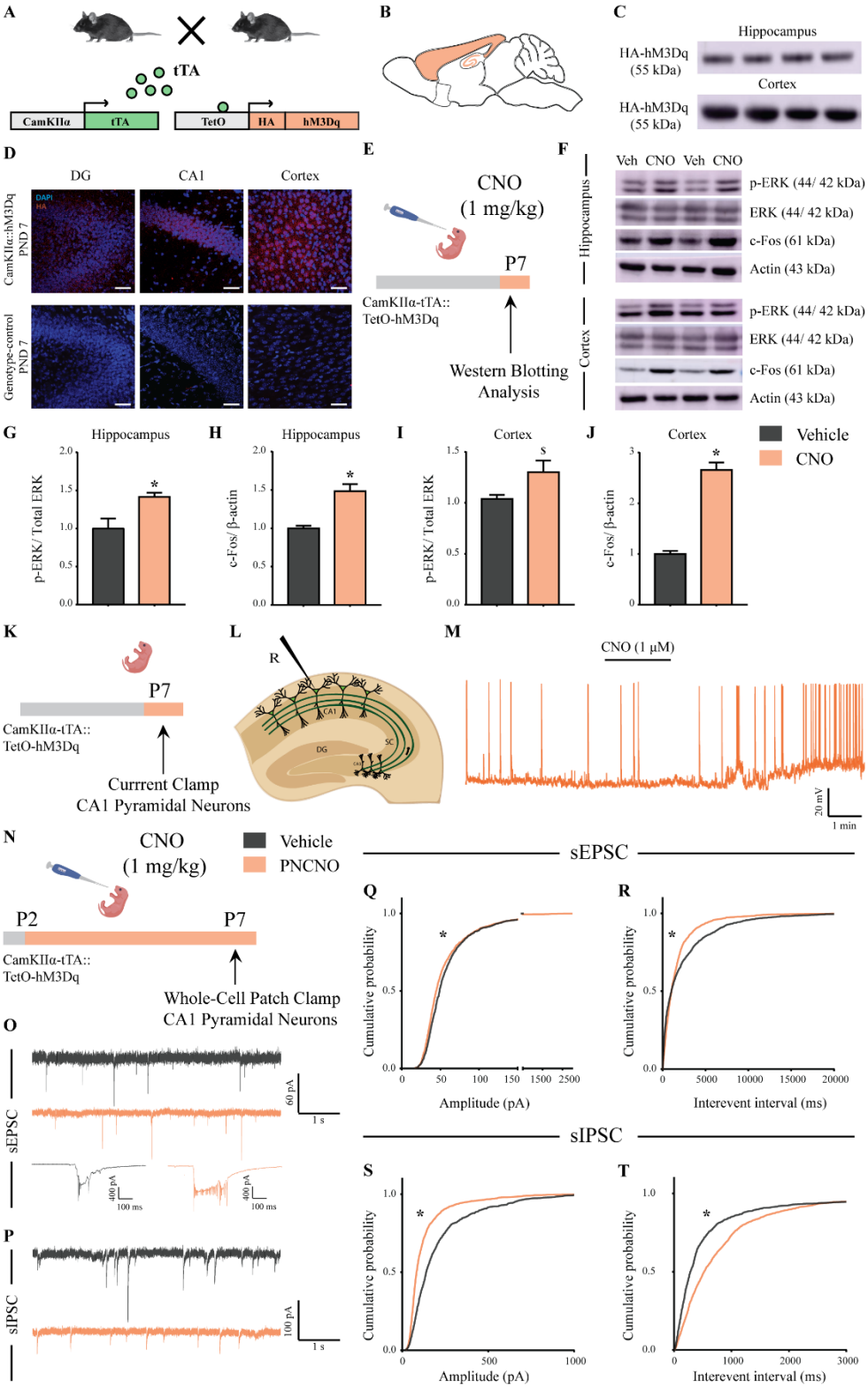

bioRxiv preprint doi: https://doi.org/10.1101/2020.02.19.956060; this version posted February 20, 2020. The copyright holder for this preprint (which was not certified by peer review) is the author/funder. All rights reserved. No reuse allowed without permission.

(A) Shown is a schematic of the experimental strategy for the generation of the bigenic CamKIIα-tTA::TetO-hM3Dq mouse line to selectively drive the expression of the hM3Dq DREADD in the CamKIIα-positive forebrain excitatory neurons. tTA – tetracycline transactivator. (B) Shown is a schematic sagittal view of the mouse brain indicating the region of hM3Dq DREADD expression. (C) Western blots indicate expression of the HA-tag in the hippocampus and the cortex confirming the presence of HA-tagged hM3Dq DREADD (n = 4). (D) Shown are representative confocal images indicating expression of hM3Dq DREADD in the DG, CA1, and cortex as identified by HA immunofluorescence, which was not observed in the genotype-control mice (n = 3 per group). (E) Shown is the experimental paradigm to assess activity-related signalling signatures following acute CNO-mediated hM3Dq DREADD activation of CamKIIα-positive forebrain excitatory neurons at P7. The mice were fed a single dose of either CNO (1 mg/kg) or vehicle and sacrificed 15 minutes later for western blotting analysis (n = 4 per group). (F) Representative western blots indicate the expression of the neuronal activity-related proteins, p-ERK and c-Fos in the hippocampus and cortex of CNO and vehicle-treated CamKIIα-tTA::TetO-hM3Dq bigenic mouse pups. Densitometric quantification revealed a significant CNO-mediated, hM3Dq DREADD activation evoked increase in p-ERK/ ERK (G) and c-Fos (H) expression in the hippocampi of CNO-treated pups as compared to the vehicle-treated controls (n = 4 per group). In the cortex, hM3Dq DREADD activation resulted in a trend towards an increase in p-ERK/ ERK (I) and a significant increase in c-Fos (J) protein levels in the CNO-treated pups. Results are expressed as the mean ± S.E.M. * $p < 0.05$, $^{\$}p = 0.07$ as compared to vehicle-treated controls using the two-tailed, unpaired Student's *t*-test. (K-L) Shown is a schematic of the experimental paradigm for whole-cell patch clamp recording from the somata of CA1 pyramidal neurons at P7 in acute hippocampal slices derived from drug-naive, bigenic CamKIIα-tTA::TetO-hM3Dq mouse pups. R – Recording electrode. (M) Bath application of CNO (1 μM) to acute hippocampal slices resulted in hM3Dq DREADD activation mediated robust spiking activity of CA1 pyramidal neurons (n = 3 cells). (N) Experimental paradigm to assess the effects of chronic CNO-mediated hM3Dq DREADD activation of CamKIIα-positive forebrain excitatory neurons using whole-cell patch clamp recording. CamKIIα-tTA::TetO-hM3Dq bigenic mouse pups were fed either CNO (1 mg/kg) or vehicle from P2 to P7 followed by recording of sEPSCs and sIPSCs. (O) Shown are representative sEPSC traces of vehicle and PNCNO-treated mice at P7. Top traces: examples of small amplitude events. Bottom traces: examples of large amplitude events. (P) Shown are representative sIPSC traces of vehicle and PNCNO-treated mice at P7. (Q) PNCNO-treated mice showed significantly altered cumulative probability of sEPSC amplitude with a small

bioRxiv preprint doi: https://doi.org/10.1101/2020.02.19.956060; this version posted February 20, 2020. The copyright holder for this preprint (which was not certified by peer review) is the author/funder. All rights reserved. No reuse allowed without permission.

decrease at lower amplitudes (<100 pA) and a significant increase in large amplitude events characterized by a long-tail as compared to vehicle-treated controls. (R) PNCNO-treated mice showed a significant decline in the cumulative probability of sEPSC interevent intervals as compared to vehicle-treated controls (n = 7 cells for vehicle; n = 10 cells for PNCNO). PNCNO-treated mice showed a significant decrease in sIPSC amplitude (S), and a concomitant increase in sIPSC interevent intervals (T) as compared to vehicle-treated controls (n = 6 cells for vehicle; n = 8 cells for PNCNO). Results are expressed as cumulative probabilities. * $p <$ 0.001 as compared to PNCNO-treated group using Kolmogorov-Smirnov two-sample comparison.

bioRxiv preprint doi: https://doi.org/10.1101/2020.02.19.956060; this version posted February 20, 2020. The copyright holder for this preprint (which was not certified by peer review) is the author/funder. All rights reserved. No reuse allowed without permission.

Figure 1 – figure supplement 1

Enhanced pERK/ERK expression following chronic postnatal hM3Dq DREADD activation in CamKIIα-positive forebrain excitatory neurons

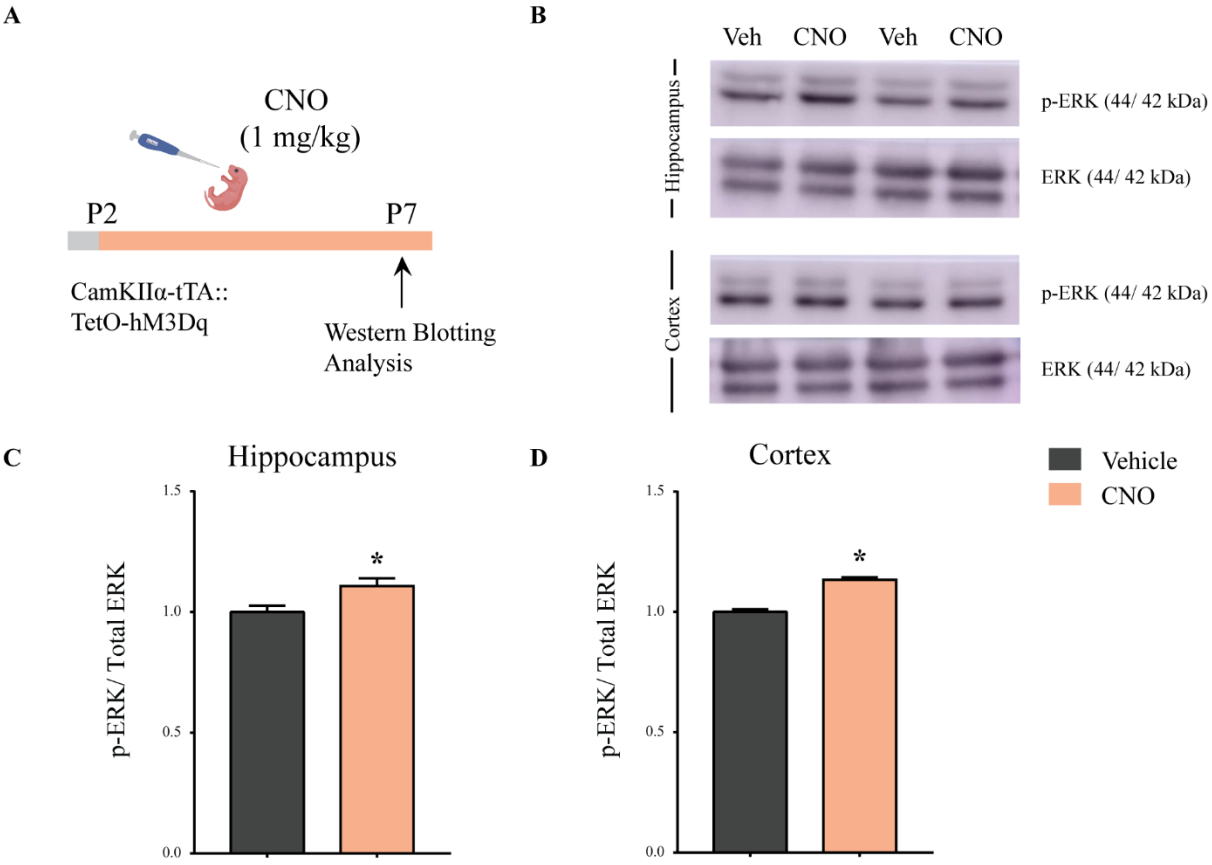

(A) Experimental paradigm to assess the influence of chronic PNCNO-mediated hM3Dq DREADD activation of CamKIIα-positive forebrain excitatory neurons on pERK/ERK expression. CamKIIα-tTA::TetO-hM3Dq bigenic mouse pups were fed either CNO (1 mg/kg) or vehicle from P2 to P7, followed by sacrifice on P7 for western blotting analysis. (B) Representative western blots indicate the expression of the neuronal activity-related protein pERK, as compared to total ERK levels in the hippocampus and cortex of vehicle and chronic PNCNO-treated CamKIIα-tTA::TetO-hM3Dq bigenic mouse pups. Densitometric quantification revealed a significant hM3Dq DREADD activation mediated increase in p-ERK/ ERK in the hippocampus (C) and the cortex (D) of the CNO-treated pups as compared to the vehicle-treated controls. Results are expressed as the mean ± S.E.M. * $p < 0.05$ as compared to vehicle-treated controls (n = 4 per group) using the two-tailed, unpaired Student's *t*-test.

bioRxiv preprint doi: https://doi.org/10.1101/2020.02.19.956060; this version posted February 20, 2020. The copyright holder for this preprint (which was not certified by peer review) is the author/funder. All rights reserved. No reuse allowed without permission.

Figure 1 – figure supplement 2

Spontaneous network activity and intrinsic excitability following chronic postnatal hM3Dq DREADD activation in CamKIIα-positive forebrain excitatory neurons

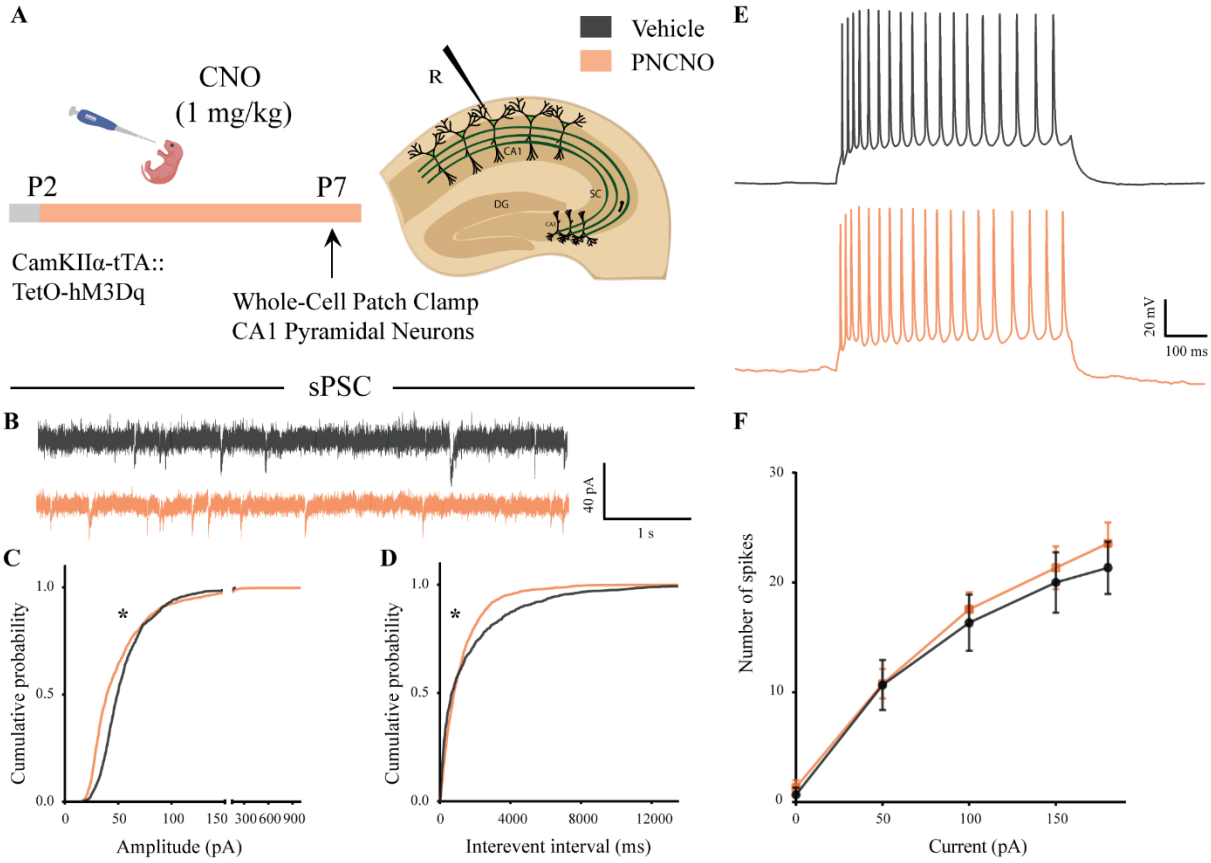

(A) Shown is the experimental paradigm to assess the effects of chronic CNO-mediated hM3Dq DREADD activation of CamKIIα-positive forebrain excitatory neurons using whole-cell patch clamp. CamKIIα-tTA::TetO-hM3Dq bigenic mouse pups were fed either CNO (1 mg/kg) or vehicle from P2 to P7, followed by recording of input-output characteristics and sPSCs. Shown is a schematic of the experimental paradigm for current clamp recording from the somata of CA1 pyramidal neurons at P7. (B) Shown are representative sPSC traces of vehicle and PNCNO-treated mice at P7. (C) PNCNO-treated mice showed significantly altered cumulative probability of sPSC amplitude with a small decrease at lower amplitudes (<100 pA) and a significant increase in large amplitude events characterized by a long-tail as compared to vehicle-treated controls. (D) PNCNO-treated mice showed a significant decline in the cumulative probability of sPSC interevent intervals as compared to vehicle-treated

bioRxiv preprint doi: https://doi.org/10.1101/2020.02.19.956060; this version posted February 20, 2020. The copyright holder for this preprint (which was not certified by peer review) is the author/funder. All rights reserved. No reuse allowed without permission.

controls (n = 7 cells for vehicle; n = 10 cells for PNCNO). Results are expressed as cumulative probabilities. *$p < 0.001$ as compared between vehicle and PNCNO-treated group using Kolmogorov-Smirnov two-sample comparison. (E) Representative traces of spikes generated by CA1 pyramidal neurons following a current injection of 100 pA. (F) No significant change was observed in the input-output characteristics of the PNCNO-treated pups as compared to vehicle-treated controls (n = 6 cells for vehicle; n = 9 cells for PNCNO).

bioRxiv preprint doi: https://doi.org/10.1101/2020.02.19.956060; this version posted February 20, 2020. The copyright holder for this preprint (which was not certified by peer review) is the author/funder. All rights reserved. No reuse allowed without permission.

Figure 1 – figure supplement 3

Distribution of spontaneous network events following chronic postnatal hM3Dq DREADD activation in CamKIIα-positive forebrain excitatory neurons

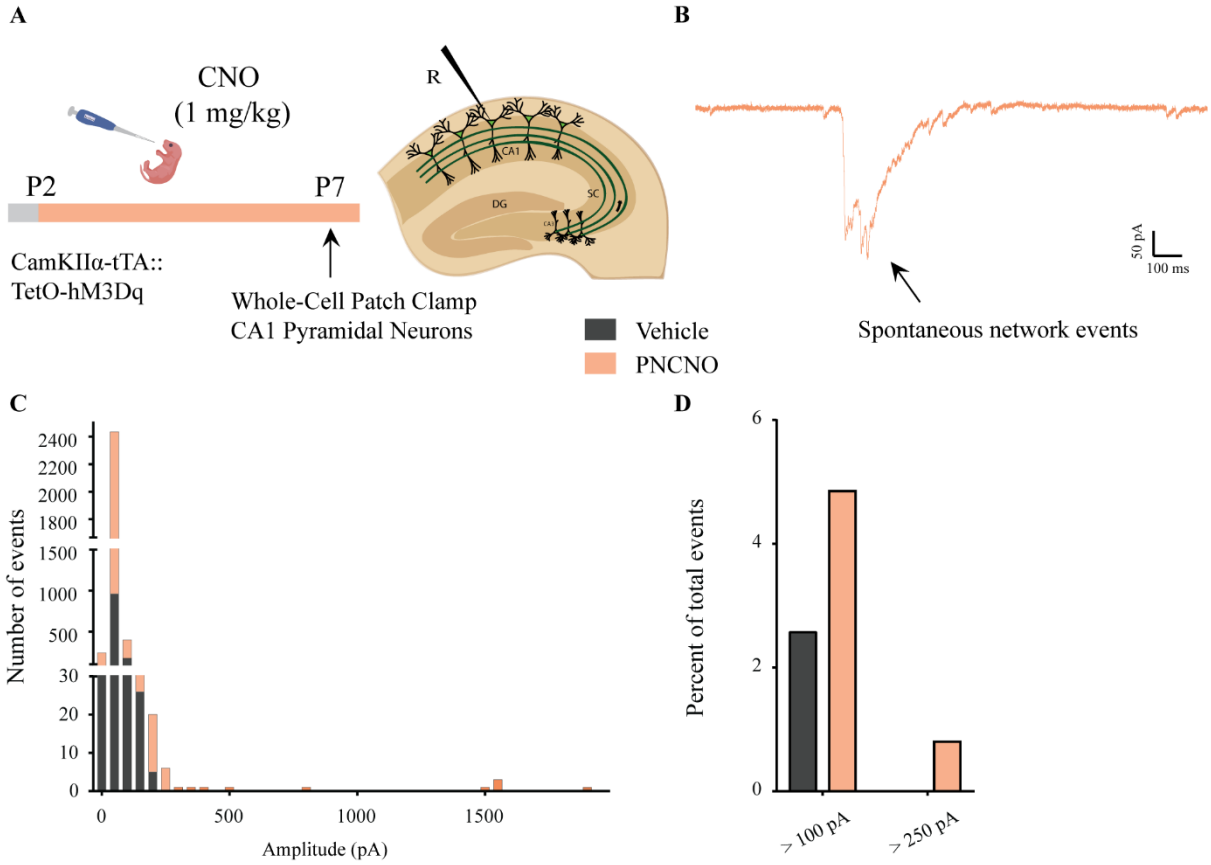

(A) Shown is an experimental paradigm to assess the effects of chronic CNO-mediated hM3Dq DREADD activation of CamKIIα-positive forebrain excitatory neurons using whole-cell patch clamp. CamKIIα-tTA::TetO-hM3Dq bigenic mouse pups were fed either CNO (1 mg/kg) or vehicle from P2 to P7 followed by recording of sPSCs (n = 7 cells for vehicle; n = 10 cells for PNCNO). (B) Example trace of a large-amplitude spontaneous network event observed in the CA1 pyramidal neuron of a PNCNO-treated pup. (C) Distribution plot for sPSC amplitudes showing a long-tail of large-amplitude events in PNCNO-treated mice. (D) Quantification of percent of total events with amplitude > 100 pA and > 250 pA. No event > 250 pA was observed in vehicle-treated pups.

bioRxiv preprint doi: https://doi.org/10.1101/2020.02.19.956060; this version posted February 20, 2020. The copyright holder for this preprint (which was not certified by peer review) is the author/funder. All rights reserved. No reuse allowed without permission.

Figure 1 – table 1

Effects of chronic postnatal hM3Dq DREADD activation in CamKIIα-positive forebrain excitatory neurons on intrinsic membrane properties.

Postnatal Day 7	CA1 Pyramidal Neurons					
	Intrinsic Properties					
Group	RMP (mV)	Input resistance (MΩ)	τ (ms)	Sag (mV)	Sag (%)	Accomodation index
Vehicle	-55.96 ± 1.923	310.2 ± 39.43	34.77 ± 4.62	-10.09 ± 2.65	10.15 ± 2.42	0.32 ± 0.06
PNCNO	-51.66 ± 1.151$^{\$}$	352.3 ± 35.23	33.62 ± 3.65	-8.99 ± 1.66	9.10 ± 1.22	0.48 ± 0.09

CamKIIα-tTA::TetO-hM3Dq bigenic mouse pups were fed either CNO (1 mg/kg) or vehicle from P2 to P7, and whole-cell patch clamp was performed at P7 to determine intrinsic membrane properties. No significant effect was noted for input resistance, membrane time constant (τ), Sag voltage, percent Sag and accommodation index across treatment groups. We noted a trend towards an increase in resting membrane potential (RMP) in hippocampi derived from the PNCNO-treated mouse pups as compared to vehicle-treated controls. $^{\$}p = 0.06$ as compared to vehicle-treated controls (n = 6 cells for vehicle; n = 9 cells for PNCNO) using the two-tailed, unpaired Student's *t*-test.

bioRxiv preprint doi: https://doi.org/10.1101/2020.02.19.956060; this version posted February 20, 2020. The copyright holder for this preprint (which was not certified by peer review) is the author/funder. All rights reserved. No reuse allowed without permission.

Figure 2 with 7 supplements

Chronic chemogenetic activation of CamKIIα-positive forebrain excitatory neurons during the early postnatal window results in a long-lasting increase in anxiety- and despair-like behavior in adult male mice

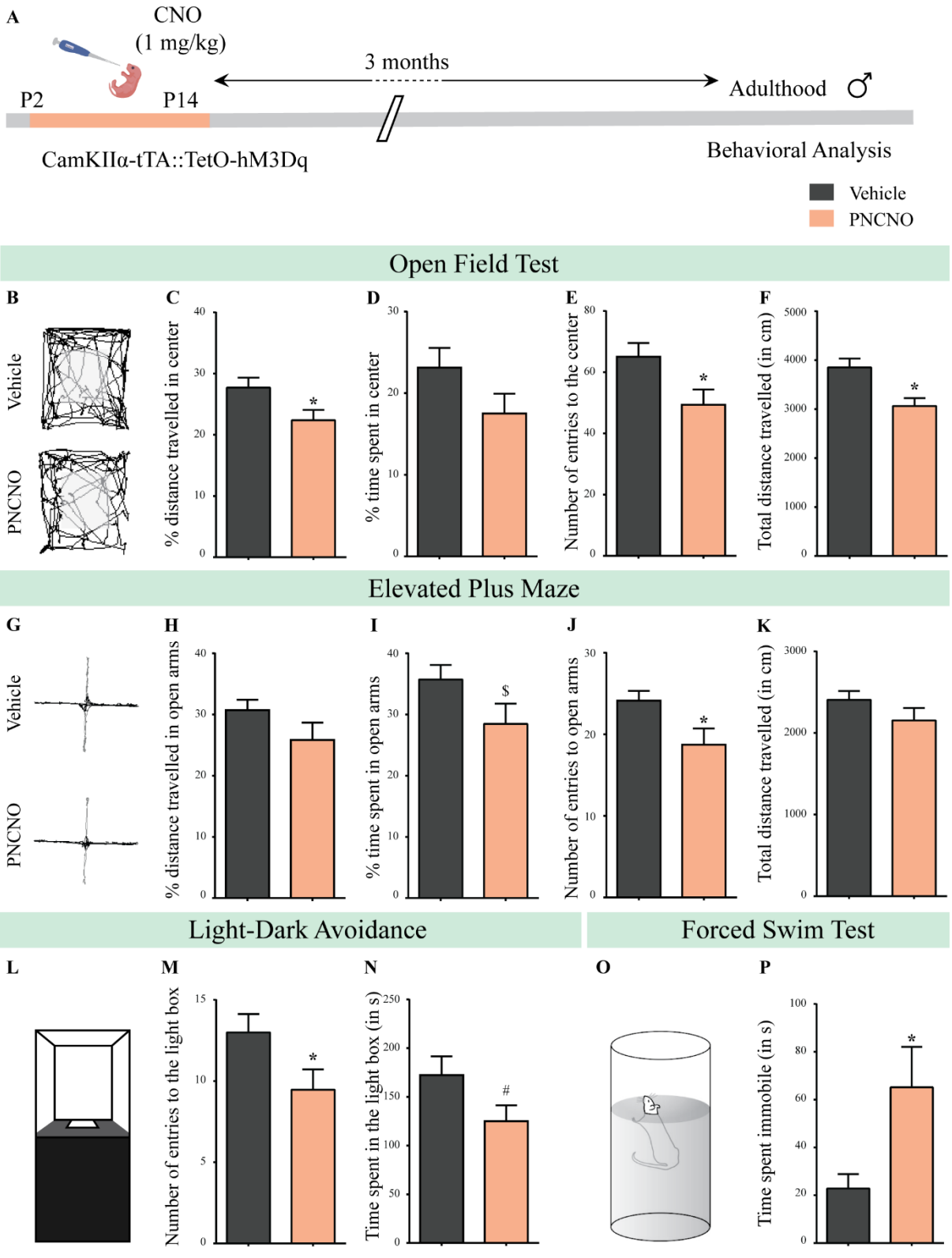

bioRxiv preprint doi: https://doi.org/10.1101/2020.02.19.956060; this version posted February 20, 2020. The copyright holder for this preprint (which was not certified by peer review) is the author/funder. All rights reserved. No reuse allowed without permission.

(A) Shown is a schematic of the experimental paradigm to induce chronic CNO-mediated hM3Dq DREADD activation in CamKIIα-positive forebrain excitatory neurons using bigenic CamKIIα-tTA::TetO-hM3Dq mouse pups that were fed CNO (PNCNO; 1 mg/kg) or vehicle from P2-P14 and then left undisturbed for three months prior to behavioral analysis performed in adulthood on male mice. (B) Shown are representative tracks of vehicle or PNCNO-treated CamKIIα-tTA::TetO-hM3Dq bigenic adult male mice in the open field test (OFT). A history of chronic postnatal hM3Dq DREADD activation of CamKIIα-positive forebrain excitatory neurons resulted in increased anxiety-like behavior on the OFT in adulthood, as noted by a significant decrease in the percent distance travelled in center (C), number of entries to the center (E), and the total distance travelled in the OFT arena (F) in PNCNO-treated mice as compared to vehicle-treated controls (n = 15 per group). The percent time spent in the center was not significantly altered (D) in PNCNO-treated mice as compared to vehicle-treated controls. (G) Shown are representative tracks of vehicle or PNCNO-treated CamKIIα-tTA::TetO-hM3Dq bigenic adult mice on the elevated plus maze (EPM). Adult mice with chronic postnatal hM3Dq DREADD activation of CamKIIα-positive forebrain excitatory neurons exhibited increased anxiety-like behavior on the EPM as revealed by a significant decrease in the number of entries to the open arms (J), and a trend towards a decrease in percent time spent in the open arms (I) in PNCNO-treated mice as compared to vehicle-treated controls (n = 15 per group). The percent distance travelled in the open arms (H) and the total distance travelled in the EPM arena (K) was not altered in PNCNO-treated mice as compared to vehicle-treated controls. (L) Shown is a schematic of the light-dark box used to assess anxiety-like behavior. Chronic postnatal hM3Dq DREADD activation of CamKIIα-positive forebrain excitatory neurons resulted in an increased anxiety-like behavior in the LD box test in adulthood, as revealed by a significant decline in the number of entries to the light box (M), and a trend toward decline in the time spent in the light box (N) in PNCNO-treated mice as compared to vehicle-treated controls (n = 15 per group). (O) Shown is a schematic representation of the forced swim test (FST) apparatus used to assess despair-like behavior. Chronic postnatal hM3Dq DREADD activation of CamKIIα-positive forebrain excitatory neurons resulted in an increased despair-like behavior on the FST in adulthood, as revealed by a significant increase in time spent immobile (P) in PNCNO-treated mice as compared to vehicle-treated controls (n = 13 per group). Results are expressed as the mean ± S.E.M. * $p < 0.05$, $^{\$}$ $p = 0.08$, $^{\#}$ $p = 0.07$; as compared to vehicle-treated controls using the two-tailed, unpaired Student's *t*-test.

bioRxiv preprint doi: https://doi.org/10.1101/2020.02.19.956060; this version posted February 20, 2020. The copyright holder for this preprint (which was not certified by peer review) is the author/funder. All rights reserved. No reuse allowed without permission.

Figure 2 – figure supplement 1

Chronic chemogenetic activation of CamKIIα-positive forebrain excitatory neurons during the early postnatal window does not alter weight during CNO administration and in adulthood

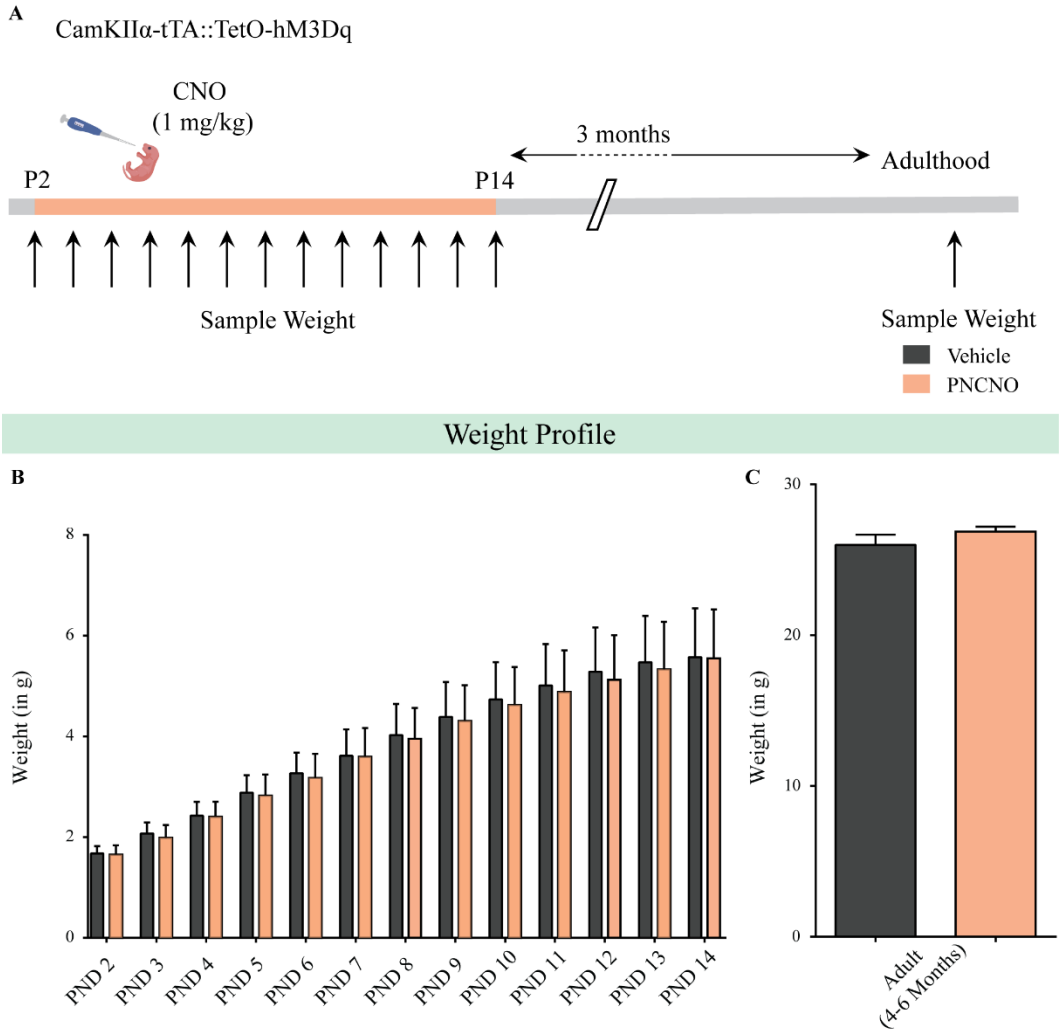

(A) Shown is a schematic of the experimental paradigm used to determine the influence of chronic CNO-mediated hM3Dq DREADD activation of CamKIIα-positive forebrain excitatory neurons in CamKIIα-tTA::TetO-hM3Dq bigenic mouse pups from P2-P14 on gross weight during the time of treatment and in adulthood. (B) CamKIIα-tTA::TetO-hM3Dq bigenic mouse pups fed with CNO (1 mg/kg) once daily from P2-14 did not show any significant change in gross weight across the duration of treatment as compared to their vehicle-treated controls (n = 9 for vehicle; n = 11 for PNCNO). (C) Adult CamKIIα-tTA::TetO-hM3Dq bigenic mice with a history of postnatal CNO treatment from P2-14 did not show any significant change in gross adult weight as compared to vehicle-treated controls (n = 9 for vehicle; n = 11 for PNCNO). Results are expressed as the mean ± S.E.M.

bioRxiv preprint doi: https://doi.org/10.1101/2020.02.19.956060; this version posted February 20, 2020. The copyright holder for this preprint (which was not certified by peer review) is the author/funder. All rights reserved. No reuse allowed without permission.

Figure 2 – figure supplement 2

Chronic chemogenetic activation of CamKIIα-positive forebrain excitatory neurons during the early postnatal window does not alter the developmental emergence of reflex behaviors

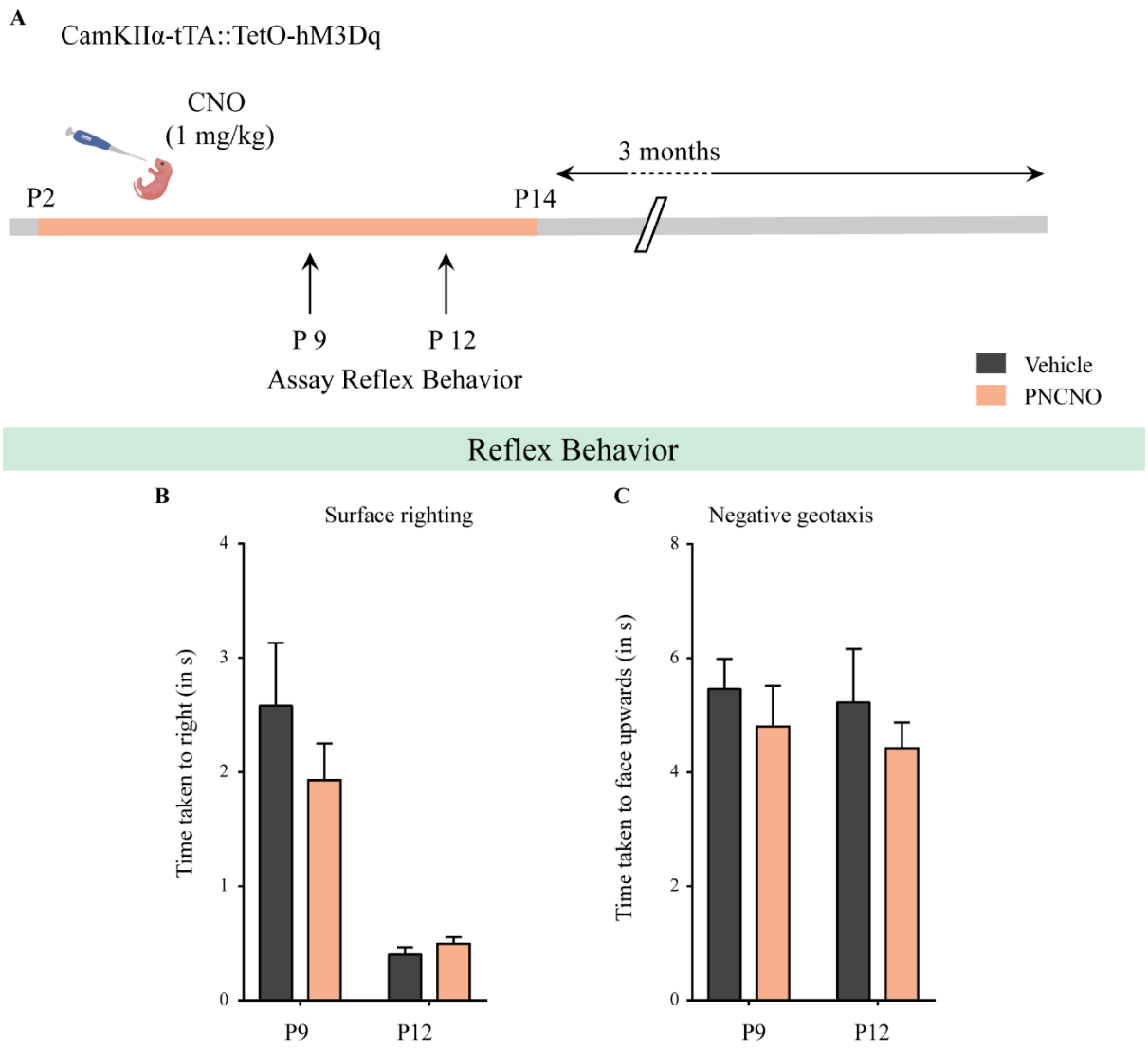

(A) Shown is a schematic of the experimental paradigm used to determine the influence of chronic CNO-mediated hM3Dq DREADD activation of CamKIIα-positive forebrain excitatory neurons in CamKIIα-tTA::TetO-hM3Dq bigenic mouse pups from P2-P14 on the postnatal emergence of reflex behaviors. (B) Surface righting was not significantly altered at P9 (n = 10 for vehicle; n = 11 for PNCNO) and P12 (n = 12 for vehicle; n = 16 for PNCNO) in PNCNO-treated mice as compared to vehicle-treated controls. (C) Negative geotaxis was not significantly altered at P9 (n = 12 for vehicle; n = 19 for PNCNO) and P12 (n = 12 for vehicle; n = 16 for PNCNO) in PNCNO-treated mice as compared to vehicle-treated controls. Results are expressed as the mean ± S.E.M.

bioRxiv preprint doi: https://doi.org/10.1101/2020.02.19.956060; this version posted February 20, 2020. The copyright holder for this preprint (which was not certified by peer review) is the author/funder. All rights reserved. No reuse allowed without permission.

Figure 2 – figure supplement 3

Chronic chemogenetic activation of CamKIIα-positive forebrain excitatory neurons during the early postnatal window results in a long-lasting increase in anxiety-like behavior in adult female mice

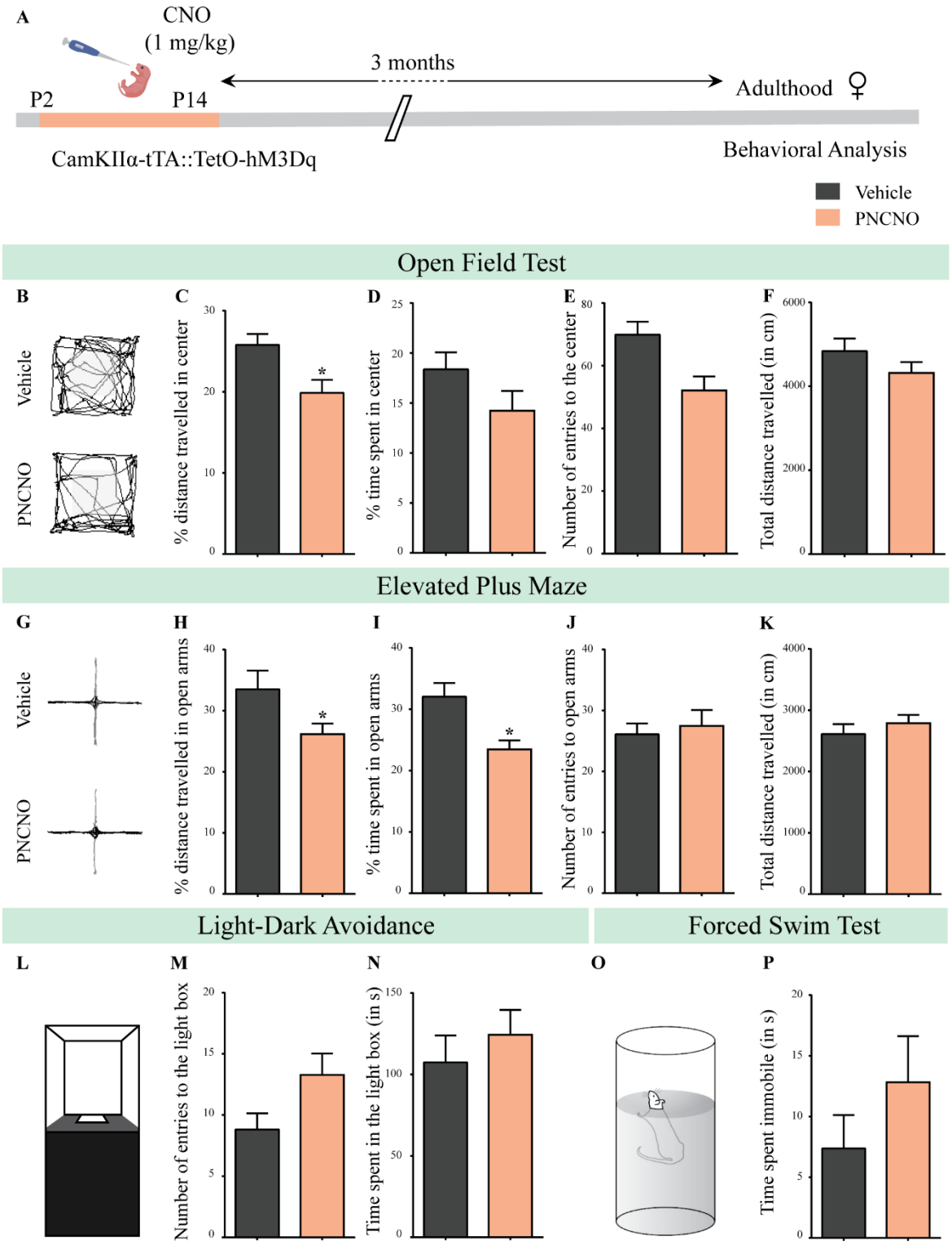

bioRxiv preprint doi: https://doi.org/10.1101/2020.02.19.956060; this version posted February 20, 2020. The copyright holder for this preprint (which was not certified by peer review) is the author/funder. All rights reserved. No reuse allowed without permission.

(A) Shown is a schematic of the experimental paradigm to induce chronic CNO-mediated hM3Dq DREADD activation in CamKIIα-positive forebrain excitatory neurons using bigenic CamKIIα-tTA::TetO-hM3Dq mouse pups that were fed CNO (PNCNO; 1 mg/kg) or vehicle from P2-P14, and then left undisturbed for three months prior to behavioral analysis performed in adulthood on female mice. (B) Shown are representative tracks of vehicle or PNCNO-treated CamKIIα-tTA::TetO-hM3Dq bigenic adult female mice in the open field test (OFT). A history of chronic postnatal hM3Dq DREADD activation of CamKIIα-positive forebrain excitatory neurons resulted in increased anxiety-like behavior on the OFT in adulthood, as noted by a significant decrease in the percent distance travelled in center (C) in PNCNO-treated mice as compared to vehicle-treated controls. The percent time spent in the center (D), the number of entries to the center (E), and the total distance travelled in the OFT arena (F) were not significantly altered across treatment groups (n = 11 per group). (G) Shown are representative tracks of vehicle or PNCNO-treated CamKIIα-tTA::TetO-hM3Dq bigenic adult mice on the elevated plus maze (EPM). Adult female mice with chronic postnatal hM3Dq DREADD activation of CamKIIα-positive forebrain excitatory neurons exhibited increased anxiety-like behavior on the EPM as revealed by a significant decrease in the percent distance travelled in the open arms (H), and a decrease in percent time spent in the open arms (I) in PNCNO-treated mice as compared to vehicle-treated controls. The number of entries to the open arms (J) and the total distance travelled in the EPM arena (K) was not altered in PNCNO-treated mice as compared to vehicle-treated controls (n = 11 per group). (L-N) Shown is a schematic of the light-dark box used to assess anxiety-like behavior. Chronic postnatal hM3Dq DREADD activation of CamKIIα-positive forebrain excitatory neurons did not alter anxiety-like behavior in the LD box test in adulthood in PNCNO-treated mice as compared to vehicle-treated controls (n = 11 per group). (O) Shown is a schematic representation of the forced swim test (FST) apparatus used to assess despair-like behavior. Chronic postnatal hM3Dq DREADD activation of CamKIIα-positive forebrain excitatory neurons did not influence despair-like behavior on the FST (P) in adulthood in PNCNO-treated female mice as compared to vehicle-treated controls (n = 14 for vehicle; n = 11 for PNCNO). Results are expressed as the mean ± S.E.M. * $p < 0.05$ as compared to vehicle-treated controls using the two-tailed, unpaired Student's *t*-test.

bioRxiv preprint doi: https://doi.org/10.1101/2020.02.19.956060; this version posted February 20, 2020. The copyright holder for this preprint (which was not certified by peer review) is the author/funder. All rights reserved. No reuse allowed without permission.

Figure 2 – figure supplement 4

Chronic chemogenetic activation of CamKIIα-positive forebrain excitatory neurons during the early postnatal window does not alter object discrimination memory in adult male mice

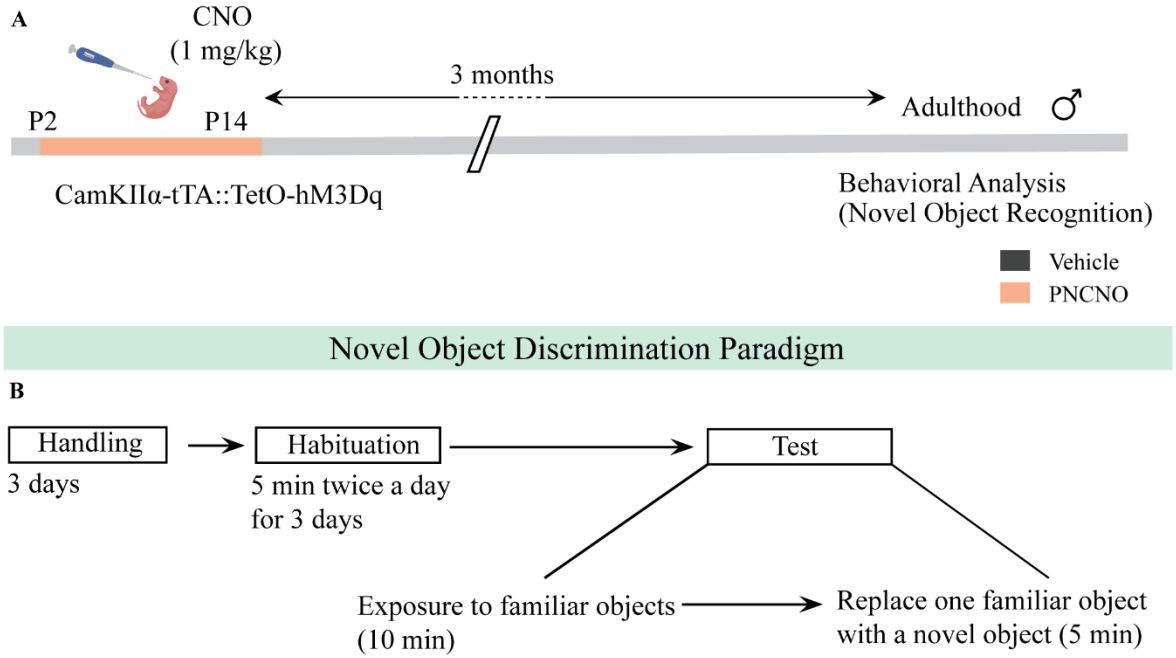

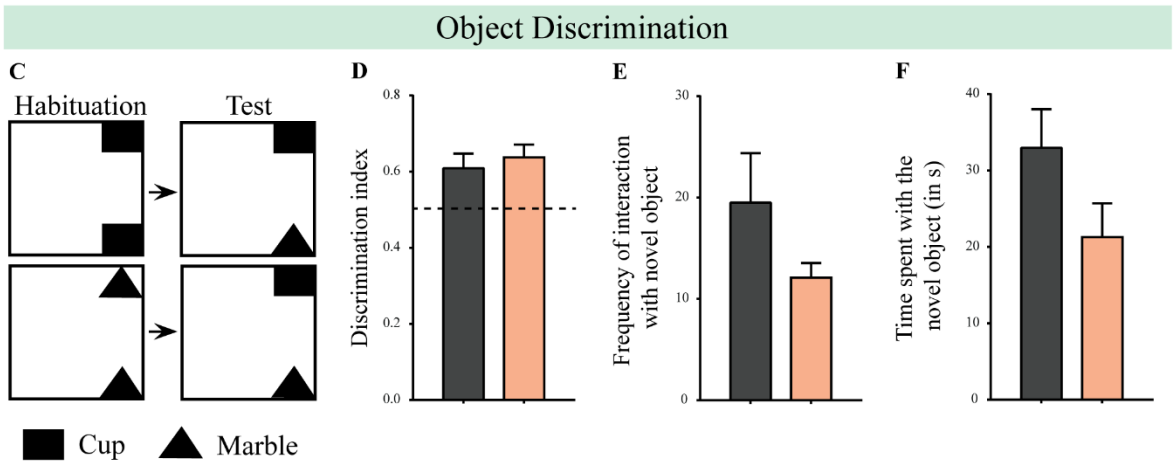

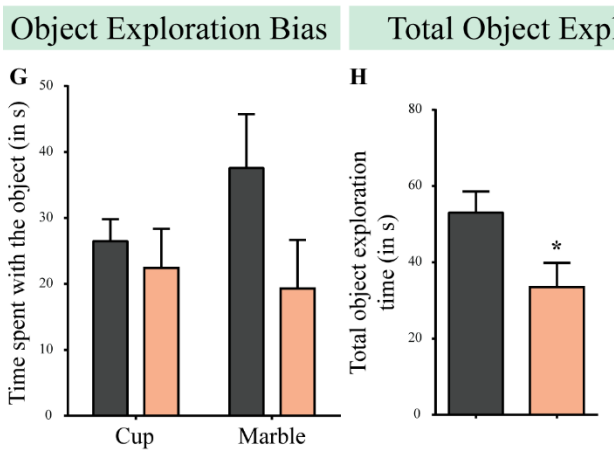

bioRxiv preprint doi: https://doi.org/10.1101/2020.02.19.956060; this version posted February 20, 2020. The copyright holder for this preprint (which was not certified by peer review) is the author/funder. All rights reserved. No reuse allowed without permission.

(A) Shown is a schematic of the experimental paradigm to induce chronic CNO-mediated hM3Dq DREADD activation in CamKIIα-positive forebrain excitatory neurons using bigenic CamKIIα-tTA::TetO-hM3Dq mouse pups that were fed CNO (PNCNO; 1 mg/kg) or vehicle from P2-P14 and then left undisturbed for three months prior to behavioral analysis to assess object discrimination memory performed in adult male mice. (B-C) Shown is a schematic showing experimental design for novel object discrimination behavior. The mice were familiarised to two identical objects during habituation of which one object was replaced with a novel object on the test day. PNCNO-treated mice did not display any significant difference in the discrimination index (D), frequency of interaction with the novel object (E), and the time spent at the novel object (F) as compared to vehicle-treated controls. Both vehicle and PNCNO-treated mice did not show any object exploration bias towards either the cup or marble filled bottle as shown by no change in the time spent with the object (G) as compared to vehicle-treated controls. A significant decrease in total object exploration time (H) was observed in the PNCNO-treated mice as compared to vehicle-treated controls (n = 12 for vehicle; n = 11 for PNCNO). Results are expressed as the mean ± S.E.M. * $p < 0.05$ as compared to vehicle-treated controls using the two-tailed, unpaired Student's *t*-test.

bioRxiv preprint doi: https://doi.org/10.1101/2020.02.19.956060; this version posted February 20, 2020. The copyright holder for this preprint (which was not certified by peer review) is the author/funder. All rights reserved. No reuse allowed without permission.

Figure 2 – figure supplement 5

Chronic chemogenetic activation of CamKIIα-positive forebrain excitatory neurons during the early postnatal window does not alter repetitive behavior in adult male mice

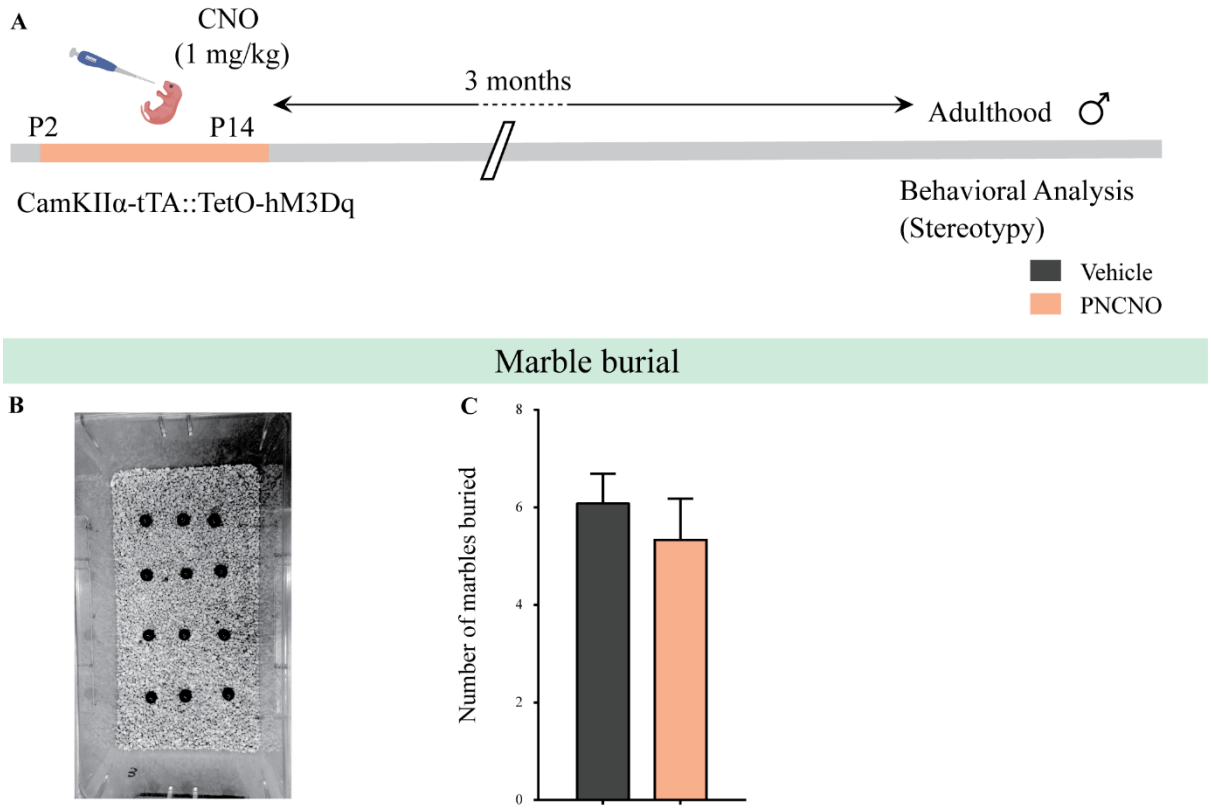

(A) Shown is a schematic of the experimental paradigm to induce chronic CNO-mediated hM3Dq DREADD activation in CamKIIα-positive forebrain excitatory neurons using bigenic CamKIIα-tTA::TetO-hM3Dq mouse pups that were fed CNO (PNCNO; 1 mg/kg) or vehicle from P2-P14 and then left undisturbed for three months prior to behavioral analysis to assess repetitive behavior on the marble burial test performed in adult male mice. (B) Shown is a representative image of marble burial test. PNCNO-treated mice did not show any significant difference in the number of marbles buried (C) as compared to vehicle-treated controls (n = 12 per group). Results are expressed as the mean ± S.E.M.

bioRxiv preprint doi: https://doi.org/10.1101/2020.02.19.956060; this version posted February 20, 2020. The copyright holder for this preprint (which was not certified by peer review) is the author/funder. All rights reserved. No reuse allowed without permission.

Figure 2 – figure supplement 6

Chronic CNO administration during the early postnatal window does not influence anxiety- and despair-like behavior in genotype-control, adult male mice

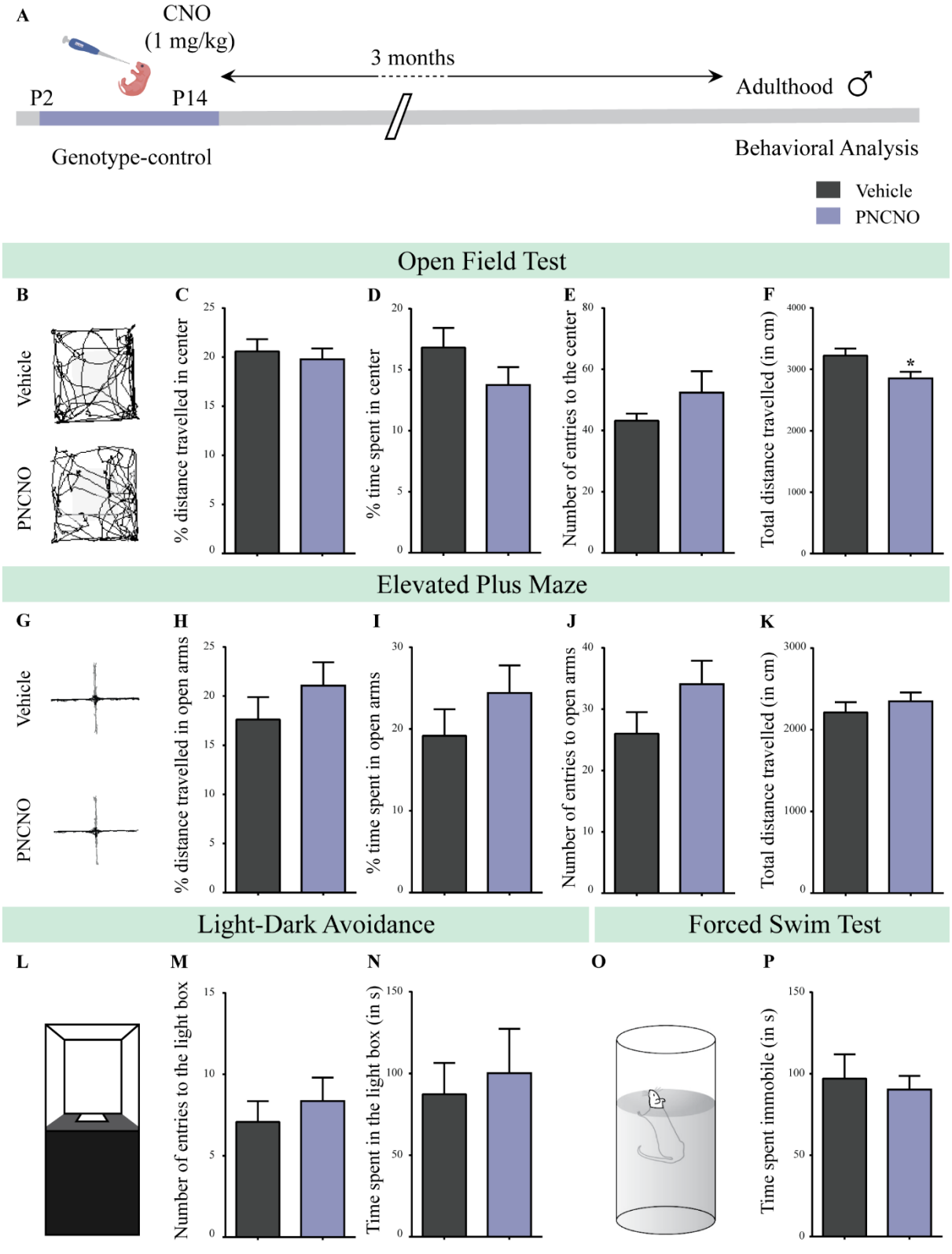

bioRxiv preprint doi: https://doi.org/10.1101/2020.02.19.956060; this version posted February 20, 2020. The copyright holder for this preprint (which was not certified by peer review) is the author/funder. All rights reserved. No reuse allowed without permission.

(A) Shown is a schematic of the experimental paradigm to assess the influence of chronic CNO administration in genotype-control mice. Mouse pups, single-positive for either CamKIIα-tTA or TetO-hM3Dq and referred to as genotype-controls, were fed CNO (PNCNO; 1 mg/kg) or vehicle from P2-P14 and then left undisturbed for three months prior to behavioral analysis performed in adulthood on male mice. (B) Shown are representative tracks of vehicle or PNCNO-treated genotype-control adult male mice in the open field test (OFT). A history of chronic postnatal CNO treatment did not influence anxiety-like behavior on the OFT in adulthood, with no change observed in the percent distance travelled in center (C), percent time spent in the center (D) and the number of entries to the center (E) of the OFT arena in PNCNO-treated genotype-control mice as compared to vehicle-treated genotype-control group (n = 13 for vehicle; n = 11 for PNCNO). We noted a small, but significant decline in the total distance traversed in the OFT arena (F) in the PNCNO-treated genotype-control mice as compared to vehicle-treated controls. (G) Shown are representative tracks of vehicle or PNCNO-treated genotype-control male mice on the elevated plus maze (EPM). Chronic postnatal CNO treatment did not alter anxiety-like behavior on the EPM, with no change observed in percent distance travelled (H), percent time spent (I), or number of entries (J) in the open arms of the EPM between PNCNO-treated genotype-control mice as compared to vehicle-treated controls (n = 13 for vehicle; n = 14 for PNCNO). The total distance travelled in the EPM arena (K) was also not different between the two groups. (L) Shown is a schematic of the light-dark box used to assess anxiety-like behavior. Chronic postnatal CNO administration did not influence anxiety-like behavior in the LD box test in adulthood, with no change noted for either the number of entries to the light box (M) or the time spent in the light box (N) in PNCNO-treated genotype-control mice as compared to vehicle-treated controls (n = 13 for vehicle; n = 14 for PNCNO). (O) Shown is a schematic representation of the forced swim test (FST) apparatus used to assess despair-like behavior. Chronic postnatal CNO administration did not influence despair-like behavior on the FST in adulthood, with no change in time spent immobile (P) in PNCNO-treated genotype-control mice as compared to vehicle-treated controls (n = 12 per group). Results are expressed as the mean ± S.E.M. * $p < 0.05$ as compared to vehicle-treated genotype-controls using the two-tailed, unpaired Student's *t*-test.

bioRxiv preprint doi: https://doi.org/10.1101/2020.02.19.956060; this version posted February 20, 2020. The copyright holder for this preprint (which was not certified by peer review) is the author/funder. All rights reserved. No reuse allowed without permission.

Figure 2 – figure supplement 7

Chronic CNO administration during the early postnatal window does not influence anxiety- and despair-like behavior in C57BL6/J adult male mice

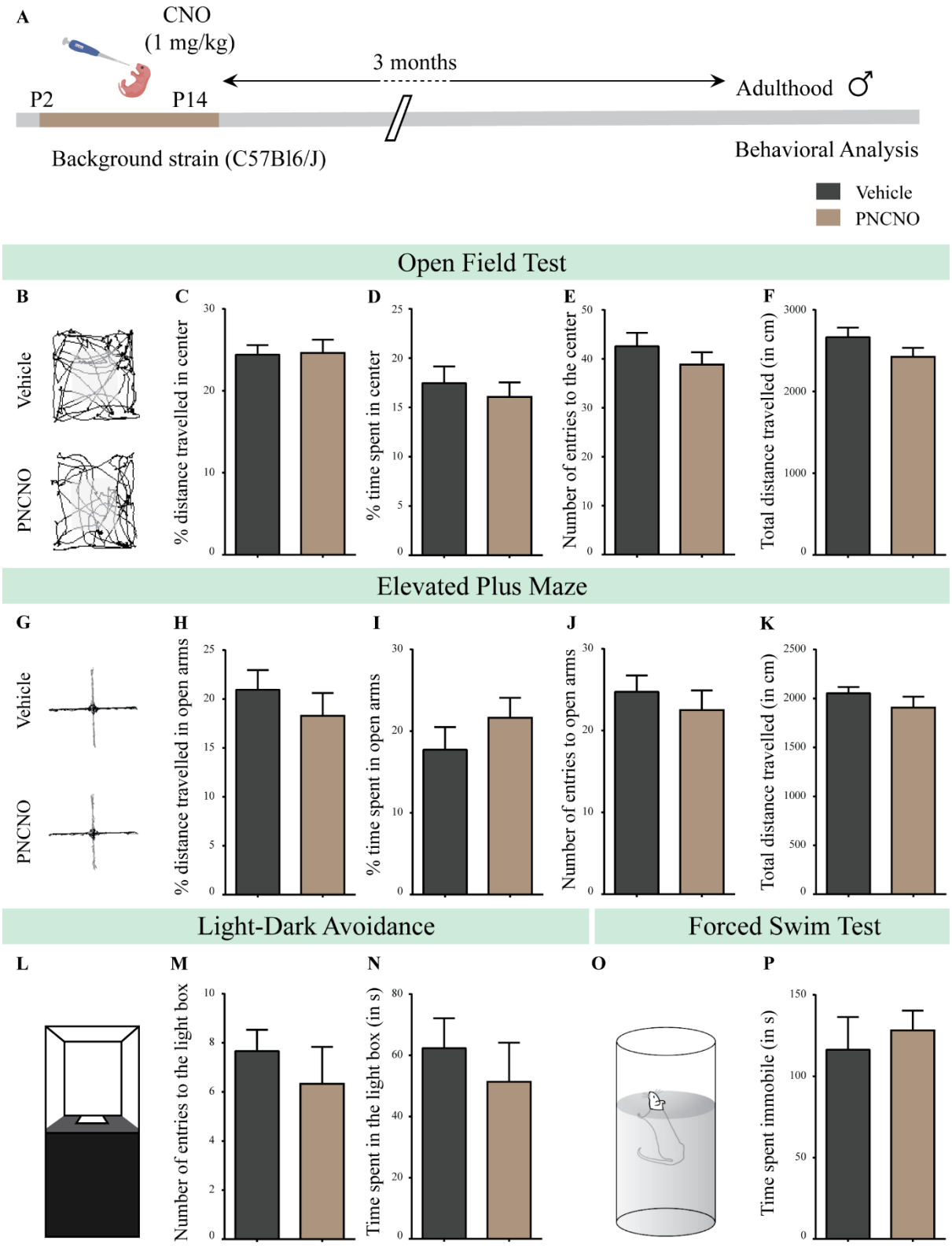

bioRxiv preprint doi: https://doi.org/10.1101/2020.02.19.956060; this version posted February 20, 2020. The copyright holder for this preprint (which was not certified by peer review) is the author/funder. All rights reserved. No reuse allowed without permission.

(A) Shown is a schematic of the experimental paradigm to assess the influence of chronic CNO administration in the background strain for the bigenic CamKIIα-tTA::TetO-hM3Dq, namely the C57BL6/J mouse strain. C57BL6/J mouse pups were fed CNO (PNCNO; 1 mg/kg) or vehicle from P2-P14 and then left undisturbed for three months prior to behavioral analysis performed in adulthood on male mice. (B) Shown are representative tracks of vehicle or PNCNO-treated background strain, adult male mice in the open field test (OFT). A history of chronic postnatal CNO treatment did not influence anxiety-like behavior on the OFT in adulthood, with no change observed in the percent distance travelled in center (C), percent time spent in the center (D), the number of entries to the center (E), or the total distance traversed in the OFT arena (F) in PNCNO-treated background strain mice as compared to the vehicle-treated background strain control group (n = 12 per group). (G) Shown are representative tracks of vehicle or PNCNO-treated background strain male mice on the elevated plus maze (EPM). Chronic postnatal CNO treatment did not alter anxiety-like behavior on the EPM, with no change observed in percent distance travelled (H), percent time spent (I), number of entries (J) in the open arms of the EPM, or the total distance travelled in the EPM arena (K) between PNCNO-treated background strain mice as compared to vehicle-treated background strain controls (n = 12 per group). (L) Shown is a schematic of the light-dark box used to assess anxiety-like behavior. Chronic postnatal CNO administration did not influence anxiety-like behavior in the LD box test in adulthood, with no change noted for either the number of entries to the light box (M) or the time spent in the light box (N) in PNCNO-treated background strain mice as compared to vehicle-treated controls (n = 12 per group). (O) Shown is a schematic representation of the forced swim test (FST) apparatus used to assess despair-like behavior. Chronic postnatal CNO administration did not influence despair-like behavior on the FST in adulthood, with no change in time spent immobile (P) in PNCNO-treated background strain mice as compared to vehicle-treated controls (n = 12 per group). Results are expressed as the mean ± S.E.M.

bioRxiv preprint doi: https://doi.org/10.1101/2020.02.19.956060; this version posted February 20, 2020. The copyright holder for this preprint (which was not certified by peer review) is the author/funder. All rights reserved. No reuse allowed without permission.

Figure 3 with 2 supplements

Chronic chemogenetic activation of CamKIIα-positive forebrain excitatory neurons during the juvenile window or in adulthood does not evoke any long-lasting changes in anxiety- and despair-like behavior in male mice

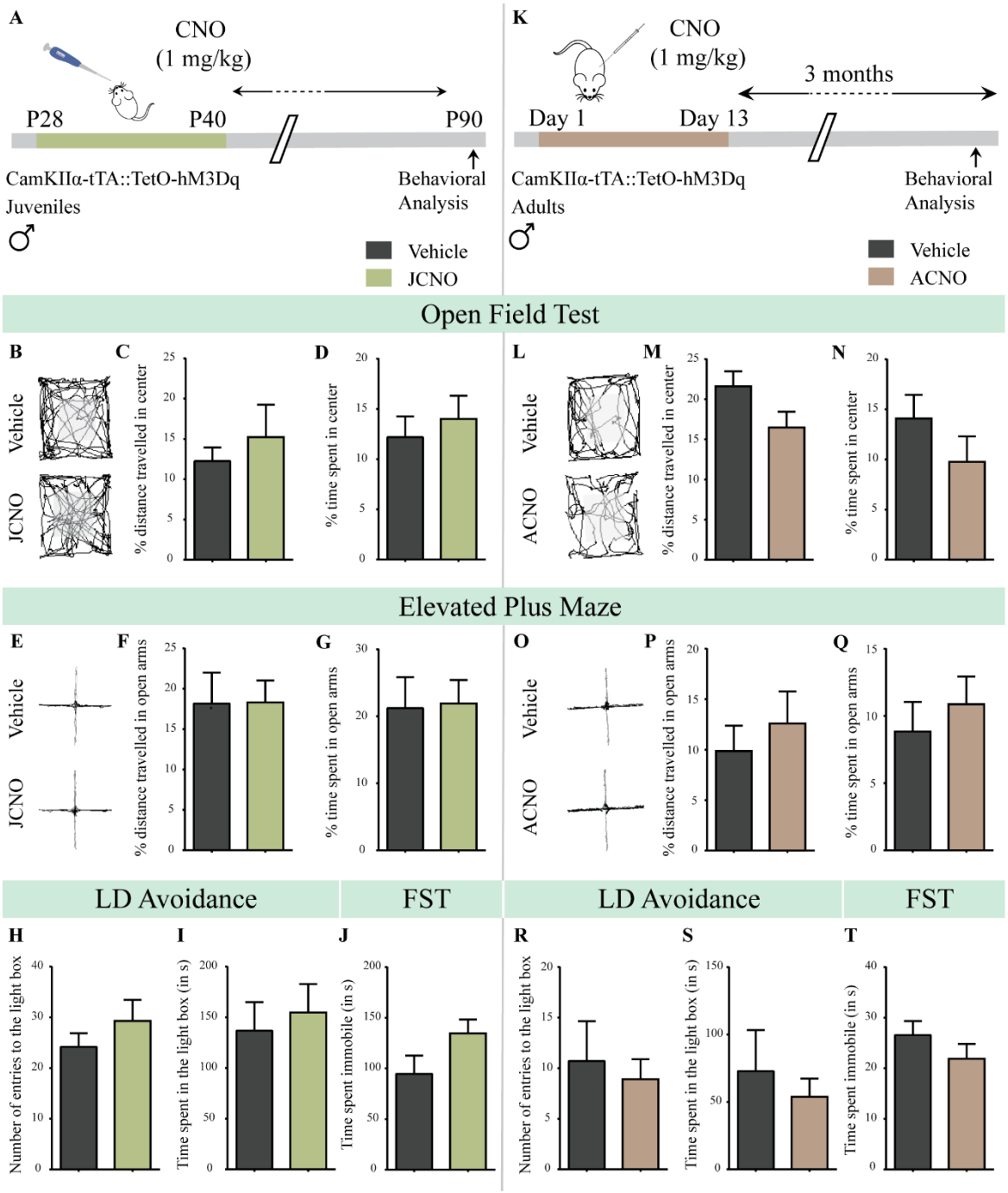

bioRxiv preprint doi: https://doi.org/10.1101/2020.02.19.956060; this version posted February 20, 2020. The copyright holder for this preprint (which was not certified by peer review) is the author/funder. All rights reserved. No reuse allowed without permission.

(A) Shown is a schematic of the experimental paradigm to induce chronic CNO-mediated hM3Dq DREADD activation in CamKIIα-positive forebrain excitatory neurons using bigenic CamKIIα-tTA::TetO-hM3Dq juvenile male mice that were fed CNO (JCNO; 1 mg/kg) or vehicle from P28-P40 and then left undisturbed till three months of age prior to behavioral analysis. (B) Shown are representative tracks of vehicle or JCNO-treated CamKIIα-tTA::TetO-hM3Dq bigenic adult male mice in the open field test (OFT). A history of chronic juvenile hM3Dq DREADD activation of CamKIIα-positive forebrain excitatory neurons does not evoke any persistent change in anxiety-like behavior on the OFT in adulthood, with no difference observed in the percent distance travelled in the center (C) and the percent time spent in the center (D) of the OFT arena in JCNO-treated mice as compared to vehicle-treated controls (n = 11 for vehicle; n = 8 for JCNO). (E) Shown are representative tracks of vehicle or JCNO-treated CamKIIα-tTA::TetO-hM3Dq bigenic adult mice on the elevated plus maze (EPM). Adult mice with chronic juvenile hM3Dq DREADD activation of CamKIIα-positive forebrain excitatory neurons did not exhibit any persistent changes in anxiety-like behavior on the EPM, with no change observed for the percent distance travelled (F) and the percent time spent (G) in the open arms of the EPM arena across treatment groups (n = 11 for vehicle; n = 10 for JCNO). Anxiety-like behavior was also assessed on the light-dark avoidance test and no significant alterations were seen in the number of entries to the light box (H) or the time spent in the light box (I) across treatment groups (n = 11 for vehicle; n = 10 for JCNO). A history of chronic juvenile hM3Dq DREADD activation of CamKIIα-positive forebrain excitatory neurons did not evoke any persistent change in despair-like behavior in the forced swim test (FST), with no difference observed in the time spent immobile (J) in JCNO-treated mice as compared to vehicle-treated controls (n = 11 per group). (K) Shown is a schematic of the experimental paradigm to induce chronic CNO-mediated hM3Dq DREADD activation in CamKIIα-positive forebrain excitatory neurons using bigenic CamKIIα-tTA::TetO-hM3Dq adult male mice (3-4 months of age) that received CNO (ACNO; 1 mg/kg) or vehicle via intraperitoneal administration (once daily for thirteen days) and were left undisturbed for three months prior to behavioral analysis. (L) Shown are representative tracks of vehicle or ACNO-treated CamKIIα-tTA::TetO-hM3Dq bigenic adult male mice in the open field test (OFT). A history of chronic hM3Dq DREADD activation of CamKIIα-positive forebrain excitatory neurons in adulthood does not evoke any persistent change in anxiety-like behavior on the OFT, with no difference observed in the percent distance travelled in the center (M) and the percent time spent in the center (N) of the OFT arena in ACNO-treated mice as compared to vehicle-treated controls (n = 7 for vehicle; n = 11 for ACNO). (O) Shown are representative

bioRxiv preprint doi: https://doi.org/10.1101/2020.02.19.956060; this version posted February 20, 2020. The copyright holder for this preprint (which was not certified by peer review) is the author/funder. All rights reserved. No reuse allowed without permission.

tracks of vehicle or ACNO-treated CamKIIα-tTA::TetO-hM3Dq bigenic adult mice on the elevated plus maze (EPM). Chronic hM3Dq DREADD activation of CamKIIα-positive forebrain excitatory neurons in adulthood did not evoke any persistent changes in anxiety-like behavior on the EPM, with no change observed for the percent distance travelled (P) and the percent time spent (Q) in the open arms of the EPM arena across treatment groups (n = 7 for vehicle; n = 11 for ACNO). Anxiety-like behavior was also studied on the light-dark avoidance test and no change was observed in the number of entries to the light box (R) or the time spent in the light box (S) across treatment groups (n = 7 for vehicle; n = 11 for ACNO). Chronic hM3Dq DREADD activation of CamKIIα-positive forebrain excitatory neurons in adulthood did not evoke any persistent change in despair-like behavior in the forced swim test (FST), with no difference observed in the time spent immobile (T) in ACNO-treated mice as compared to vehicle-treated controls (n = 10 for vehicle; n = 9 for ACNO). Results are expressed as the mean ± S.E.M.

bioRxiv preprint doi: https://doi.org/10.1101/2020.02.19.956060; this version posted February 20, 2020. The copyright holder for this preprint (which was not certified by peer review) is the author/funder. All rights reserved. No reuse allowed without permission.

Figure 3 – figure supplement 1

Chronic chemogenetic activation of CamKIIα-positive forebrain excitatory neurons during the juvenile window or in adulthood does not evoke any long-lasting changes in anxiety-like behavior in male mice

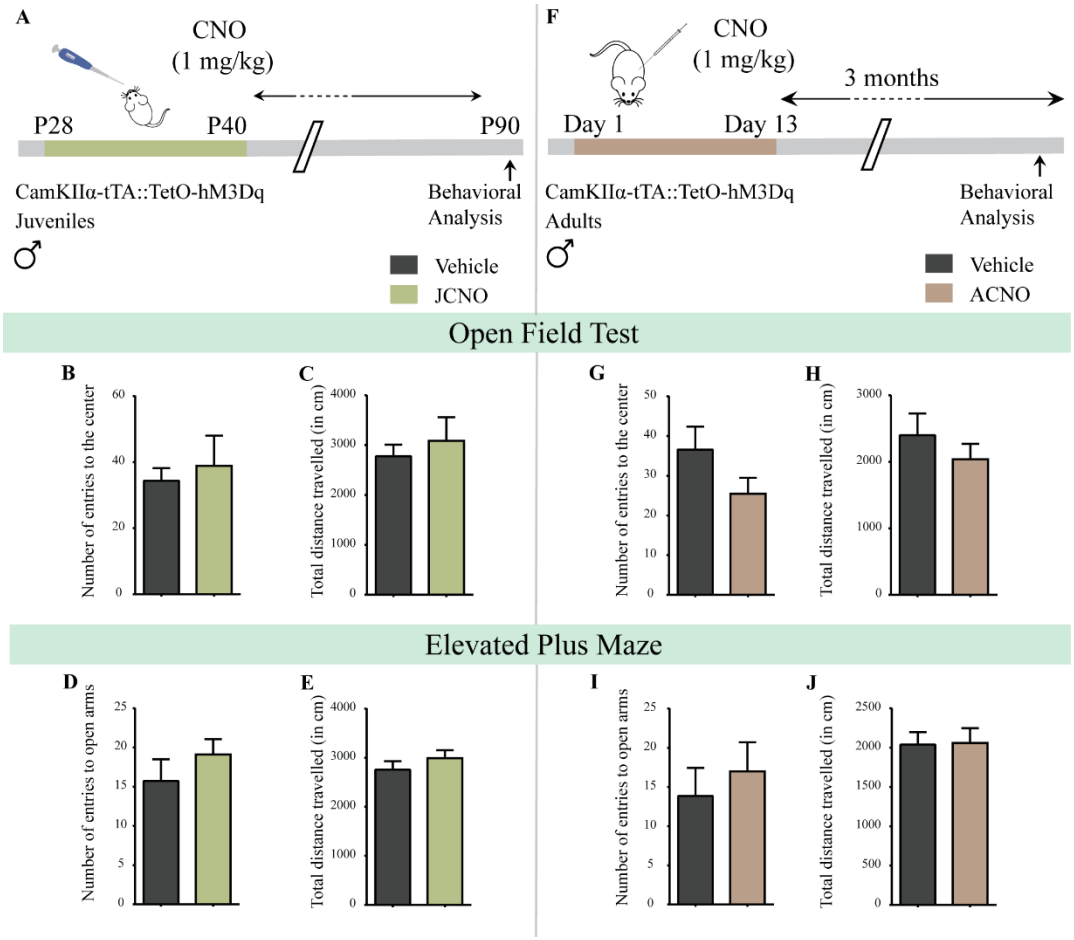

(A) Shown is a schematic of the experimental paradigm to induce chronic CNO-mediated hM3Dq DREADD activation in CamKIIα-positive forebrain excitatory neurons using bigenic CamKIIα-tTA::TetO-hM3Dq juvenile male mice that were fed CNO (JCNO; 1 mg/kg) or vehicle from P28-P40 and then left undisturbed till three months of age prior to behavioral analysis. A history of chronic juvenile hM3Dq DREADD activation of CamKIIα-positive forebrain excitatory neurons does not evoke any persistent change in anxiety-like behavior on the OFT in adulthood, with no difference observed in the number of entries to the center (B) and the total distance travelled in the OFT arena (C) in JCNO-treated mice as compared to vehicle-treated controls (n = 11 for vehicle; n = 8 for JCNO). Adult mice with chronic juvenile hM3Dq DREADD activation of CamKIIα-positive forebrain excitatory neurons did not exhibit

bioRxiv preprint doi: https://doi.org/10.1101/2020.02.19.956060; this version posted February 20, 2020. The copyright holder for this preprint (which was not certified by peer review) is the author/funder. All rights reserved. No reuse allowed without permission.

any persistent changes in anxiety-like behavior on the EPM, with no change observed for the number of entries to the open arms (D) and the total distance travelled in the EPM arena (E) across treatment groups (n = 11 for vehicle; n = 10 for JCNO). (F) Shown is a schematic of the experimental paradigm to induce chronic CNO-mediated hM3Dq DREADD activation in CamKIIα-positive forebrain excitatory neurons using bigenic CamKIIα-tTA::TetO-hM3Dq adult male mice (3-4 months of age) that received CNO (ACNO; 1 mg/kg) or vehicle via intraperitoneal administration (once daily for thirteen days) and were left undisturbed for three months prior to behavioral analysis. A history of chronic hM3Dq DREADD activation of CamKIIα-positive forebrain excitatory neurons in adulthood does not evoke any persistent change in anxiety-like behavior on the OFT, with no difference observed in the number of entries to the center (G) and the total distance travelled in the OFT arena (H) in ACNO-treated mice as compared to vehicle-treated controls (n = 7 for vehicle; n = 11 for ACNO). Chronic hM3Dq DREADD activation of CamKIIα-positive forebrain excitatory neurons in adulthood did not evoke any persistent changes in anxiety-like behavior on the EPM, with no change observed for the number of entries to the open arms (I) and the total distance travelled in the EPM arena (J) across treatment groups (n = 7 for vehicle; n = 11 for ACNO). Results are expressed as the mean ± S.E.M.

bioRxiv preprint doi: https://doi.org/10.1101/2020.02.19.956060; this version posted February 20, 2020. The copyright holder for this preprint (which was not certified by peer review) is the author/funder. All rights reserved. No reuse allowed without permission.

Figure 3 – figure supplement 2

Chronic chemogenetic activation of CamKIIα-positive forebrain excitatory neurons in adulthood does not evoke any long-lasting changes in anxiety-like behavior in male mice during or soon after cessation of CNO treatment

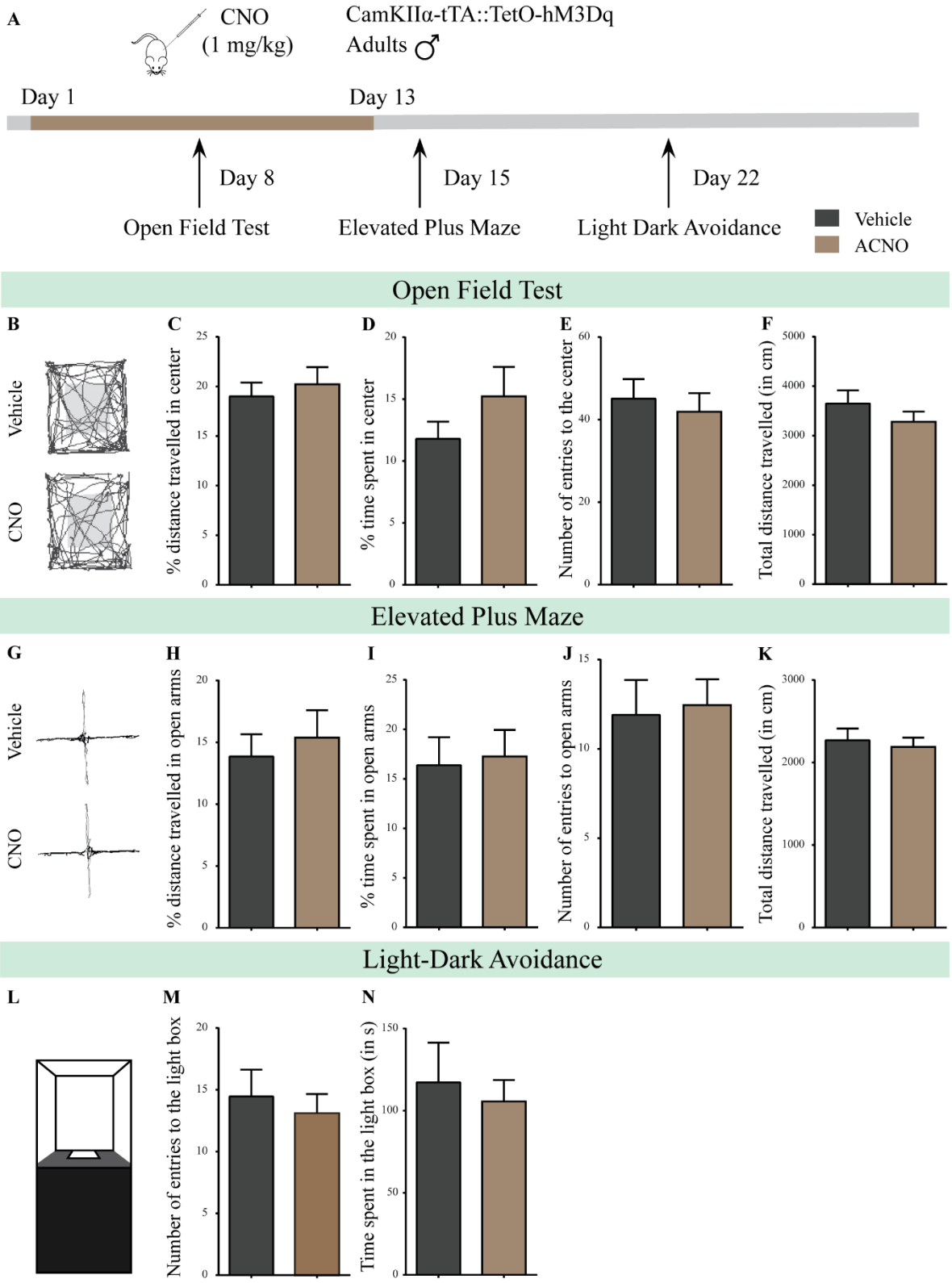

bioRxiv preprint doi: https://doi.org/10.1101/2020.02.19.956060; this version posted February 20, 2020. The copyright holder for this preprint (which was not certified by peer review) is the author/funder. All rights reserved. No reuse allowed without permission.

(A) Shown is a schematic of the experimental paradigm to induce chronic CNO-mediated hM3Dq DREADD activation in CamKIIα-positive forebrain excitatory neurons using bigenic CamKIIα-tTA::TetO-hM3Dq adult male mice (3-4 months of age) that received CNO (ACNO; 1 mg/kg) or vehicle via intraperitoneal administration (once daily for thirteen days) and were assayed for anxiety-like behavior during (OFT- performed on Day 8) and soon after cessation of CNO treatment (EPM performed on Day 15; LD avoidance test performed on Day 22). (B) Shown are representative tracks of vehicle or ACNO-treated bigenic CamKIIα-tTA::TetO-hM3Dq adult male mice in the open field test (OFT). Chronic CNO treatment in adulthood did not influence anxiety-like behavior on the OFT as tested on Day 8 of a 13 day treatment regime, with no change observed in the percent distance travelled in center (C), percent time spent in the center (D), the number of entries to the center (E), or the total distance traversed in the OFT arena (F) in ACNO-treated male mice as compared to the vehicle-treated controls (n = 11 per group). (G) Shown are representative tracks of vehicle or ACNO-treated adult male mice on the elevated plus maze (EPM). Chronic CNO treatment did not alter anxiety-like behavior on the EPM soon after cessation of CNO treatment, with no change observed in percent distance travelled (H), percent time spent (I), number of entries (J) in the open arms of the EPM, or the total distance travelled in the EPM arena (K) between ACNO-treated CamKIIα-tTA::TetO-hM3Dq mice as compared to vehicle-treated controls (n = 11 per group). (L) Shown is a schematic of the light-dark box used to assess anxiety-like behavior. Chronic CNO administration did not influence anxiety-like behavior in the LD box test in adulthood soon after cessation of CNO treatment, with no change noted for either the number of entries to the light box (M) or the time spent in the light box (N) in ACNO-treated bigenic adult male mice as compared to vehicle-treated controls (n = 11 per group). Results are expressed as the mean ± S.E.M.

bioRxiv preprint doi: https://doi.org/10.1101/2020.02.19.956060; this version posted February 20, 2020. The copyright holder for this preprint (which was not certified by peer review) is the author/funder. All rights reserved. No reuse allowed without permission.

Figure 4 with 2 supplements

Chronic chemogenetic activation of CamKIIα-positive forebrain excitatory neurons during the early postnatal window evokes impaired sensorimotor gating in adulthood.

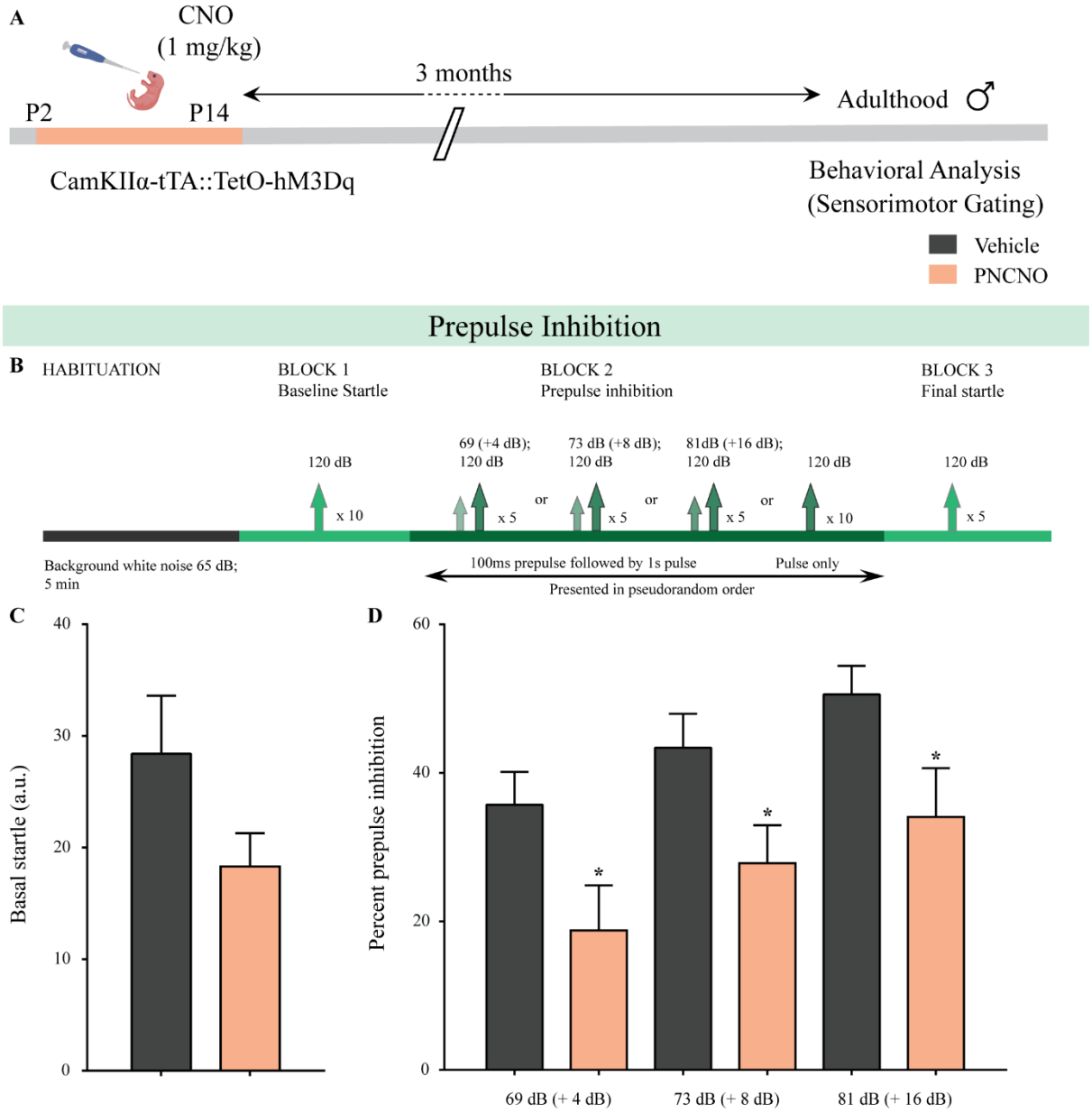

bioRxiv preprint doi: https://doi.org/10.1101/2020.02.19.956060; this version posted February 20, 2020. The copyright holder for this preprint (which was not certified by peer review) is the author/funder. All rights reserved. No reuse allowed without permission.

(A) Shown is a schematic of the experimental paradigm to induce chronic CNO-mediated hM3Dq DREADD activation in CamKIIα-positive forebrain excitatory neurons using bigenic CamKIIα-tTA::TetO-hM3Dq mouse pups that were fed CNO (PNCNO; 1 mg/kg) or vehicle from P2-P14 and then left undisturbed for three months prior to behavioral analysis for sensorimotor gating, using the prepulse inhibition test, in adulthood on male mice. (B) Shown is the test paradigm for prepulse inhibition to assess sensorimotor gating. Adult male mice with a history of postnatal CNO administration (PNCNO) did not show any significant change in basal startle response (C) as compared to vehicle-treated controls. PNCNO-treated adult mice exhibited deficits in sensorimotor gating, as noted via a significant decrease in pre-pulse inhibition (D) at + 4 dB (69 dB), + 8 dB (73 dB), and + 16 dB (81 dB) above background noise (65 dB) when compared to vehicle-treated controls (n = 12 per group). Results are expressed as the mean ± S.E.M. *$p < 0.05$, as compared to vehicle-treated controls using two-tailed, unpaired Student's *t*-test.

bioRxiv preprint doi: https://doi.org/10.1101/2020.02.19.956060; this version posted February 20, 2020. The copyright holder for this preprint (which was not certified by peer review) is the author/funder. All rights reserved. No reuse allowed without permission.

Figure 4 – figure supplement 1

Chronic chemogenetic activation of CamKIIα-positive forebrain excitatory neurons during the juvenile window does not alter sensorimotor gating behavior.

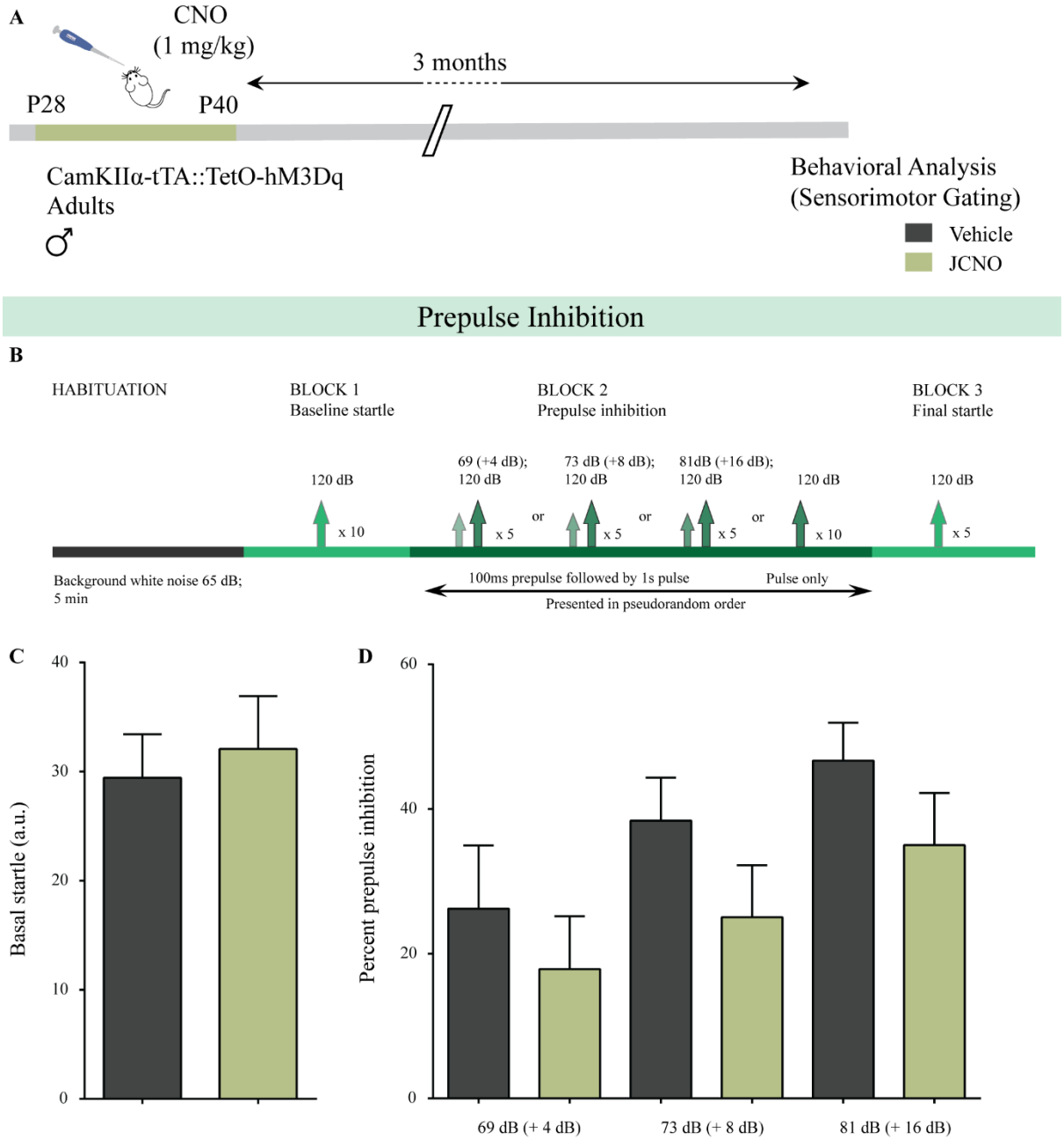

bioRxiv preprint doi: https://doi.org/10.1101/2020.02.19.956060; this version posted February 20, 2020. The copyright holder for this preprint (which was not certified by peer review) is the author/funder. All rights reserved. No reuse allowed without permission.

(A) Shown is a schematic of the experimental paradigm to induce chronic CNO-mediated hM3Dq DREADD activation in CamKIIα-positive forebrain excitatory neurons using bigenic CamKIIα-tTA::TetO-hM3Dq juvenile male mice (P28-40) that were fed CNO (JCNO; 1 mg/kg) or vehicle, and subjected to behavioral analysis using the prepulse inhibition test in adulthood. (B) Shown is the experimental paradigm for prepulse inhibition to assess sensorimotor gating. JCNO-treated mice did not show any significant change in basal startle response (C) as compared to vehicle-treated controls. (D) Pre-pulse inhibition at + 4 dB (69 dB), + 8 dB (73 dB), and + 16 dB (81 dB) above background noise (65 dB) was unaltered in JCNO-treated mice as compared to vehicle-treated controls (n = 8 for vehicle and n = 9 for JCNO). Results are expressed as the mean ± S.E.M.

bioRxiv preprint doi: https://doi.org/10.1101/2020.02.19.956060; this version posted February 20, 2020. The copyright holder for this preprint (which was not certified by peer review) is the author/funder. All rights reserved. No reuse allowed without permission.

Figure 4 – figure supplement 2

Chronic chemogenetic activation of CamKIIα-positive forebrain excitatory neurons in adulthood does not alter sensorimotor gating behavior.

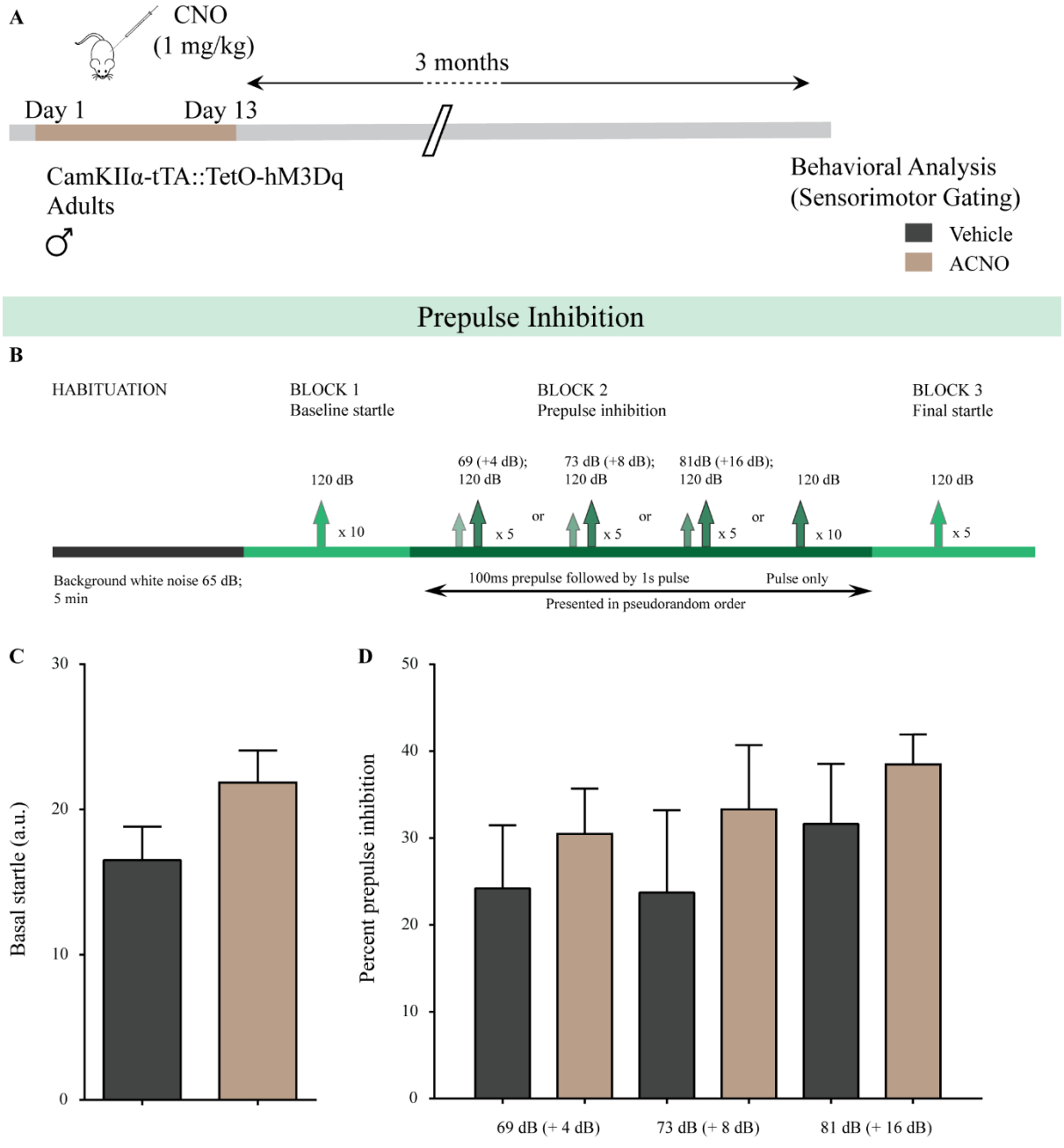

bioRxiv preprint doi: https://doi.org/10.1101/2020.02.19.956060; this version posted February 20, 2020. The copyright holder for this preprint (which was not certified by peer review) is the author/funder. All rights reserved. No reuse allowed without permission.

(A) Shown is a schematic of the experimental paradigm to induce chronic CNO-mediated hM3Dq DREADD activation in CamKIIα-positive forebrain excitatory neurons using bigenic CamKIIα-tTA::TetO-hM3Dq adult male mice (3-4 months of age) that received CNO (ACNO; 1 mg/kg) or vehicle via intraperitoneal administration (once daily for thirteen days) and were left undisturbed for three months prior to behavioral analysis using the prepulse inhibition test. (B) Shown is the experimental paradigm for prepulse inhibition to assess sensorimotor gating. ACNO-treated mice did not show any significant change in basal startle response (C) as compared to vehicle-treated controls. (D) Pre-pulse inhibition at + 4 dB (69 dB), + 8 dB (73 dB), and + 16 dB (81 dB) above background noise (65 dB) was unaltered in ACNO-treated mice as compared to vehicle-treated controls (n = 10 per group). Results are expressed as the mean ± S.E.M.

bioRxiv preprint doi: https://doi.org/10.1101/2020.02.19.956060; this version posted February 20, 2020. The copyright holder for this preprint (which was not certified by peer review) is the author/funder. All rights reserved. No reuse allowed without permission.

Figure 5 with 4 supplements

Chronic chemogenetic activation of CamKIIα-positive forebrain excitatory neurons during the early postnatal window results in long-lasting alterations in neurotransmitter cycling flux and neuronal metabolic rate in hippocampus and cortex.

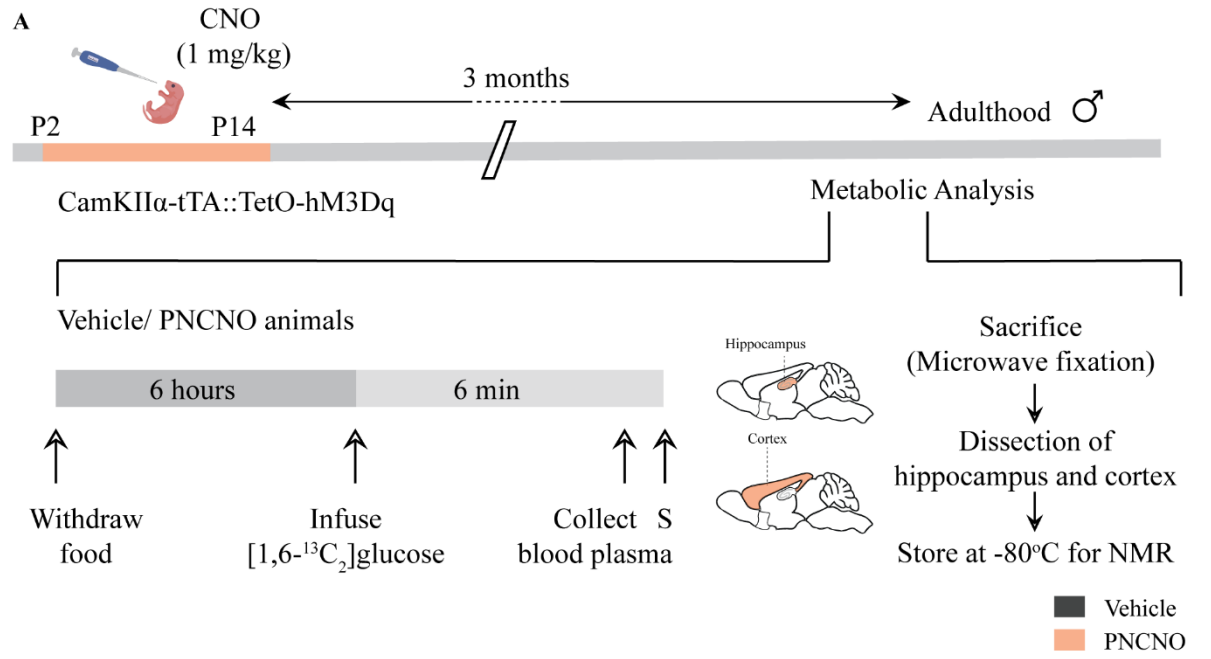

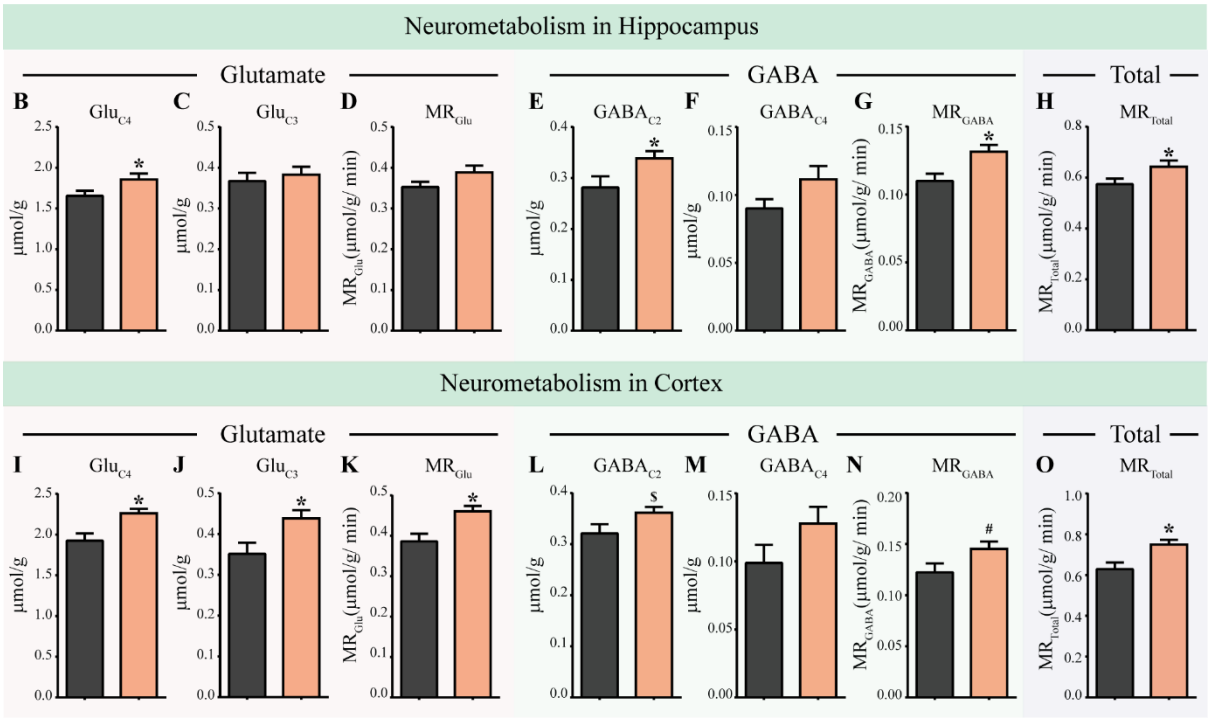

bioRxiv preprint doi: https://doi.org/10.1101/2020.02.19.956060; this version posted February 20, 2020. The copyright holder for this preprint (which was not certified by peer review) is the author/funder. All rights reserved. No reuse allowed without permission.

(A) Shown is a schematic of the experimental paradigm to induce chronic CNO-mediated hM3Dq DREADD activation in CamKIIα-positive forebrain excitatory neurons using bigenic CamKIIα-tTA::TetO-hM3Dq mouse pups that were fed CNO (PNCNO; 1 mg/kg) or vehicle from P2-P14 and then left undisturbed for three months prior to metabolic analysis performed in adulthood on male mice using ^{1}H-[^{13}C]-NMR spectroscopy. Adult male mice, with a history of PNCNO or vehicle administration, were subjected to fasting for 6 hours, following which [1,6-$^{13}C_2$]glucose was infused via the tail-vein. Blood plasma was collected and mice were sacrificed 6 minutes following glucose infusion, followed by dissection of hippocampus and cortex for NMR analysis. PNCNO-treated mice exhibited a higher rate of glutamate and GABA synthesis from [1,6-$^{13}C_2$]glucose in the hippocampus as revealed by significantly higher levels of ^{13}C-labelled metabolites Glu_{C4} (B) and $GABA_{C2}$ (E) as compared to vehicle-treated controls. Levels of ^{13}C-labelled metabolites Glu_{C3} (C) and $GABA_{C4}$ (F) was not altered across treatment groups in the hippocampus. No significant change was observed in the metabolic rate of glucose oxidation in glutamatergic neurons of the hippocampus (D) across treatment groups. There was a significant increase in the metabolic rate of glucose oxidation in GABAergic neurons of the hippocampus (G) and the overall neuronal metabolic rate of the hippocampus (H), in PNCNO-treated mice as compared to vehicle-treated controls. PNCNO-treated mice had a higher rate of glutamate and GABA synthesis from [1,6-$^{13}C_2$]glucose in the cortex as revealed by significantly higher levels of ^{13}C-labelled metabolites Glu_{C4} (I), Glu_{C3} (J), and the metabolic rate of glucose oxidation in glutamatergic neurons of the cortex (K) as compared to vehicle-treated controls. There was a trend towards an increase in levels of ^{13}C-labelled metabolite $GABA_{C2}$ (L) and the metabolic rate of glucose oxidation in GABAergic neurons of the cortex (N) in the PNCNO-treated mice as compared to the vehicle-treated controls. The levels of ^{13}C-labelled $GABA_{C4}$ (M) was not altered across treatment groups. There was a significant increase in the overall neuronal metabolic rate of the cortex (O), in PNCNO-treated mice as compared to vehicle-treated controls (n = 7 per group). Results are expressed as the mean ± S.E.M. *$p < 0.05$, $^{\$}$ $p = 0.08$, $^{\#}$ $p = 0.06$; as compared to vehicle-treated controls using the two-tailed, unpaired Student's *t*-test.

bioRxiv preprint doi: https://doi.org/10.1101/2020.02.19.956060; this version posted February 20, 2020. The copyright holder for this preprint (which was not certified by peer review) is the author/funder. All rights reserved. No reuse allowed without permission.

Figure 5 – figure supplement 1

Schematic of ^{13}C labelling of various metabolites from [1,6-$^{13}C_2$]glucose in a three-compartment metabolic model

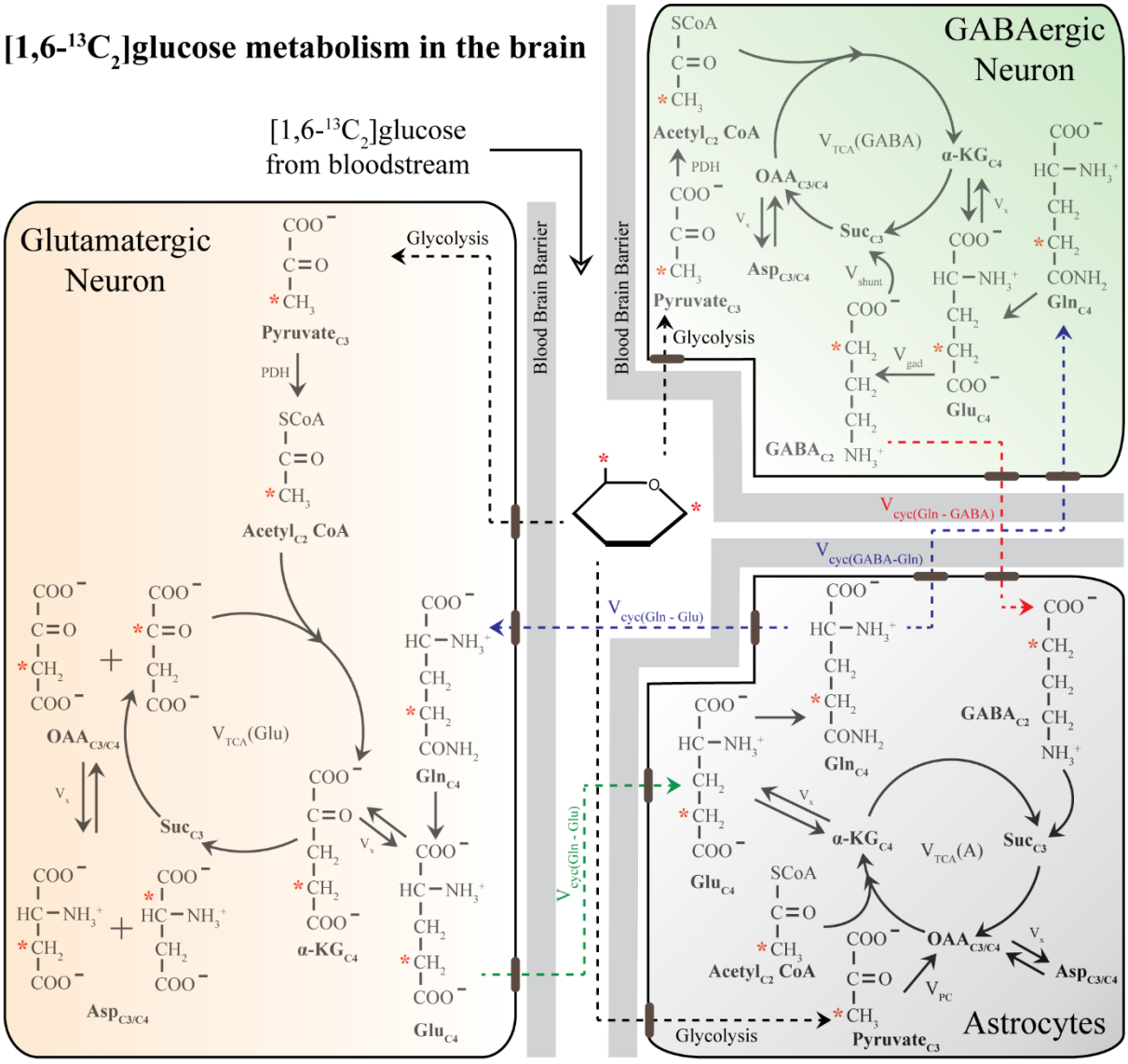

[1,6-$^{13}C_2$]glucose is converted to Pyruvate$_{C3}$ via glycolysis and subsequently enters the TCA cycle. Metabolism of [1,6-$^{13}C_2$]glucose in glutamatergic and GABAergic neurons produces Glu$_{C4}$, which is then decarboxylated to GABA$_{C2}$ by GAD enzyme in GABAergic neurons. The glutamate-glutamine and GABA-glutamine cycle operating between neurons and astrocytes produce Gln$_{C4}$. Other versions of ^{13}C-labelled glutamate (Glu$_{C4}$) and GABA (GABA$_{C4}$) are produced in the subsequent metabolism of Glu$_{C4}$ and GABA$_{C2}$. In the astrocytes, Pyruvate$_{C3}$ can enter the TCA cycle via the pyruvate carboxylate pathway and subsequently produce the

bioRxiv preprint doi: https://doi.org/10.1101/2020.02.19.956060; this version posted February 20, 2020. The copyright holder for this preprint (which was not certified by peer review) is the author/funder. All rights reserved. No reuse allowed without permission.

^{13}C-labelled metabolites namely Gln_{C2}, Glu_{C2}, and $GABA_{C4}$. Only the first round of TCA cycle is depicted here for simplicity. Abbreviations: αKG: α-ketoglutarate; OAA: oxaloacetate; Asp: aspartate; Suc: succinate; GABA: γ-aminobutyric acid; GAD: glutamic acid decarboxylase; Glu: glutamate; Gln: glutamine; $V_{cyc(GABA-Gln)}$: GABA-glutamine cycling flux; $V_{cyc(Glu-Gln)}$: glutamate–glutamine cycling flux; V_{gad}: glutamate decarboxylase flux; V_{gln}: glutamine synthesis rate; V_{pc}: pyruvate carboxylase flux; V_{shunt}: flux of GABA shunt; V_{TCA}(A): Astroglial TCA cycle flux; V_{TCA}(GABA), GABAergic TCA cycle flux; V_{TCA}(Glu): glutamatergic TCA cycle flux; V_x: exchange rate between a ketoglutarate and glutamate. $*$ represents the position of the ^{13}C carbon.

bioRxiv preprint doi: https://doi.org/10.1101/2020.02.19.956060; this version posted February 20, 2020. The copyright holder for this preprint (which was not certified by peer review) is the author/funder. All rights reserved. No reuse allowed without permission.

Figure 5 – figure supplement 2

Representative ^{1}H-[^{13}C]-NMR spectra from the cortex of vehicle and PNCNO-treated CamKIIα-tTA::TetO-hM3Dq adult male mice

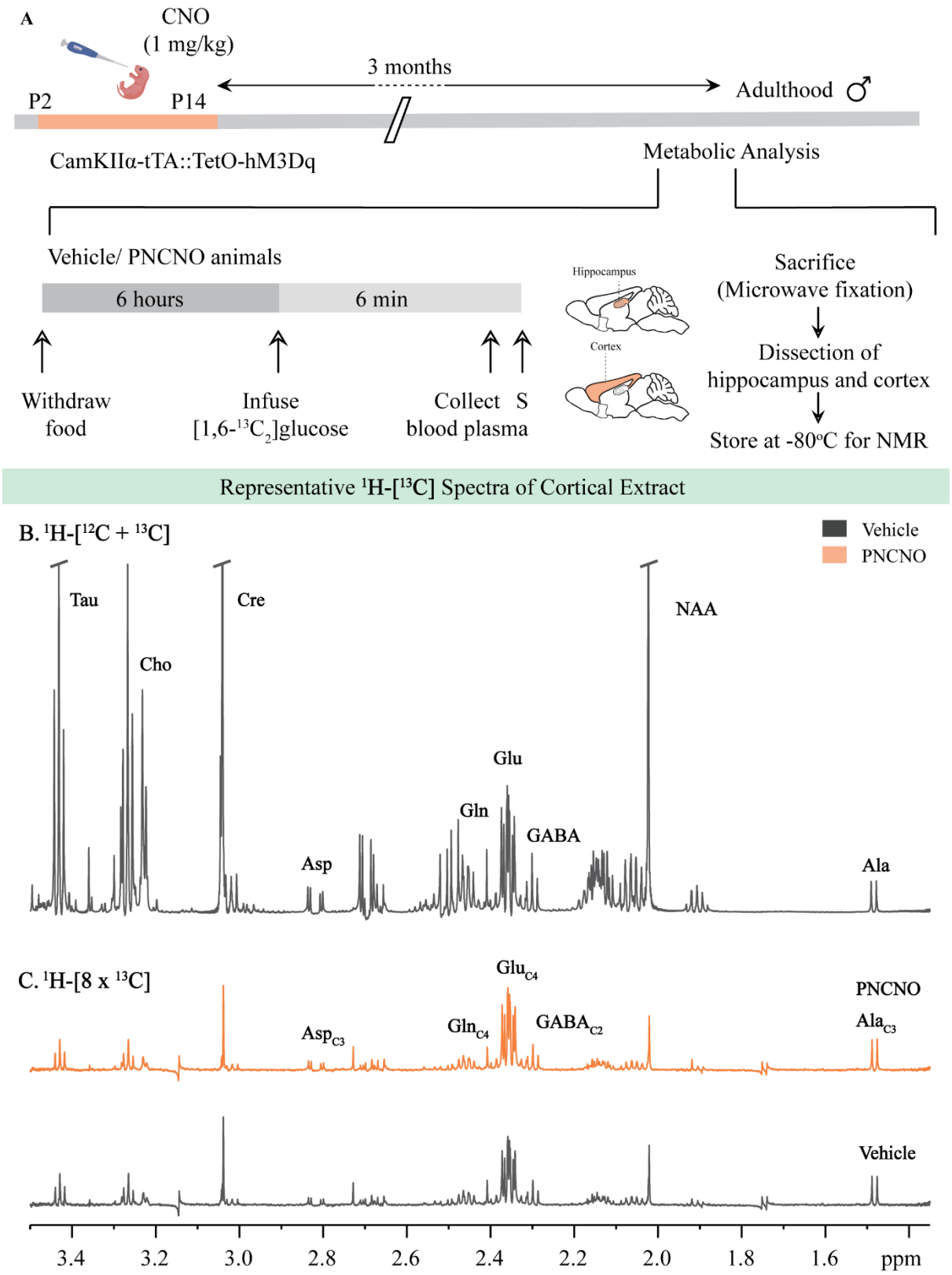

bioRxiv preprint doi: https://doi.org/10.1101/2020.02.19.956060; this version posted February 20, 2020. The copyright holder for this preprint (which was not certified by peer review) is the author/funder. All rights reserved. No reuse allowed without permission.

(A) Shown is a schematic of the experimental paradigm to induce chronic CNO-mediated hM3Dq DREADD activation in CamKIIα-positive forebrain excitatory neurons using bigenic CamKIIα-tTA::TetO-hM3Dq mouse pups that were fed CNO (PNCNO; 1 mg/kg) or vehicle from P2-P14 and then left undisturbed for three months prior to metabolic analysis performed in adulthood on male mice using ^{1}H-[^{13}C]-NMR spectroscopy. Adult male mice, with a history of PNCNO or vehicle administration, were subjected to fasting for 6 hours, following which [1,6-$^{13}C_2$]glucose was infused via the tail-vein. Blood plasma was collected and mice were sacrificed 6 minutes following glucose infusion, followed by dissection of hippocampus and cortex for NMR analysis. (B) ^{1}H-[^{12}C + ^{13}C] spectra represents the total concentration of metabolites. (C) ^{1}H-[8 x ^{13}C] depicts ^{13}C labelling of metabolites from [1,6-$^{13}C_2$]glucose. Peak labels: Asp: aspartate; Ala: alanine; Cho: Choline; Cre: Creatine; NAA: N-acetylaspartate; GABA: γ-aminobutyric acid; Glu: glutamate; Gln: glutamine; Ala_{C3}: alanine-C3; Asp_{C3}: asparate-C3; $GABA_{C2}$: GABA-C2; Gln_{C4}: glutamine-C4; Glu_{C4}: glutamate-C4.

bioRxiv preprint doi: https://doi.org/10.1101/2020.02.19.956060; this version posted February 20, 2020. The copyright holder for this preprint (which was not certified by peer review) is the author/funder. All rights reserved. No reuse allowed without permission.

Figure 5 – figure supplement 3

Influence of chronic chemogenetic activation of CamKIIα-positive forebrain excitatory neurons during the early postnatal window on the levels of other ^{13}C-labelled metabolites in the hippocampus and cortex in adult male mice.

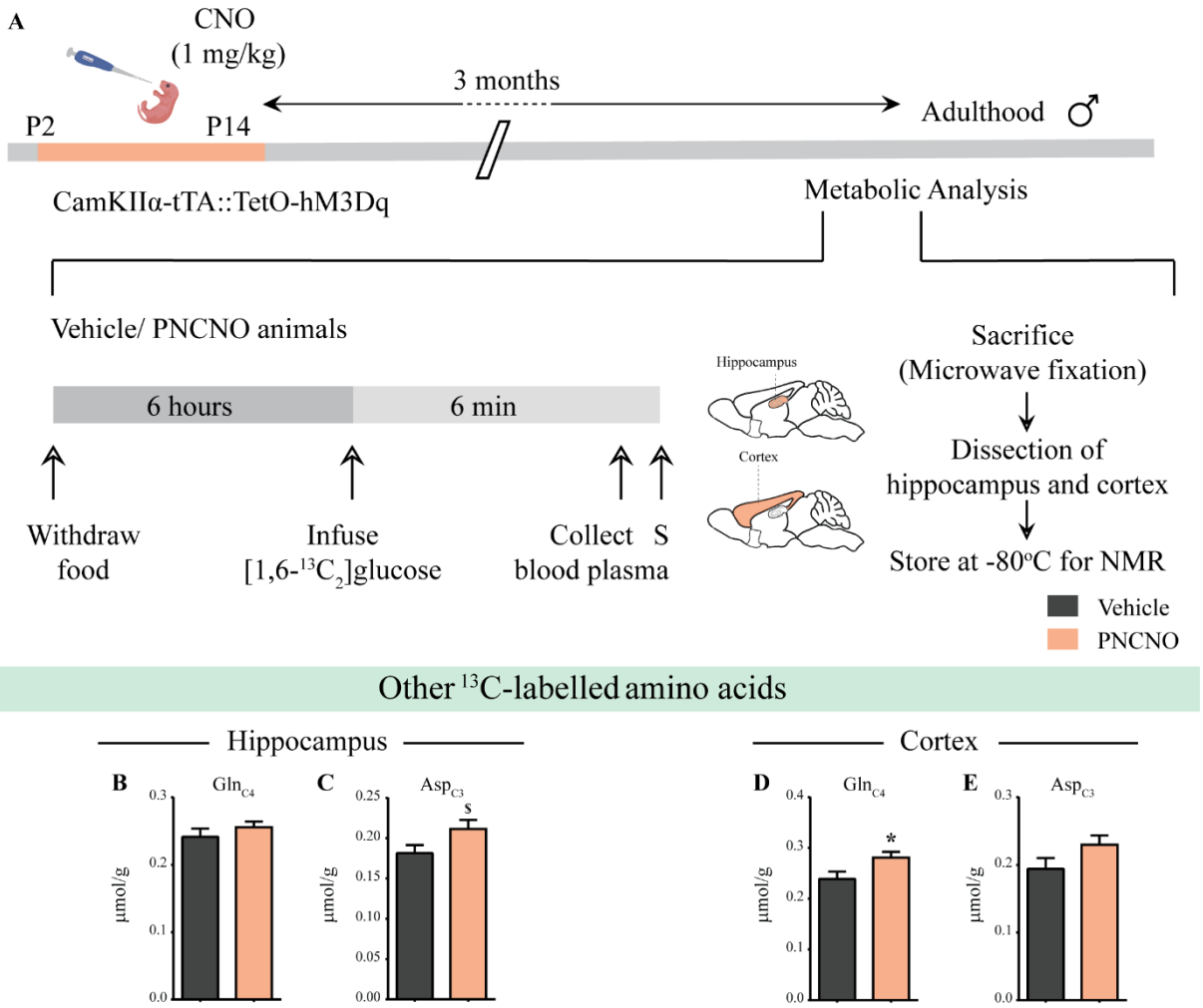

(A) Shown is a schematic of the experimental paradigm to induce chronic CNO-mediated hM3Dq DREADD activation in CamKIIα-positive forebrain excitatory neurons using bigenic CamKIIα-tTA::TetO-hM3Dq mouse pups that were fed CNO (PNCNO; 1 mg/kg) or vehicle from P2-P14 and then left undisturbed for three months prior to metabolic analysis performed in adulthood on male mice using ^{1}H-[^{13}C]-NMR spectroscopy. Adult male mice, with a history of PNCNO or vehicle administration, were subjected to fasting for 6 hours, following which [1,6-$^{13}C_2$]glucose was infused via the tail-vein. Blood plasma was collected and mice were sacrificed 6 minutes following glucose infusion, followed by dissection of hippocampus and

bioRxiv preprint doi: https://doi.org/10.1101/2020.02.19.956060; this version posted February 20, 2020. The copyright holder for this preprint (which was not certified by peer review) is the author/funder. All rights reserved. No reuse allowed without permission.

cortex for NMR analysis. (B) No significant change was observed in the levels of Gln_{C4} in the hippocampus across treatment groups. (C) There was a trend towards an increase observed in the ^{13}C-labelled metabolite, Asp_{C3} in the hippocampi of PNCNO-treated adult male mice as compared to vehicle-treated controls. (D) A significant increase was noted in the ^{13}C-labelled Gln_{C4} in the cortex of PNCNO-treated mice as compared to vehicle-treated controls. (E) No significant change was observed in the levels of Asp_{C3} in the cortex across treatment groups (n = 7 per group). Results are expressed as the mean ± S.E.M. $*p < 0.05$, $^{\$}\ p = 0.07$; as compared to vehicle-treated controls using the two-tailed, unpaired Student's *t*-test.

bioRxiv preprint doi: https://doi.org/10.1101/2020.02.19.956060; this version posted February 20, 2020. The copyright holder for this preprint (which was not certified by peer review) is the author/funder. All rights reserved. No reuse allowed without permission.

Figure 5 – table 2

Influence of chronic chemogenetic activation of CamKIIα-positive forebrain excitatory neurons during the early postnatal window on the total levels of metabolites relative to [2-^{13}C]glycine in the hippocampus and cortex in adult male mice.

		[1,6-^{13}C]glucose Infusion										
		Concentration of brain metabolites determined relative to [2-^{13}C]glycine (μmol/g)										
Brain Region	Group	Glu	GABA	Gln	Asp	NAA	Ala	Lac	Ino	Tau	Cho	Cre
Hippocampus	Vehicle	13.5 ± 0.3	3.6 ± 0.2	5.0 ± 0.1	2.3 ± 0.1	8.9 ± 0.1	0.7 ± 0.1	3.0 ± 0.6	7.3 ± 0.2	8.6 ± 0.2	2.3 ± 0.1	13.5 ± 0.2
	PNCNO	13.7 ± 0.3	3.7 ± 0.2	4.8 ± 0.1	2.5 ± 0.1	9.0 ± 0.1	0.6 ± 0.1*	2.3 ± 0.2	7.5 ± 0.2	8.5 ± 0.2	2.3 ± 0.1	13.5 ± 0.3
Cortex	Vehicle	13.5 ± 0.3	3.4 ± 0.1	4.7 ± 0.1	2.9 ± 0.1	9.5 ± 0.4	0.7 ± 0.1	7.0 ± 1.3	6.0 ± 0.2	9.1 ± 0.1	2.0 ± 0.1	12.9 ± 0.1
	PNCNO	14.0 ± 0.2	3.3 ± 0.1	4.5 ± 0.1	3.2 ± 0.1$^{\$}$	9.6 ± 0.4	0.6 ± 0.1	5.3 ± 0.5	6.0 ± 0.1	9.1 ± 0.2	2.1 ± 0.1	12.9 ± 0.2

Chronic CNO-mediated hM3Dq DREADD activation in CamKIIα-positive forebrain excitatory neurons was achieved using bigenic CamKIIα-tTA::TetO-hM3Dq mouse pups that were fed CNO (PNCNO; 1 mg/kg) or vehicle from P2-P14 and then left undisturbed for three months prior to metabolic analysis performed in adulthood on male mice and NMR spectroscopy on the hippocampus and cortex was performed to acquire ^{1}H-[^{12}C + ^{13}C] spectra. The concentration of metabolites was determined relative to [2-^{13}C]glycine. Glu: Glutamate; GABA: γ-aminobutyric acid; Gln: Glutamine; Asp: Aspartate; NAA: N-acetylaspartate; Suc: Succinate; Ala: Alanine; Lac: Lactose; Ino; Inositol; Tau: Taurine; Cho: Choline; Cre: Creatine. Results are expressed as the mean ± S.E.M (n = 7 per group). *$p < 0.05$, $^{\$}$ $p = 0.06$; as compared to vehicle-treated controls using the two-tailed, unpaired Student's *t*-test.

bioRxiv preprint doi: https://doi.org/10.1101/2020.02.19.956060; this version posted February 20, 2020. The copyright holder for this preprint (which was not certified by peer review) is the author/funder. All rights reserved. No reuse allowed without permission.

Figure 6 with 1 supplement

Chronic chemogenetic activation of CamKIIα-positive forebrain excitatory neurons during the early postnatal window results in a long-lasting decline in neuronal activity-related gene expression, and c-Fos immunopositive cell numbers, in the adult hippocampus.

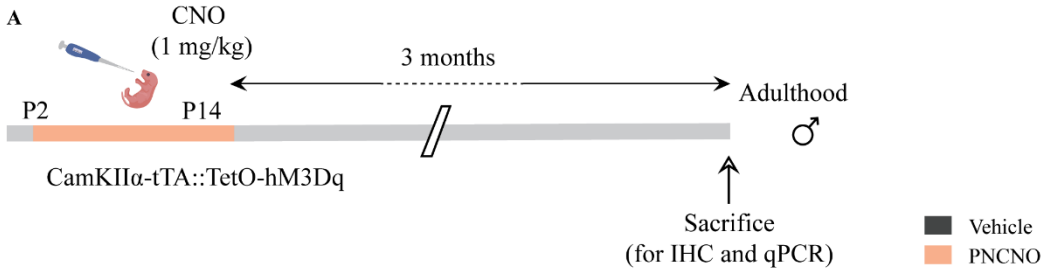

Activity-related Gene Expression

B

Genes	Vehicle	PNCNO	*p* Value	FDR
c-Fos	1.00 ± 0.12	0.71 ± 0.06*	0.0485	0.0417
Erk1	1.00 ± 0.08	0.77 ± 0.03*	0.0131	0.0201
Nr4a1	1.00 ± 0.16	0.87 ± 0.10	0.4998	0.3374
Npas4	1.00 ± 0.15	0.48 ± 0.06*	0.0050	0.0095
JunB	1.00 ± 0.12	0.93 ± 0.07	0.6300	0.3969
Staufen1	1.00 ± 0.05	0.69 ± 0.05*	0.0003	0.0028
Staufen2	1.00 ± 0.06	0.81 ± 0.05*	0.0172	0.0203
Nrxn1	1.00 ± 0.06	0.77 ± 0.07*	0.0283	0.0297
Gphn	1.00 ± 0.06	0.81 ± 0.04*	0.0149	0.0201
Shank	1.00 ± 0.07	0.73 ± 0.04*	0.0036	0.0095
Nlgn1	1.00 ± 0.15	0.97 ± 0.06	0.8628	0.4796
Nlgn2	1.00 ± 0.16	0.87 ± 0.05	0.4387	0.3189
Psd95	1.00 ± 0.08	0.82 ± 0.03*	0.0381	0.0360
Fmrp	1.00 ± 0.07	0.71 ± 0.06*	0.0047	0.0095
Mecp2	1.00 ± 0.22	0.75 ± 0.04	0.2687	0.2116
Mef2c	1.00 ± 0.19	0.88 ± 0.19	0.6748	0.3986
Synapsin1b	1.00 ± 0.06	0.74 ± 0.03*	0.0009	0.0043

c-Fos Immunoreactivity

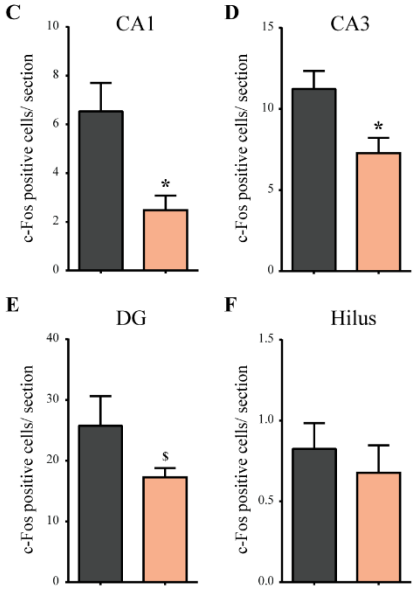

(A) Shown is a schematic of the experimental paradigm to induce chronic CNO-mediated hM3Dq DREADD activation in CamKIIα-positive forebrain excitatory neurons using bigenic CamKIIα-tTA::TetO-hM3Dq mouse pups that were fed CNO (PNCNO; 1 mg/kg) or vehicle from P2-P14 and then left undisturbed for three months prior to qPCR analysis for neuronal activity-related gene expression and c-Fos immunohistochemistry performed in adulthood on male mice. (B) Shown are normalized gene expression levels for specific neuronal activity-related genes in PNCNO-treated mice represented as fold-change of their vehicle-treated controls (n = 11 per group). Heat maps indicate the extent of gene regulation. *$p < 0.05$ as compared to vehicle-treated controls using the two-tailed, unpaired Student's *t*-test. Also

bioRxiv preprint doi: https://doi.org/10.1101/2020.02.19.956060; this version posted February 20, 2020. The copyright holder for this preprint (which was not certified by peer review) is the author/funder. All rights reserved. No reuse allowed without permission.

shown are false-discovery rate (FDR) corrected *p* values. Cell counting analysis for c-Fos immunopositive cells within the hippocampus, indicated a significant reduction in the number of c-Fos positive cells/section within the CA1 (C), CA3 (D), and DG (E) hippocampal subfields in PNCNO-treated mice as compared to vehicle-treated controls (n = 10 for vehicle; n = 12 for PNCNO). c-Fos immunopositive cell numbers were unaltered in the hilar subfield of the hippocampus (F) in PNCNO-treated mice as compared to vehicle-treated controls. Results are expressed as the mean ± S.E.M. $*p < 0.05$ as compared to vehicle-treated controls using the two-tailed unpaired Student's *t*-test.

bioRxiv preprint doi: https://doi.org/10.1101/2020.02.19.956060; this version posted February 20, 2020. The copyright holder for this preprint (which was not certified by peer review) is the author/funder. All rights reserved. No reuse allowed without permission.

Figure 6 – table 3

List of qPCR primers

Genes	Forward Primer (5'-3')	Reverse Primer (5'-3')
c-Fos	AGGGAGCTGACAGATACACTCC	TGCAACGCAGACTTCTCATC
Erk1	GCCACCTTCTCTCACTTTGC	TGTCAGGGAAAATGGGGTGG
Nr4a1	GGGTGACCCCACTATTTGTC	ATGGAAGGAGAGCGGAAGAG
Npas4	CCTTCCAGACTCACTTGCCC	CTGAGCTTTCTGTCAACTGTCC
JunB	ATCAGCTACCTCCCACATGC	GCTTTCGCTCCACTTTGATG
Staufen1	CAGACAGCCCCGGATTATGG	TGCCCAACCTTTACCTGCAT
Staufen2	GTGGCCCGCAGTTTTGTG	CAACAGCTTGTTGGGCCTTC
Nrxn1	ATTGGACACGCTATGGTGACA	ACTGACTGGTGACCCTGGAA
Gphn	TGGGTGGGACTATATCGGCA	TTTGTGGCCTCTGGAGTGAC
Shank	ACCAGGTCCCATAAGGCTACA	TTCAGGCATACACAGGCACC
Nlgn1	GCTTGGGGTACTTGGCTTCT	AGGTTGACACATGAACCCCC
Nlgn2	ACTTCGCCAAGACTGGTGAC	ACCTTGTTGGCACGGTAGTT
Psd95	TAGTGACAACCAAGAAATACCGC	TCCGTTCACCTGCAACTCATA
Fmrp	CAAGGCTTGGCAGGGTATGG	CCAATTTGTCGCAACTGCTCA
Mecp2	AAACAGCGGCGCTCCATTA	AAAGCTTTTCCCTGGGGATTGA
Mef2c	CAACAAAGCCCTCAGCAGGT	TGCATTCGTTCCCTCTGCAC
Synapsin1b	TACCATCCACCAAGCAGTCC	TGGAGGTTGGAGGAAGATGC

bioRxiv preprint doi: https://doi.org/10.1101/2020.02.19.956060; this version posted February 20, 2020. The copyright holder for this preprint (which was not certified by peer review) is the author/funder. All rights reserved. No reuse allowed without permission.

Figure 7 with 3 supplement

Chronic chemogenetic activation of CamKIIα-positive forebrain excitatory neurons during the early postnatal window alters excitatory and inhibitory spontaneous currents in the hippocampi of adult male mice.

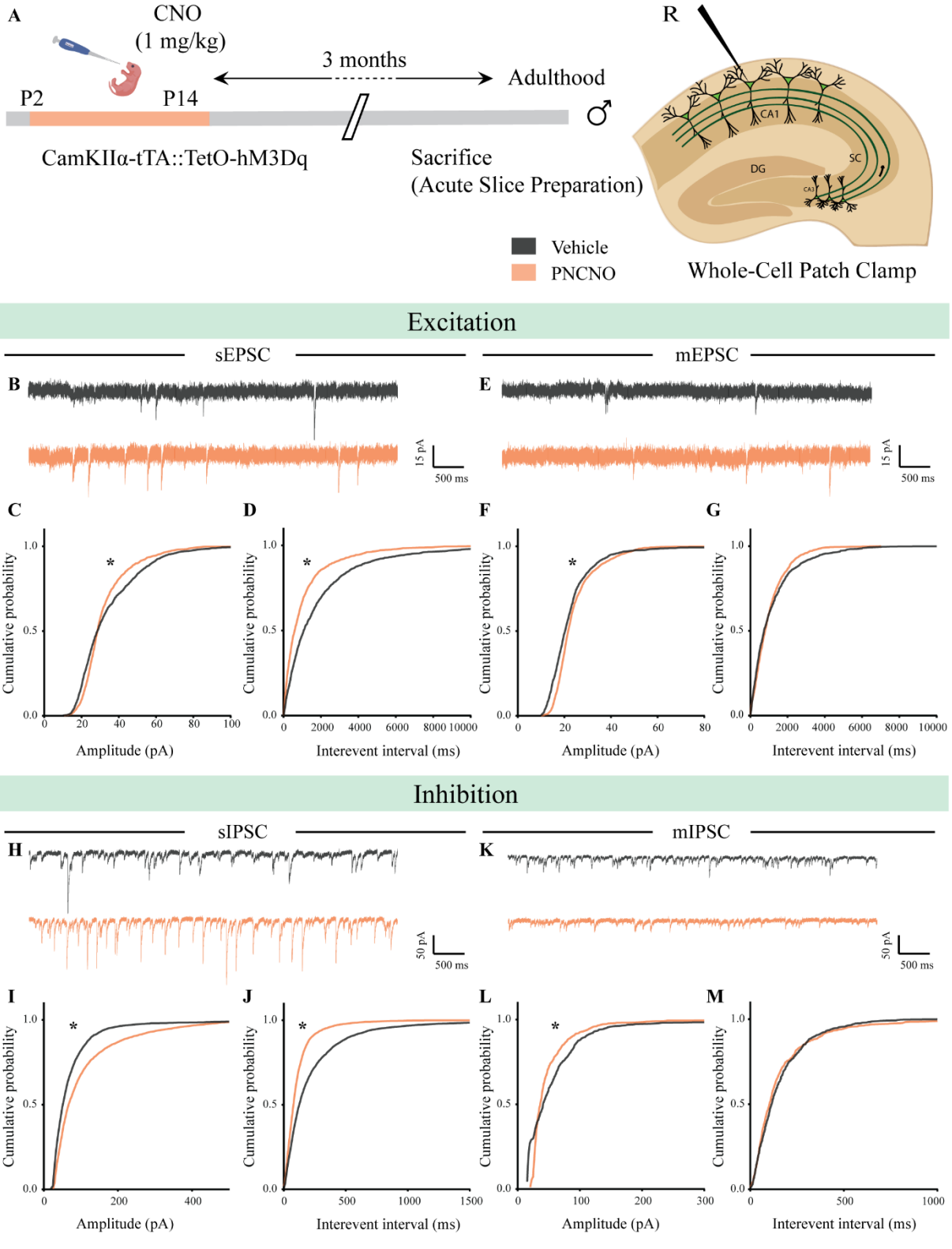

bioRxiv preprint doi: https://doi.org/10.1101/2020.02.19.956060; this version posted February 20, 2020. The copyright holder for this preprint (which was not certified by peer review) is the author/funder. All rights reserved. No reuse allowed without permission.

(A) Shown is a schematic of the experimental paradigm to induce chronic CNO-mediated hM3Dq DREADD activation in CamKIIα-positive forebrain excitatory neurons using bigenic CamKIIα-tTA::TetO-hM3Dq mouse pups that were fed CNO (PNCNO; 1 mg/kg) or vehicle from P2-P14 and then left undisturbed for three months prior to electrophysiological analysis, in acute hippocampal slices derived from adult male mice. Whole-cell patch clamp was performed to record sEPSCs/ mEPSCs and sIPSCs/ mIPSCs in the somata of CA1 pyramidal neurons. R – Recording electrode. (B) Shown are representative sEPSC traces of CA1 pyramidal neurons from vehicle and PNCNO-treated mice. (C) PNCNO-treated mice showed significantly altered cumulative probability of sEPSC amplitude with a small increase at lower amplitudes (< 30 pA) and a significant decline in large amplitude events as compared to vehicle-treated controls. (D) PNCNO-treated mice showed a significant decline in the cumulative probability of sEPSC interevent intervals as compared to vehicle-treated controls (n = 8 cells for vehicle; n = 5 cells for PNCNO). (E) Shown are representative mEPSC traces of CA1 pyramidal neurons from vehicle and PNCNO-treated mice. (F) PNCNO-treated mice showed significantly enhanced cumulative probability of sEPSC amplitude as compared to vehicle-treated controls. (G) No significant change was observed in the cumulative probability of sEPSC interevent intervals in PNCNO-treated mice as compared to vehicle-treated controls (n = 5 cells for vehicle; n = 6 cells for PNCNO). (H) Shown are representative sIPSC traces of CA1 pyramidal neurons from vehicle and PNCNO-treated mice. PNCNO-treated mice showed a significant increase in the cumulative probability of sIPSC amplitude (I), along with a significant decline in the cumulative probability of sIPSC interevent intervals (J) as compared to vehicle-treated controls (n = 8 cells for vehicle; n = 7 cells for PNCNO). (K) Shown are representative mIPSC traces of CA1 pyramidal neurons from vehicle and PNCNO-treated mice. (L) PNCNO-treated mice showed a significant decline in the cumulative probability of mIPSC amplitude as compared to vehicle-treated controls (n = 6 cells for vehicle; n = 7 cells for PNCNO). (M) No significant change was observed in the cumulative probability of mIPSC interevent intervals across treatment groups. Results are expressed as cumulative probabilities. * $p < 0.001$ as compared to PNCNO-treated group using the Kolmogorov-Smirnov two-sample comparison.

bioRxiv preprint doi: https://doi.org/10.1101/2020.02.19.956060; this version posted February 20, 2020. The copyright holder for this preprint (which was not certified by peer review) is the author/funder. All rights reserved. No reuse allowed without permission.

Figure 7 – figure supplement 1

Chronic chemogenetic activation of CamKIIα-positive forebrain excitatory neurons during the early postnatal window does not change intrinsic excitability but alters spontaneous network activity in the hippocampi of adult male mice.

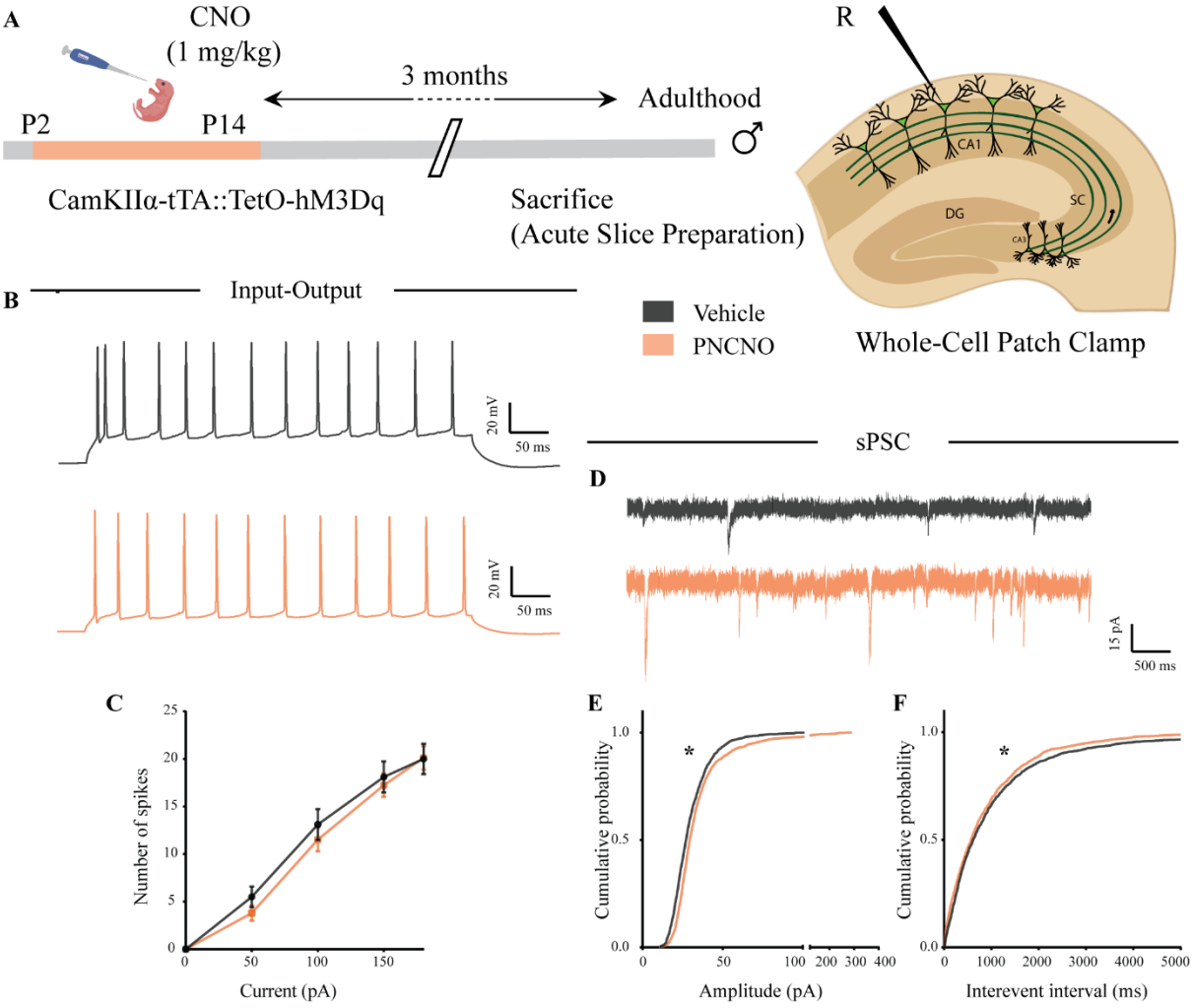

(A) Shown is a schematic of the experimental paradigm to induce chronic CNO-mediated hM3Dq DREADD activation in CamKIIα-positive forebrain excitatory neurons using bigenic CamKIIα-tTA::TetO-hM3Dq mouse pups that were fed CNO (PNCNO; 1 mg/kg) or vehicle from P2-P14 and then left undisturbed for three months prior to electrophysiological analysis, in acute hippocampal slices derived from adult male mice. Whole-cell patch clamp was performed to record sPSCs and input-output characteristics in the somata of CA1 pyramidal neurons. R – Recording electrode. (B) Shown are representative traces of spikes generated by CA1 pyramidal neurons following a current injection of 100 pA in vehicle and PNCNO-treated

bioRxiv preprint doi: https://doi.org/10.1101/2020.02.19.956060; this version posted February 20, 2020. The copyright holder for this preprint (which was not certified by peer review) is the author/funder. All rights reserved. No reuse allowed without permission.

adult male mice. (C) No significant change was observed in the input-output characteristics of CA1 pyramidal neurons in acute hippocampal slices derived from PNCNO-treated mice as compared to vehicle-treated controls (n = 18 cells for vehicle; n = 25 cells for PNCNO). Results are expressed as the mean ± S.E.M. (D) Shown are representative sPSC traces of CA1 pyramidal neurons from vehicle and PNCNO-treated mice. (E) PNCNO-treated mice showed significantly enhanced cumulative probability of sPSC amplitude in addition to the presence of a long-tail as compared to vehicle-treated controls. (F) PNCNO-treated mice showed a significant decline in the cumulative probability of sPSC interevent intervals as compared to vehicle-treated controls (n = 8 cells for vehicle; n = 6 cells for PNCNO). Results are expressed as cumulative probabilities. * $p < 0.001$ as compared between vehicle and PNCNO-treated group using the Kolmogorov-Smirnov two-sample comparison.

bioRxiv preprint doi: https://doi.org/10.1101/2020.02.19.956060; this version posted February 20, 2020. The copyright holder for this preprint (which was not certified by peer review) is the author/funder. All rights reserved. No reuse allowed without permission.

Figure 7 – figure supplement 2

Effect of chronic chemogenetic activation of CamKIIα-positive forebrain excitatory neurons during the early postnatal window on the distribution of spontaneous network events in hippocampi of adult male mice

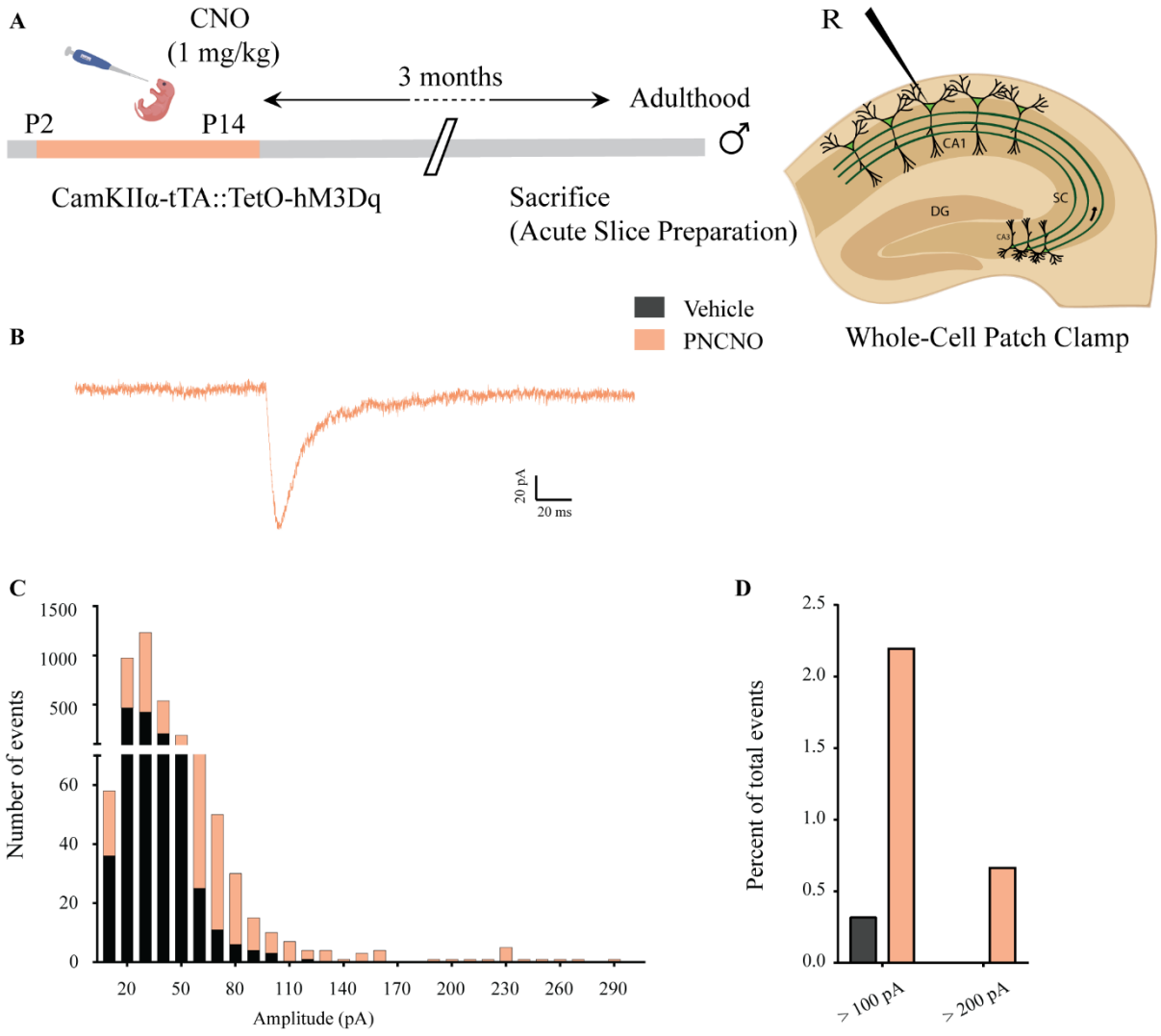

(A) Shown is a schematic of the experimental paradigm to induce chronic CNO-mediated hM3Dq DREADD activation in CamKIIα-positive forebrain excitatory neurons using bigenic CamKIIα-tTA::TetO-hM3Dq mouse pups that were fed CNO (PNCNO; 1 mg/kg) or vehicle from P2-P14 and then left undisturbed for three months prior to electrophysiological analysis, in acute hippocampal slices derived from adult male mice. Whole-cell patch clamp was performed to record sPSCs in the somata of CA1 pyramidal neurons. R – Recording electrode. (B) Shown is an example trace of a large-amplitude spontaneous network event observed in a

bioRxiv preprint doi: https://doi.org/10.1101/2020.02.19.956060; this version posted February 20, 2020. The copyright holder for this preprint (which was not certified by peer review) is the author/funder. All rights reserved. No reuse allowed without permission.

CA1 pyramidal neuron of a PNCNO-treated mouse. (C) Distribution plot for sPSC amplitudes showing a long-tail of large-amplitude events in PNCNO-treated mice. (D) Quantification of percent of total events with amplitude > 100 pA and > 200 pA. No event > 200 pA was observed in vehicle-treated controls.

bioRxiv preprint doi: https://doi.org/10.1101/2020.02.19.956060; this version posted February 20, 2020. The copyright holder for this preprint (which was not certified by peer review) is the author/funder. All rights reserved. No reuse allowed without permission.

Figure 7 – table 4

Effect of chronic chemogenetic activation of CamKIIα-positive forebrain excitatory neurons during the early postnatal window on intrinsic membrane properties in adulthood.

Adults	CA1 Pyramidal Neurons					
	Intrinsic Properties					
Group	RMP (mV)	Input resistance (MΩ)	τ (ms)	Sag (mV)	Sag (%)	Accomodation index
Vehicle	-62.3 ± 0.655	195.1 ± 10.89	18.87 ± 1.574	-4.282 ± 0.288	4.956 ± 0.317	0.375 ± 0.054
PNCNO	-62.81 ± 0.682	180.2 ± 10.46	18.66 ± 1.269	-3.603 ± 0.397	4.173 ± 0.420	0.392 ± 0.046

Chronic CNO-mediated hM3Dq DREADD activation of CamKIIα-positive forebrain excitatory neurons was performed using bigenic CamKIIα-tTA::TetO-hM3Dq mouse pups that were fed CNO (PNCNO; 1 mg/kg) or vehicle from P2-P14 and then left undisturbed for three months prior to electrophysiological analysis, in acute hippocampal slices derived from adult male mice. Whole-cell patch clamp was performed to determine intrinsic properties in the somata of CA1 pyramidal neurons. RMP: Resting membrane potential, τ: Membrane time constant. Results are expressed as the mean ± S.E.M. (n = 18 cells for vehicle; n = 25 cells for PNCNO).